

Dinuclear Ce(IV) Aryloxides: Highly Active Catalysts for Anhydride/Epoxide Ring-Opening Copolymerization

Steven J. Gray[†], Karen Brown[†], Francis Y. T. Lam^{†,‡}, Jennifer A. Garden[†] and Polly L. Arnold^{†,‡,*}

[†] EaStCHEM School of Chemistry, The University of Edinburgh, Joseph Black Building, David Brewster Road, Edinburgh, EH9 3FJ, UK

[‡] Current address: Department of Chemistry, University of California, Berkeley, Berkeley CA 94720, USA. Chemical Sciences Division, Lawrence Berkeley National Laboratory, One Cyclotron Road, Berkeley 94720, USA. e-mail: pla@berkeley.edu

Contents

S1 General Details	2
S2 Compound Syntheses	3
S2.1 Synthesis of H ₄ (<i>p</i> TP ^{Ad})	3
S2.2 Synthesis of H ₄ (<i>m</i> TP ^{Ad})	4
S2.3 Synthesis of [NEt ₄] ₂ [Ce ₂ Cl ₆ (<i>p</i> TP ^t)]	6
S2.4 [NEt ₄] ₂ [Ce ₂ Cl ₂ (OSiMe ₃) ₄ (<i>p</i> TP ^t)]	8
S2.5 [NEt ₄] ₂ [Ce ₂ Cl ₂ (OSiMe ₃) ₄ (<i>m</i> TP ^t)]	11
S2.6 [NEt ₄] ₂ [Ce ₂ Cl ₂ (OSiMe ₃) ₄ (<i>p</i> TP ^{Ad})]	13
S2.7 [NEt ₄] ₂ [Ce ₂ Cl ₂ (OSiMe ₃) ₄ (<i>m</i> TP ^{Ad})]	15
S2.8 [NEt ₄] ₂ [Ce ₂ (OSiMe ₃) ₆ (<i>p</i> TP ^{Ad})]	17
S2.9 [NEt ₄] ₂ [Ce ₂ Cl ₄ (ODipp) ₂ (<i>p</i> TP ^t)]	17
S2.10 Synthesis of [NEt ₄] ₂ [Ce ₂ Cl ₆ (<i>mTer</i> TP ^t)]	20
S2.11 Synthesis of neutral di-Ce(IV) complex	22
S2.12 Cyclic voltammetry studies	24
S2.13 UV-Vis	26
S3 ROCOP Protocols	27
S3.1 Example procedure for PA/CHO reactions, using [NEt ₄] ₂ [Ce ₂ Cl ₂ (OSiMe ₃) ₄ (<i>p</i> TP ^t)] as catalyst.	27
S3.2 Example procedure for ROCOP substrate scope	31
S3.3 Rate equation determination experiments	35
S3.4 ROCOP Mechanistic discussion	36
S3.5 SEC Traces	38
S3.6 MALDI Data	45
S4. Crystallography	49
S5. References	50

S1 General Details

All moisture and air sensitive materials were manipulated using standard high-vacuum Schlenk-line techniques and MBraun gloveboxes and stored under an atmosphere of dried and deoxygenated dinitrogen. All gases were supplied by BOC gases UK. All glassware items, cannulae and Fisherbrand 1.2 μm retention glass microfibre filters were dried in a 160 °C oven overnight before use.

Hexane, tetrahydrofuran and toluene for use with moisture and air sensitive compounds were dried using a Vac Atmospheres solvent purification system and stored over activated 4 Å molecular sieves. The solvent was cycled through a drying column containing molecular sieves for 12 hours before collection. All solvents were degassed and stored for 2 days prior to use. Benzene- d_6 and pyridine- d_5 were refluxed over potassium metal for 24 hours, freeze-pump-thaw degassed and distilled by trap-to-trap distillation prior to use. All solvents were purchased from Sigma-Aldrich or Fisher Scientific.

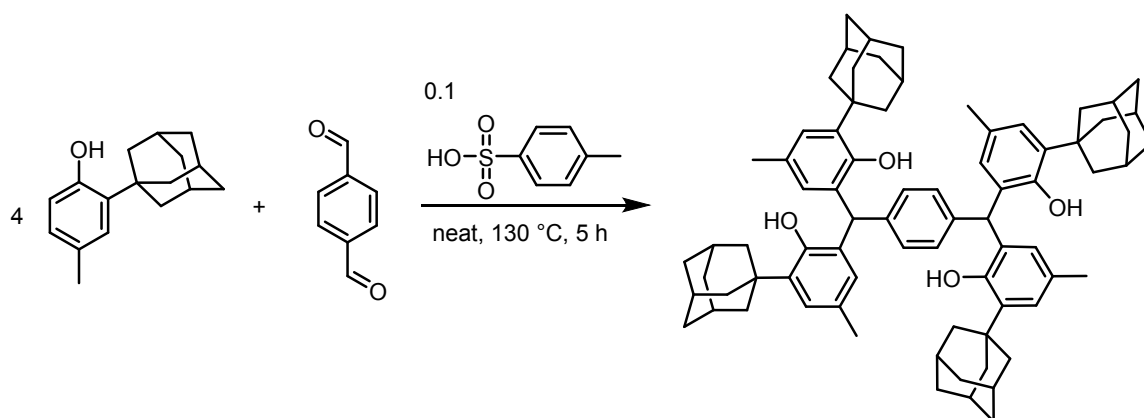
NaOSiMe_3 was sublimed prior to use and phthalic anhydride and succinic anhydride were sublimed three times prior to use. Cyclohexene oxide, (\pm)-propylene oxide and (+)-limonene oxide were dried over CaH_2 and distilled prior to use. $\text{H}_4(p\text{TP}^t)$,¹ $\text{H}_4(m\text{TP}^t)$,¹ $\text{H}_4(m\text{TerTP}^t)$,² 2-adamantyl-*p*-cresol,³ $\text{NaN}(\text{SiMe}_3)_2$,⁴ $[\text{NEt}_4]_2\text{CeCl}_6$,⁵ and NaODipp ,^{6, 7} were prepared using published methods. All other chemicals were used as received.

Unless stated otherwise, all NMR spectroscopic analyses were recorded at 298 K using a Bruker Avance III 500.12 MHz spectrometer with ^1H NMR spectra run at 500.12 MHz, ^{13}C NMR spectra run at 126 MHz and ^{29}Si NMR spectra at 99.37 MHz. The ^1H NMR spectra were referenced internally using residual solvent signals and are reported relative to external tetramethylsilane. Chemical shifts are quoted in ppm and coupling constants in Hz. IR spectra were recorded using a Nicolet Avatar 360 FT-IR spectrometer between 4000–400 cm^{-1} on a powdered sample. Elemental analyses were carried out at the London Metropolitan University.

SEC analyses of the filtered polymer samples were carried out in SEC grade THF at a flow rate of 1 $\text{mL}\cdot\text{min}^{-1}$ at 35 °C on a 1260 Infinity II GPC/SEC single detection system with mixed bed C PLgel columns (300 x 7.5 mm). MALDI-ToF MS analyses were performed using a Bruker Daltonics UltrafleXtreme™ MALDI-ToF/ToF MS instrument. The sample to be analysed, dithranol matrix and KI (cationizing agent) were dissolved in THF at 10 $\text{mg}\cdot\text{mL}^{-1}$ and the solutions were mixed in a 2:2:1 volume ratio, respectively. A droplet (2 μL) of the resultant mixture was spotted on to the sample plate and submitted for MALDI-ToF MS analysis.

S2 Compound Syntheses

S2.1 Synthesis of H₄(pTP^{Ad})



Equation S1: Synthesis of H₄(pTP^{Ad}).

A 250 mL round-bottomed flask was charged with 2-adamantyl-*p*-cresol (3.52 g, 14.5 mmol, 4.4 equiv.), terephthalaldehyde (0.440 g, 3.3 mmol, 1 equiv.), *p*-toluenesulfonic acid (0.063 g, 0.33 mmol, 0.1 equiv.) and a stir bar, the contents heated to 130 °C and stirred for 5 hours. The resulting red-orange solid was suspended in acetonitrile (200 cm³) and stirred with sonication until the mixture was homogenous. The light red mixture was then filtered and dried under suction, washed with boiling ethanol (3 x 50 cm³) and dried under dynamic vacuum for 16 hours at 50 °C to give the pale red/pink solid H₄(pTP^{Ad}). Yield: 3.81 g (82%).

¹H NMR (500 MHz, benzene-*d*₆) δ_H 7.08 (br, 4H, Ar-H), 7.07 (br, 4H, Ar-H), 6.73 (s, 4H, Ar-H), 5.63 (s, 2H, benzylic C-H), 4.98 (s, 4H, -OH), 2.19, (m, 24H, -CH₂), 2.11 (br, 12H), 2.02 (br, 12H), 1.74 (m, 24H, -CH₂).

¹³C{¹H} NMR (126 MHz, benzene-*d*₆) δ_C 151.9 (ArC), 140.5 (ArC), 138.3 (ArC), 130.6 (ArC), 130.2 (ArC), 128.7 (ArC), 67.8 (benzylic CH), 47.7, 40.9, 37.4, 37.3, 29.6, 25.8, 21.2.

Elemental analysis (C₇₆H₉₀O₄): C 85.51%, H 8.50%, N 0.00% calculated; C 85.33%, H 8.37%, N 0.00% found.

Figure S1: ¹H NMR spectrum of H₄(pTP^{Ad}) in C₆D₆.

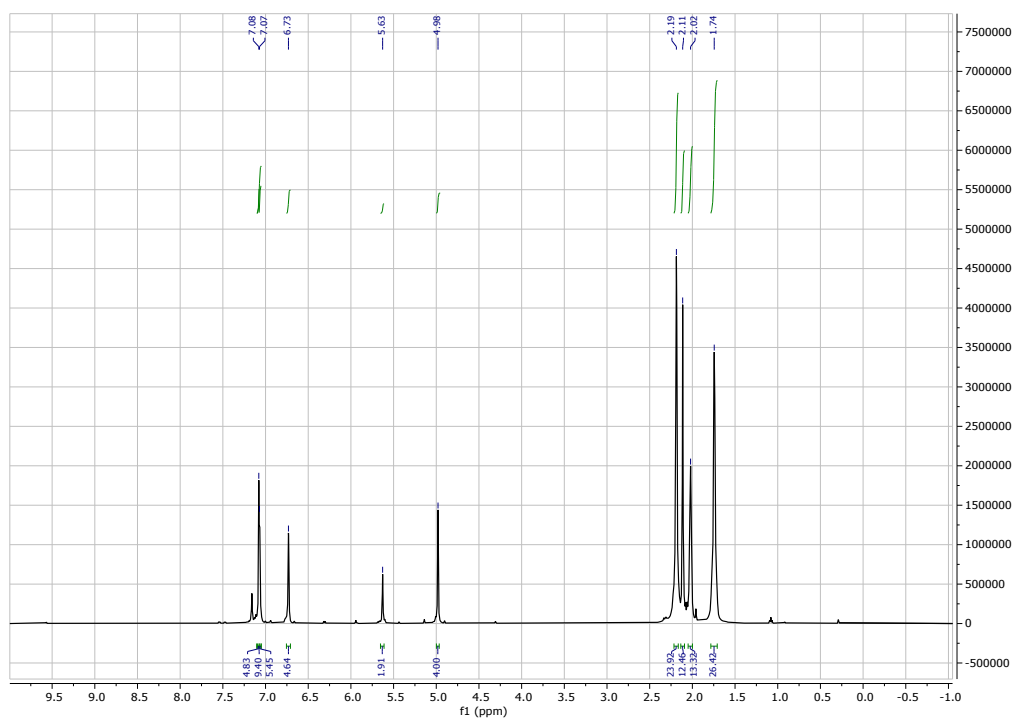
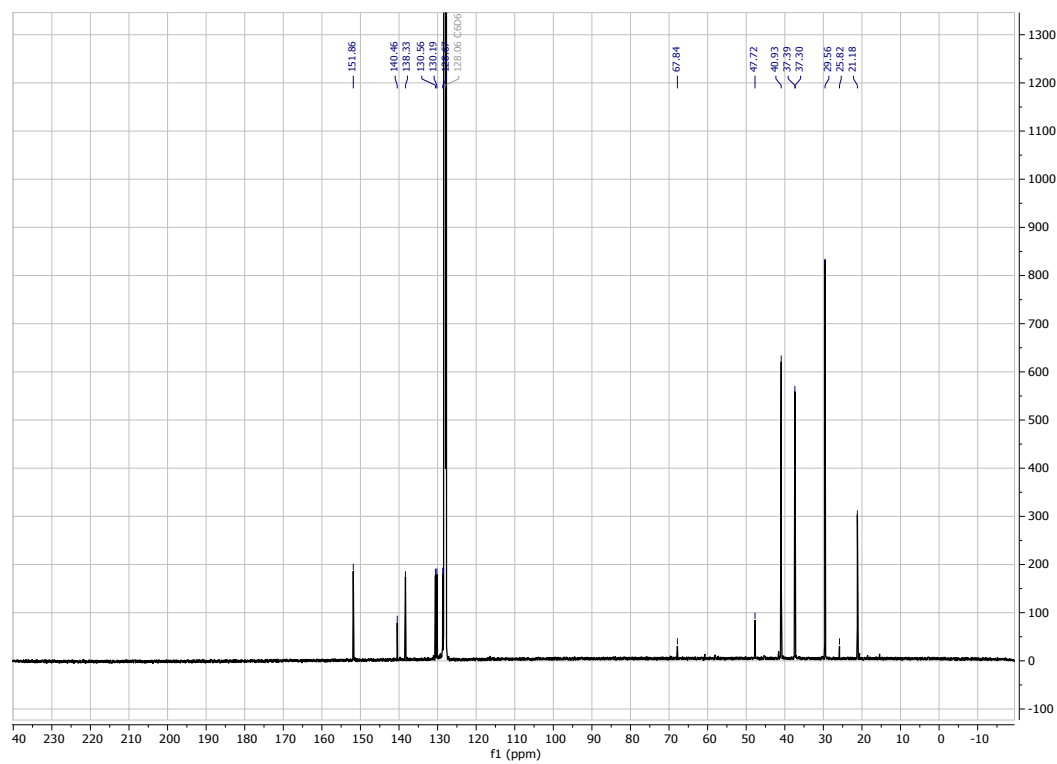
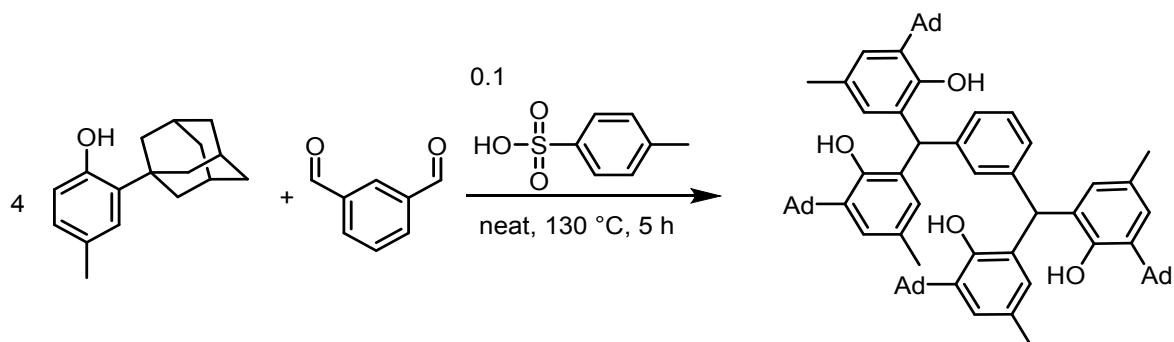


Figure S2: $^{13}\text{C}\{^1\text{H}\}$ NMR spectrum of $\text{H}_4(\text{pTPAd})$ in C_6D_6 .



S2.2 Synthesis of $\text{H}_4(\text{mTPAd})$



Equation S2: Synthesis of $H_4(mTP^{Ad})$.

Synthesised by analogous procedure to $H_4(pTP^{Ad})$. 2-adamantyl-*p*-cresol (3.52 g, 14.5 mmol, 4.4 equiv.), isophthalaldehyde (0.440 g, 3.3 mmol, 1 equiv.) and *p*-toluenesulfonic acid (0.063 g, 0.33 mmol, 0.1 equiv.) were combined, heated to 130 °C and stirred for 5 hours. An identical work-up yielded $H_4(mTP^{Ad})$ as a pale-yellow solid, yield: 3.05 g (66%).

1H NMR (500 MHz, benzene- d_6) δ_H 7.05 (br, 8H, Ar-H), 6.71 (br, 4H, Ar-H), 5.53 (s, 2H, benzylic C-H), 4.95 (s, 4H, -OH), 2.18, (m, 24H, -CH $_2$), 2.12 (br, 12H), 2.03 (br, 12H), 1.76 (m, 24H, -CH $_2$).

$^{13}C\{^1H\}$ NMR (126 MHz, benzene- d_6) δ_C 151.8 (ArC), 142.1 (ArC), 138.3 (ArC), 131.2 (ArC), 130.2 (ArC), 130.0, 128.9 (ArC), 128.5 (ArC), 128.4 (ArC), 128.0 (ArC), 48.1, 40.9, 37.4, 37.3, 29.6, 21.2.

Elemental analysis (C $_{76}$ H $_{90}$ O $_4$): C 85.51%, H 8.50%, N 0.00% calculated; C 85.67%, H 8.78%, N 0.00% found.

Figure S3: 1H NMR spectrum of $H_4(mTP^{Ad})$ in C $_6$ D $_6$.

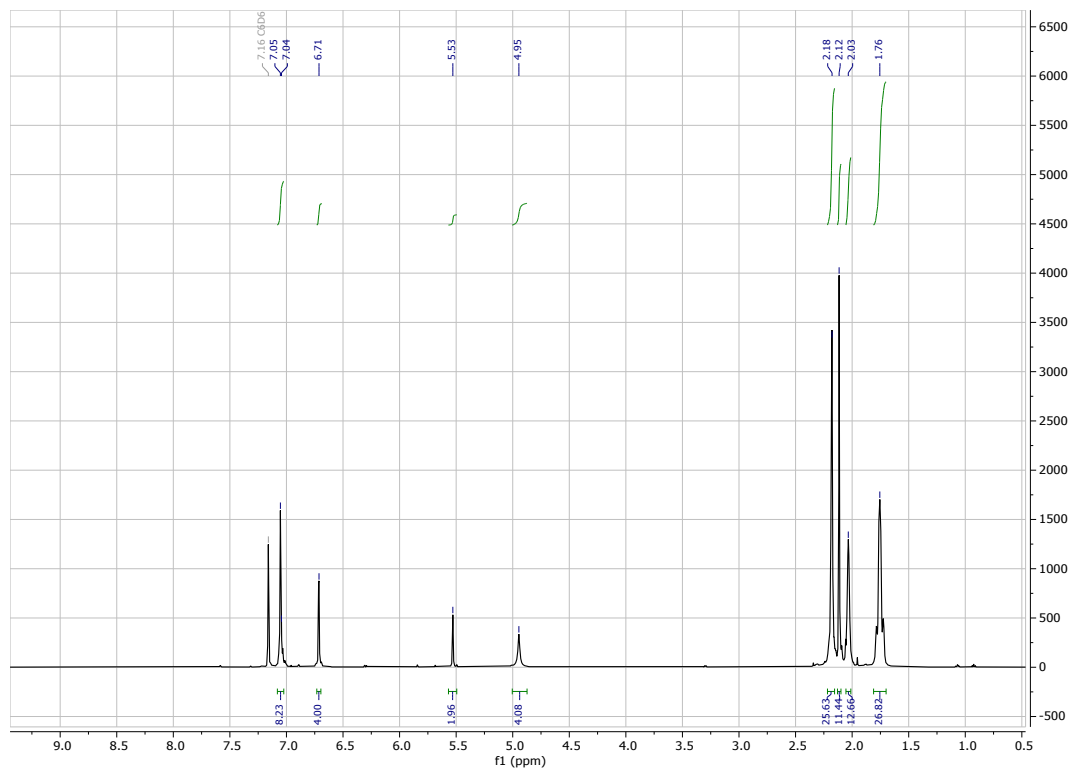
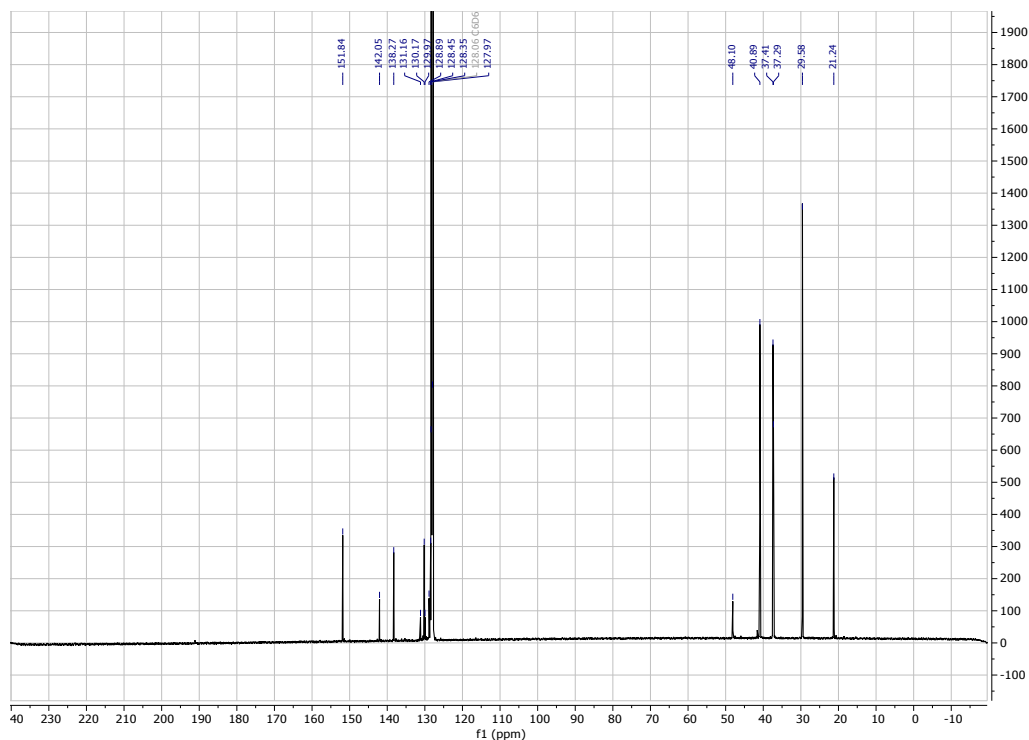
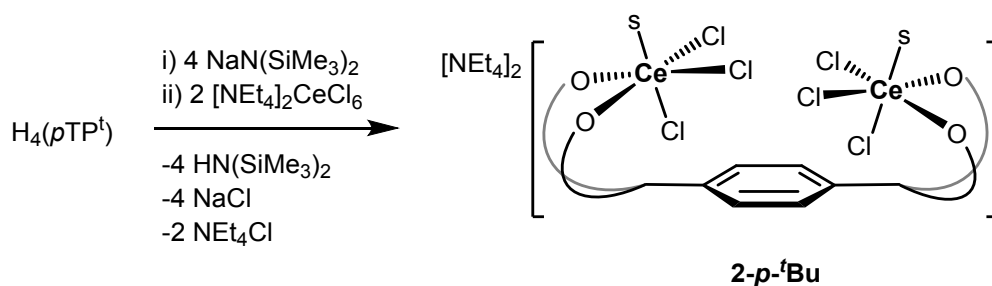


Figure S4: $^{13}C\{^1H\}$ NMR spectrum of $H_4(mTP^{Ad})$ in C $_6$ D $_6$.



S2.3 Synthesis of $[\text{NEt}_4]_2[\text{Ce}_2\text{Cl}_6(\text{pTP}^t)]$



Equation S3: Synthesis of $[\text{NEt}_4]_2[\text{Ce}_2\text{Cl}_6(\text{pTP}^t)]$.

$\text{H}_4(\text{pTP}^t)$ (1.11 g, 1.20 mmol, 1 equiv.) and $\text{NaN}(\text{SiMe}_3)_2$ (0.850 g, 4.90 mmol, 4.1 equiv.) were dissolved in THF (25 mL) and the resulting yellow-brown solution stirred for 2 hours. $[\text{NEt}_4]_2\text{CeCl}_6$ (1.55 g, 2.52 mmol, 2.1 equiv.) was suspended in THF (15 mL) at 0 °C and to this was slowly added the $\text{Na}_4(\text{pTP}^t)$ solution, forming a deep purple solution which was stirred vigorously for 16 hours at room temperature. The mixture was centrifuged then cooled in an ice-bath, filtered *via* cannula whilst cold and the volatiles of the filtrate evaporated under reduced pressure presenting the crude product as a purple solid. This material was dried under reduced pressure then triturated with hexane (3 x 10 mL) before drying again, yielding $[\text{NEt}_4]_2[\text{Ce}_2\text{Cl}_6(\text{pTP}^t)]$ **2-p-tBu** (1.12 g, 56%) as a purple powder.

^1H NMR (500 MHz, pyridine- d_5) δ_{H} 8.14 (d, $J = 2.5$ Hz, 2H Aryloxide A), 8.08 (d, $J = 2.5$ Hz, 2H Aryloxide B), 7.82 (s, 2H, benzyl protons), 7.60 (s, 4H, spacer), 7.48 (d, $J = 2.5$ Hz, 2H, Aryloxide A), 7.16 (d, $J = 2.5$ Hz, 2H Aryloxide B), 3.32 (q, 16H, $(^+\text{N}(\text{CH}_2\text{CH}_3)_4)$), 1.91 (s, 18H, ^tBu), 1.53 (s, 18H, ^tBu), 1.41 (s, 18H, ^tBu), 1.40 (s, 18H, ^tBu), 1.20 (t, 24H, $(^+\text{N}(\text{CH}_2\text{CH}_3)_4)$).

$^{13}\text{C}\{^1\text{H}\}$ NMR (126 MHz, pyridine- d_5) δ_{C} 170.0 (q, ArC-O), 166.5 (q, ArC-O), 143.4 (q, ArC), 139.0 (q, ArC), 138.2 (q, ArC), 137.8 (q, ArC), 134.0 (q, ArC), 133.8 (q, ArC), 130.1 (spacer, ArC-H), 125.6 (Aryloxide B ArC-H), 124.9 (Aryloxide A ArC-H), 119.4 (Aryloxide A ArC-H), 119.1 (Aryloxide B ArC-H), 53.0 ($(^+\text{N}(\text{CH}_2\text{CH}_3)_4)$), 45.1 (benzylic C-

H), 36.2 (q, ^tBu), 36.1 (q, ^tBu), 35.0 (q, ^tBu), 34.8 (q, ^tBu), 33.1 (CH₃, ^tBu), 33.0 (CH₃, ^tBu), 32.5 (CH₃, ^tBu), 32.3 (CH₃, ^tBu), 7.8 (⁺N(CH₂CH₃)₄).

IR: $\nu_{\text{max}}/\text{cm}^{-1}$ 2951m, 1433m, 1252s, 1120, 1010m, 830s, 530s, 432s.

Elemental analysis ([NEt₄]₂[Ce₂Cl₆(*p*TP^t)(THF)₂): C 58.17%, H 7.88%, N 1.54% calculated; C 58.22%, H 7.41%, N 1.94% found.

Figure S5: ¹H NMR spectrum of [NEt₄]₂[Ce₂Cl₆(*p*TP^t)] in C₅D₅N.

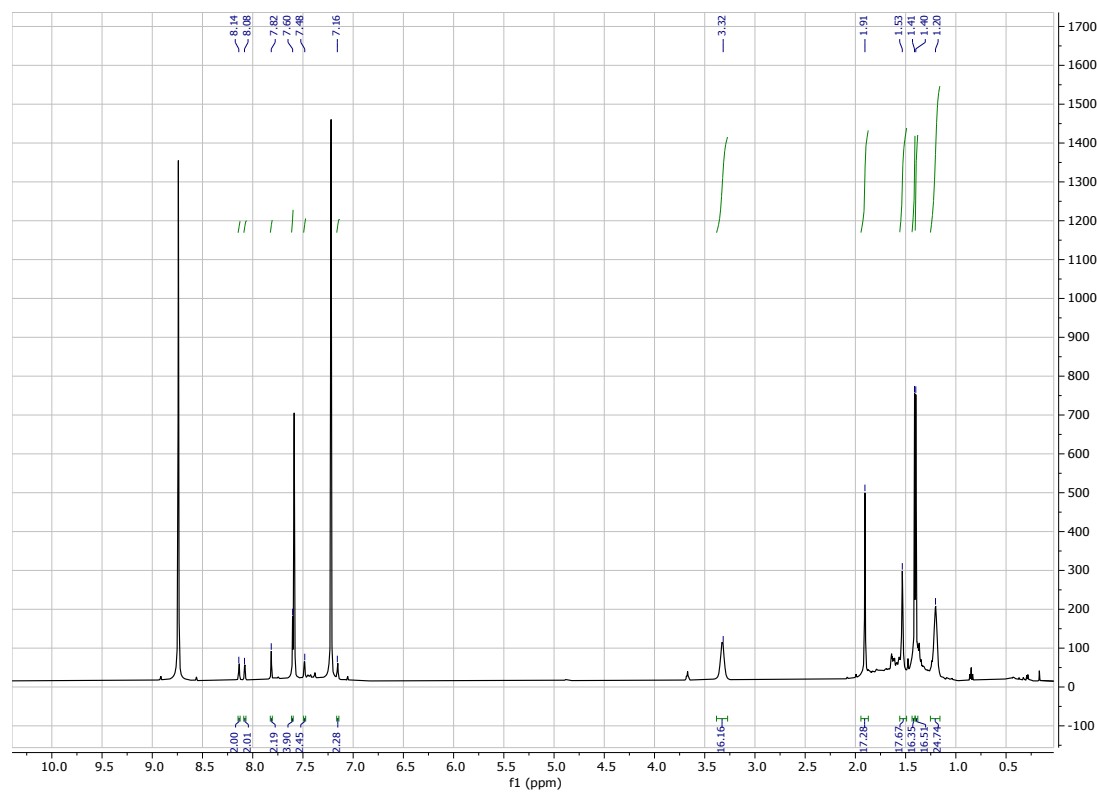
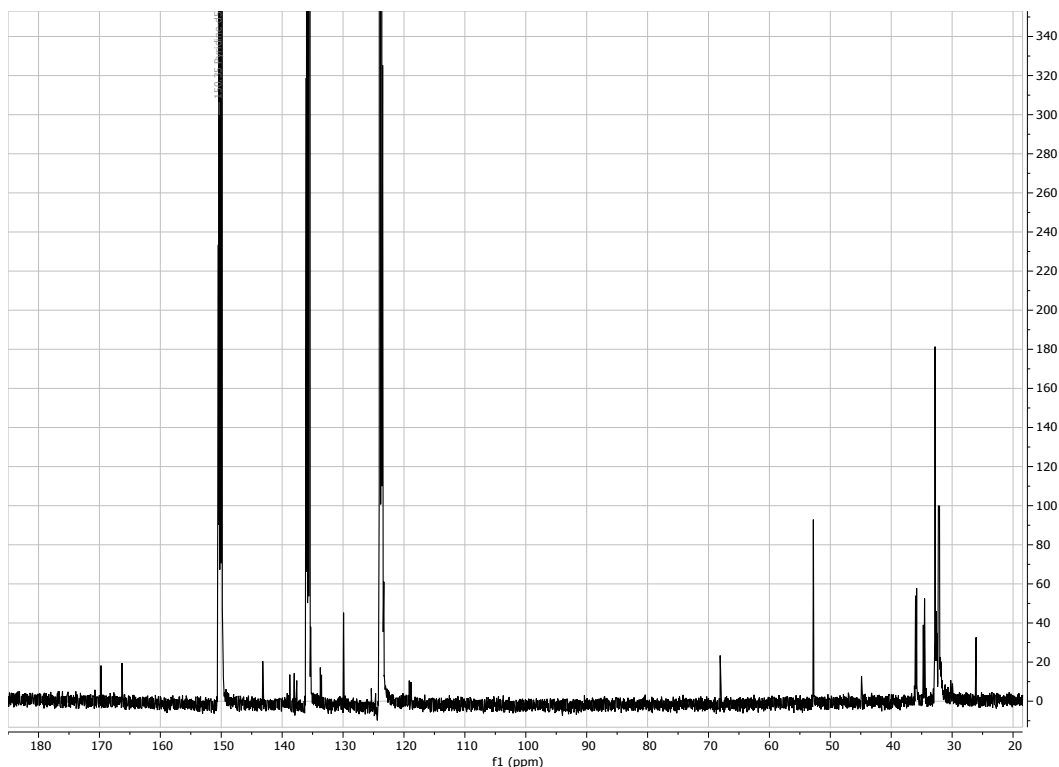
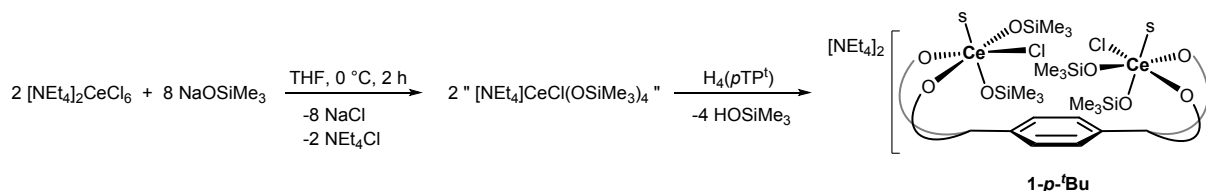


Figure S6: ¹³C{¹H} NMR spectrum of [NEt₄]₂[Ce₂Cl₆(*p*TP^t)] in C₅D₅N.



S2.4 [NEt₄]₂[Ce₂Cl₂(OSiMe₃)₄(pTP^t)]

Method A



Equation S4: Synthesis of [NEt₄]₂[Ce₂Cl₂(OSiMe₃)₂(pTP^t)] by *in situ* formation of a “Ce-siloxide” complex.

[NEt₄]₂CeCl₆ (613 mg, 1 mmol, 2 equiv.) and sodium trimethylsiloxide (449 mg, 4 mmol, 8 equiv.) were combined in a Schlenk flask, cooled in a salt-ice bath, and suspended in THF (15 mL). The yellow suspension was stirred at 0 °C for 2 hours before adding dropwise to a THF solution (15 mL) of H₄(pTP^t) (462 mg, 0.5 mmol, 1 equiv.) over a period of 20 minutes. An initial green colour was observed which afterwards turned red-brown once the addition was completed. The reaction was stirred for a further 16 hours and the now purple mixture was centrifuged, filtered *via* cannula and the solids extracted with toluene (2 x 10 mL). The filtrates were combined, volatiles were removed under reduced pressure giving the crude product, which was recrystallised from hot toluene yielding [NEt₄]₂[Ce₂Cl₂(OSiMe₃)₄(pTP^t)] **1-*p*-^tBu** as a purple solid (740 mg, 72%).

¹H NMR (500 MHz, pyridine-*d*₅) δ_H 7.64 (s, 4H), 7.63 (d, J = 2.4 Hz, 4H), 7.34 (d, J = 2.4 Hz, 4H), 6.96 (s, 1H, benzylic C-H), 6.88 (s, 1H, benzylic C-H), 3.21 (q, 16H, (⁺N(CH₂CH₃)₄)), 1.94 (s, 36H, ^tBu), 1.40 (s, 36H, ^tBu), 1.17 (t, 24H, (⁺N(CH₂CH₃)₄)), 0.43 (s, 36H, OSiMe₃).

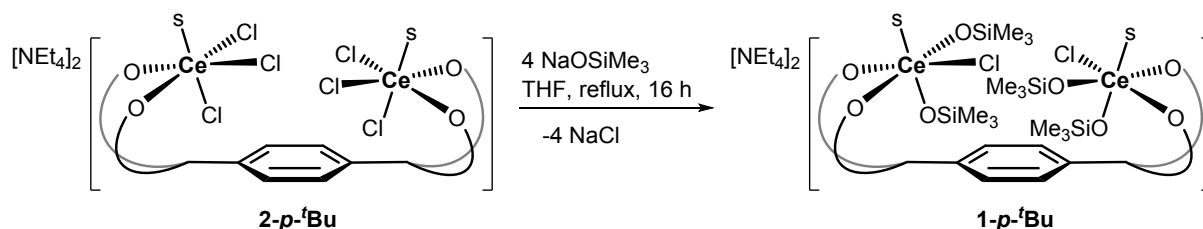
¹³C DEPTQ NMR (126 MHz, pyridine-*d*₅) δ_C 167.4 (q, ArC-O), 144.8 (q, ArC), 138.5 (q, ArC), 138.4 (q, ArC), 135.4 (q, ArC), 129.2 (spacer, ArC-H), 125.2 (ArC-H), 119.9 (ArC-H), 53.2 (⁺N(CH₂CH₃)₄), 36.5 (q, ^tBu), 35.0 (q, ^tBu), 33.2 (CH₃, ^tBu), 32.7 (CH₃, ^tBu), 8.0 (⁺N(CH₂CH₃)₄), 5.4 (CH₃, OSiMe₃).

^{29}Si NMR (99 MHz, pyridine- d_5) δ_{Si} 7.47

Elemental analysis ($[\text{NEt}_4]_2[\text{Ce}_2\text{Cl}_2(\text{OSiMe}_3)_4(\rho\text{TP}^t)(\text{THF})_2]$): C 59.11%, H 8.83%, N 1.38% calculated; C 58.73%, H 8.81%, N 1.41% found.

IR: $\nu_{\text{max}}/\text{cm}^{-1}$ 2952w, 1434w, 1251m, 1239m, 981w, 897s, 832s, 744m.

Method B



Equation S5: Synthesis of $[\text{NEt}_4]_2[\text{Ce}_2\text{Cl}_2(\text{OSiMe}_3)_2(\rho\text{TP}^t)]$ from **2-*p*-^tBu**.

To a purple THF solution (20 mL) of $[\text{NEt}_4]_2[\text{Ce}_2\text{Cl}_6(\rho\text{TP}^t)]$ (1.00 g, 0.61 mmol, 1 equiv.) was added, with stirring, a clear THF solution (20 mL) of sodium trimethylsilyoxide (273 mg, 2.44 mmol, 4 equiv.). The resulting purple solution was heated under reflux for 16 hours before allowing to cool to room temperature, centrifuged, filtered *via* cannula and the solids extracted with toluene (2 x 10 mL). The filtrates were combined, volatiles were removed under reduced pressure giving the crude product, which was recrystallised from hot toluene yielding $[\text{NEt}_4]_2[\text{Ce}_2\text{Cl}_2(\text{OSiMe}_3)_4(\rho\text{TP}^t)]$ **1-*p*-^tBu** as a purple solid (790 mg, 69%).

Figure S7: ^1H NMR spectrum of $[\text{NEt}_4]_2[\text{Ce}_2\text{Cl}_2(\text{OSiMe}_3)_4(\rho\text{TP}^t)]$ in $\text{C}_5\text{D}_5\text{N}$.

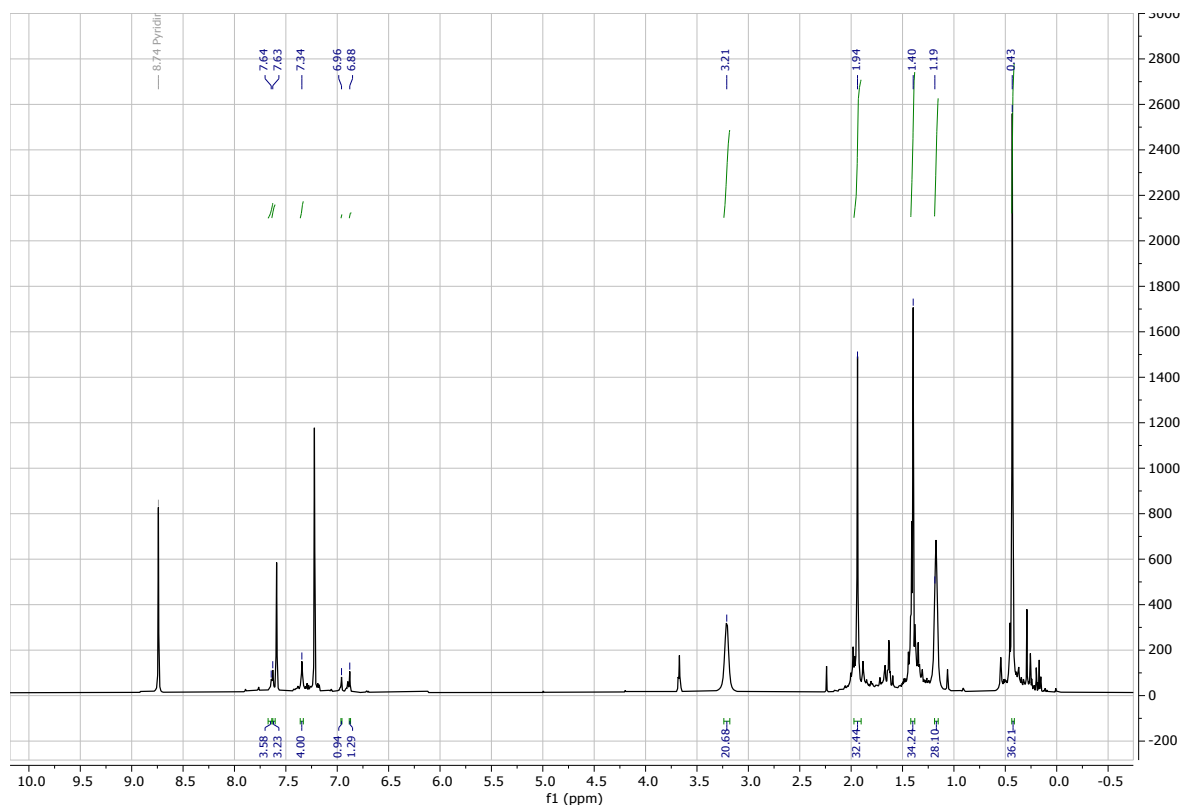
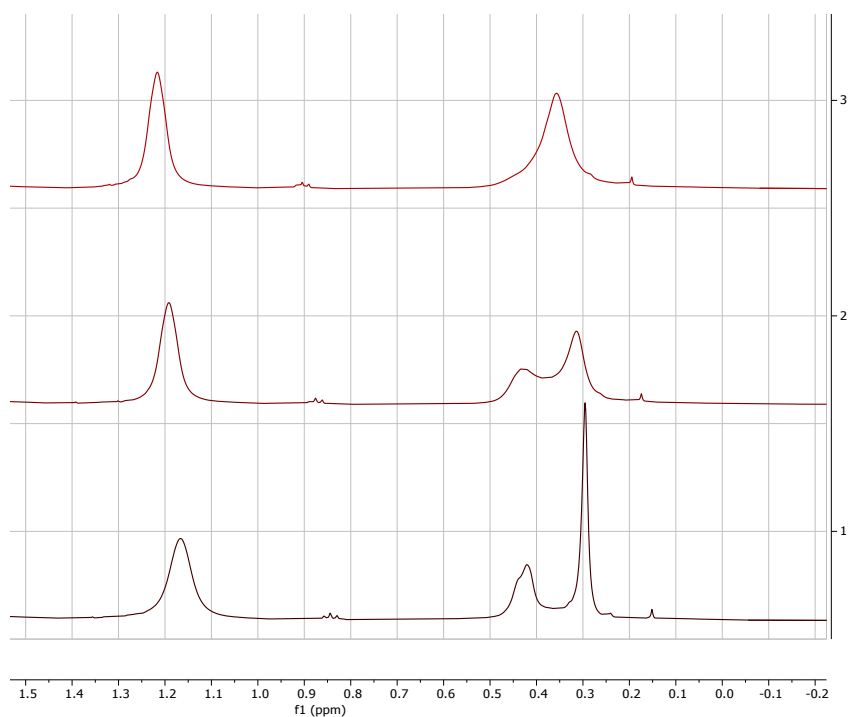


Figure S8: Section of variable temperature ^1H NMR spectra of $[\text{NEt}_4]_2[\text{Ce}_2\text{Cl}_2(\text{OSiMe}_3)_4(\rho\text{TP}^t)]$ in $\text{C}_5\text{D}_5\text{N}$.



The top spectrum is at 340 K and shows a coalescence of both $-\text{OSiMe}_3$ signals into one, indicating that upon even mild heating, there is sufficient energy for free rotation between the two conformers.

The middle spectrum is at 320 K.

The bottom spectrum is at 300 K and shows two signals for the $-\text{OSiMe}_3$ ligands, at 0.4 and 0.3 ppm – one each for the *anti* and *syn* conformers.

^1H - ^1H NOESY spectrum of $[\text{NEt}_4]_2[\text{Ce}_2\text{Cl}_2(\text{OSiMe}_3)_4(\rho\text{TP}^t)]$ in $\text{C}_5\text{D}_5\text{N}$. No cross-peaks are observable that correspond to siloxide ligands in close proximity.

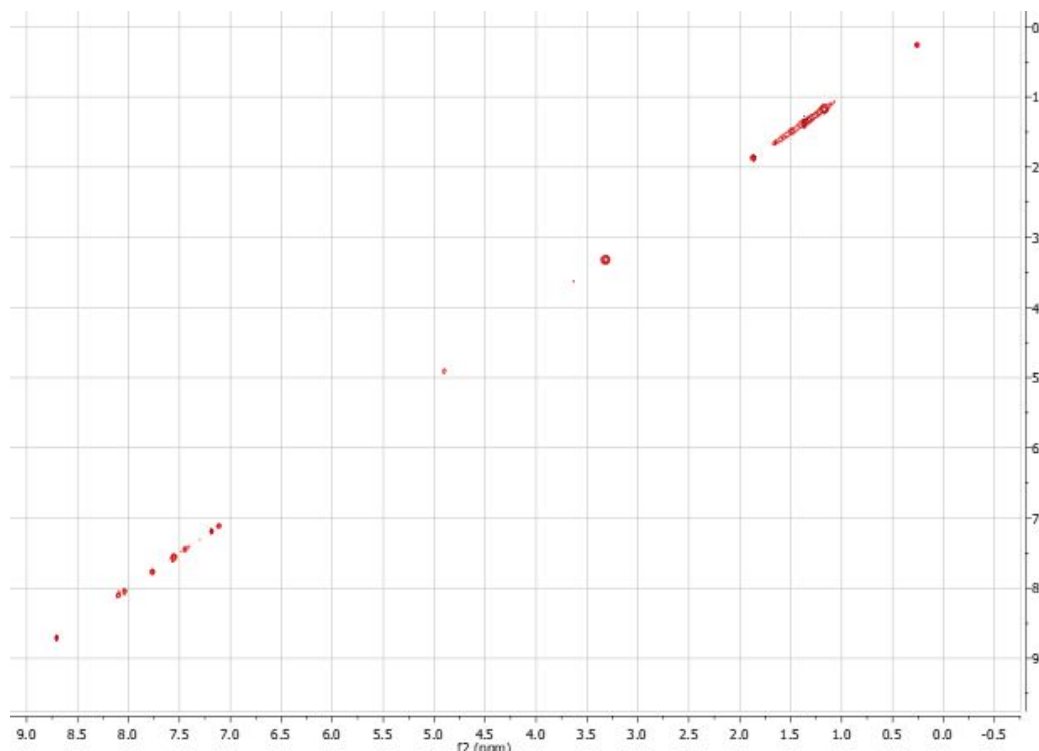
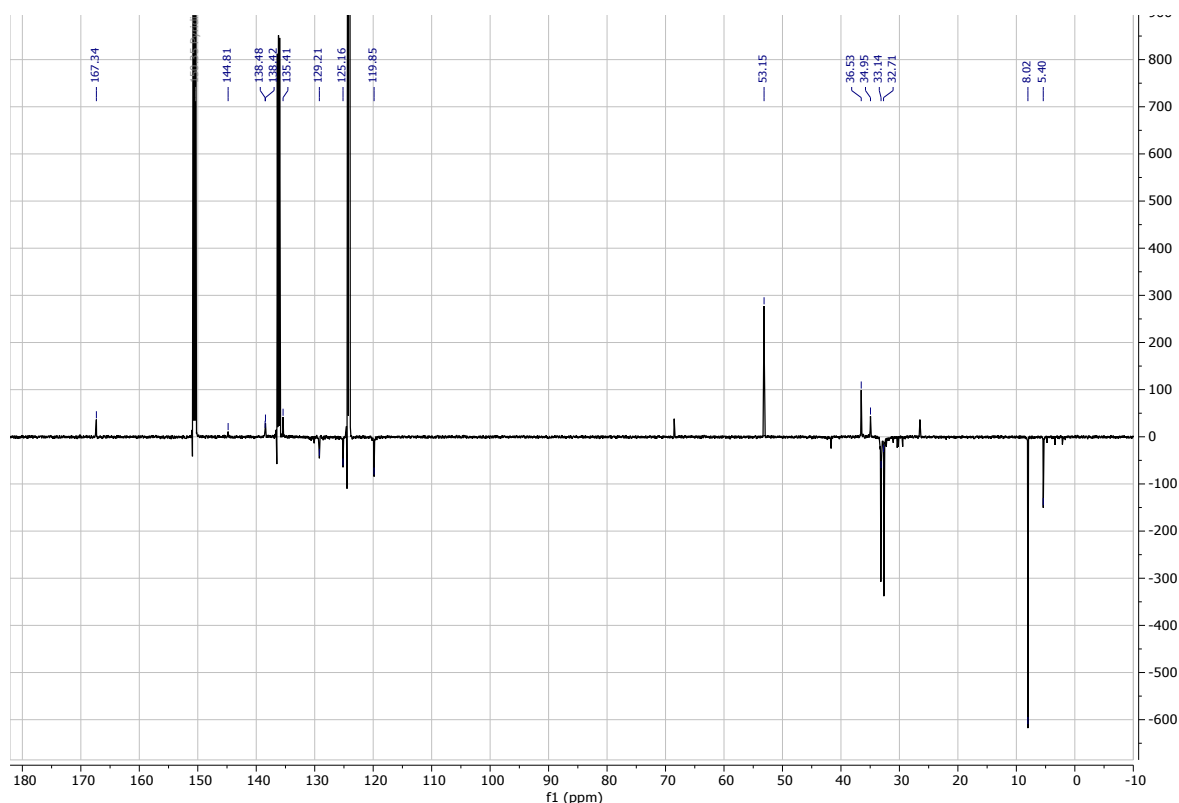
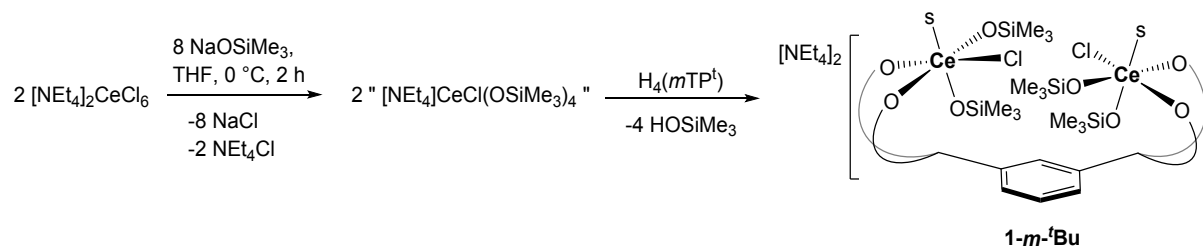


Figure S9: ^{13}C DEPTQ NMR spectrum of $[\text{NEt}_4]_2[\text{Ce}_2\text{Cl}_2(\text{OSiMe}_3)_4(p\text{TP}^t)]$ in $\text{C}_5\text{D}_5\text{N}$.



S2.5 $[\text{NEt}_4]_2[\text{Ce}_2\text{Cl}_2(\text{OSiMe}_3)_4(m\text{TP}^t)]$



Equation S6: Synthesis of $[\text{NEt}_4]_2[\text{Ce}_2\text{Cl}_2(\text{OSiMe}_3)_4(m\text{TP}^t)]$.

By analogous procedure to S2.4A.

$[\text{NEt}_4]_2\text{CeCl}_6$ (681 mg, 1.11 mmol, 2 equiv.) and sodium trimethylsiloxide (498 mg, 4.44 mmol, 8 equiv.) were combined in a Schlenk flask, cooled in a salt-ice bath, and suspended in THF (15 mL). The yellow suspension was stirred at 0°C for 2 hours before adding dropwise to a THF solution (15 mL) of $\text{H}_4(m\text{TP}^t)$ (513 mg, 0.55 mmol, 1 equiv.). An initial green colour was observed which afterwards turned red-brown once the addition was completed. The reaction was stirred for a further 16 hours and worked up in an identical manner to S2.4A. The purple solid $[\text{NEt}_4]_2[\text{Ce}_2\text{Cl}_2(\text{OSiMe}_3)_4(m\text{TP}^t)]$ **1-m^tBu** was obtained (735 mg, 71%).

^1H NMR (500 MHz, pyridine- d_5) δ_{H} 7.56 (m, 1H), 7.53 (m, 1H), 7.43 (m, 1H), 7.40 (m, 1H), 7.35 (m, 4H), 7.31 (m, 4H), 6.94 (s, 2H, benzylic C-H), 3.33 (q, 16H, $^+\text{N}(\text{CH}_2\text{CH}_3)_4$), 2.02 (br s, 36H, ^tBu), 1.36 (s, 36H, ^tBu), 1.23 (t, 24H, $^+\text{N}(\text{CH}_2\text{CH}_3)_4$), 0.45 (br s, 36H, OSiMe₃).

^{13}C DEPTQ NMR (126 MHz, pyridine- d_5) δ_{C} 166.6 (q, ArC-O), 147.0 (q, ArC), 146.6 (q, ArC), 134.9 (q, ArC), 134.8 (q, ArC), 119.7 (ArC-H), 119.5 (ArC-H), 52.8 ($^+\text{N}(\text{CH}_2\text{CH}_3)_4$), 36.2 (q, ^tBu), 36.0 (q, ^tBu), 33.0 (CH₃, ^tBu), 32.9 (CH₃, ^tBu), 32.4 (CH₃, ^tBu), 31.9 (CH₃, ^tBu), 7.6 ($^+\text{N}(\text{CH}_2\text{CH}_3)_4$), 3.0 (CH₃, OSiMe₃).

^{29}Si NMR (99 MHz, pyridine- d_5) δ_{Si} 1.40.

Elemental analysis ($[\text{NEt}_4]_2[\text{Ce}_2\text{Cl}_2(\text{OSiMe}_3)_4(m\text{TP}^t)(\text{THF})_2]$): C 59.11%, H 8.83%, N 1.38% calculated; C 59.58%, H 8.62%, N 1.53% found.

IR: $\nu_{\text{max}}/\text{cm}^{-1}$ 2952w, 1595w, 1435w, 1255m, 972w, 891m, 832s, 744m.

Figure S10: ^1H NMR spectrum of $[\text{NEt}_4]_2[\text{Ce}_2\text{Cl}_2(\text{OSiMe}_3)_4(m\text{TP}^t)]$ in $\text{C}_5\text{D}_5\text{N}$.

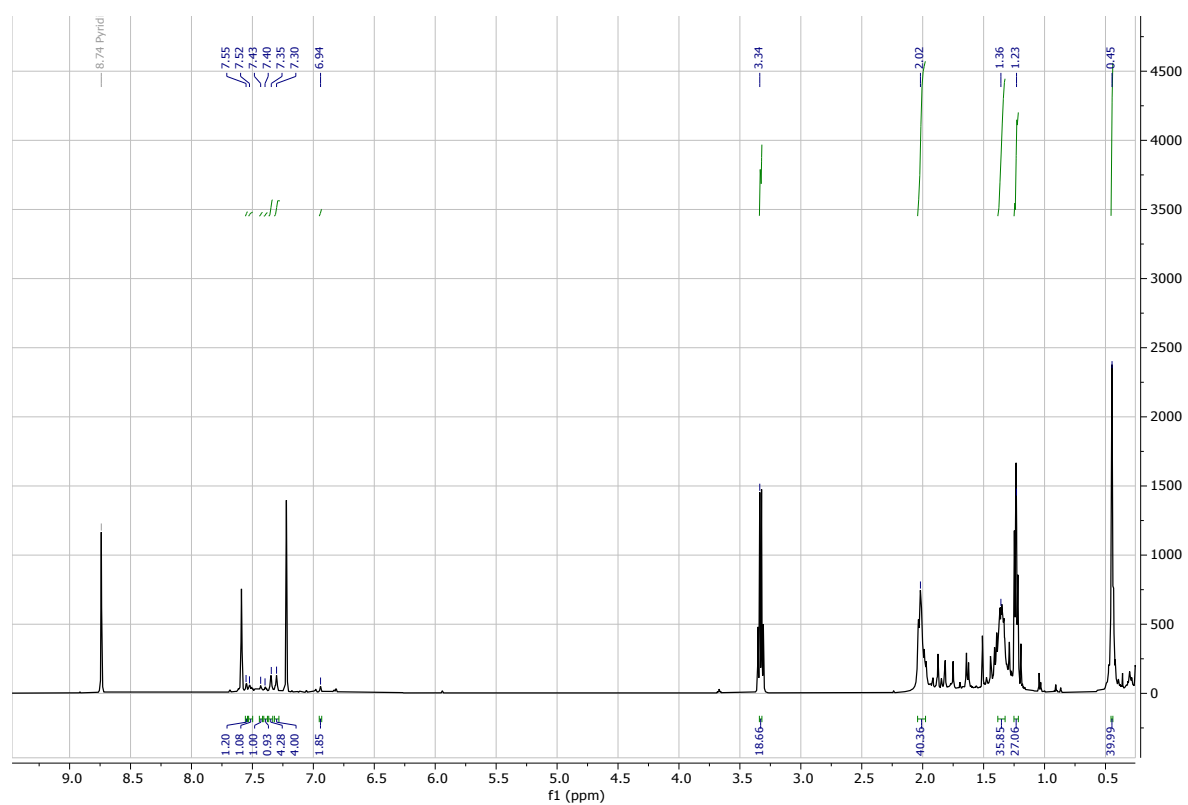
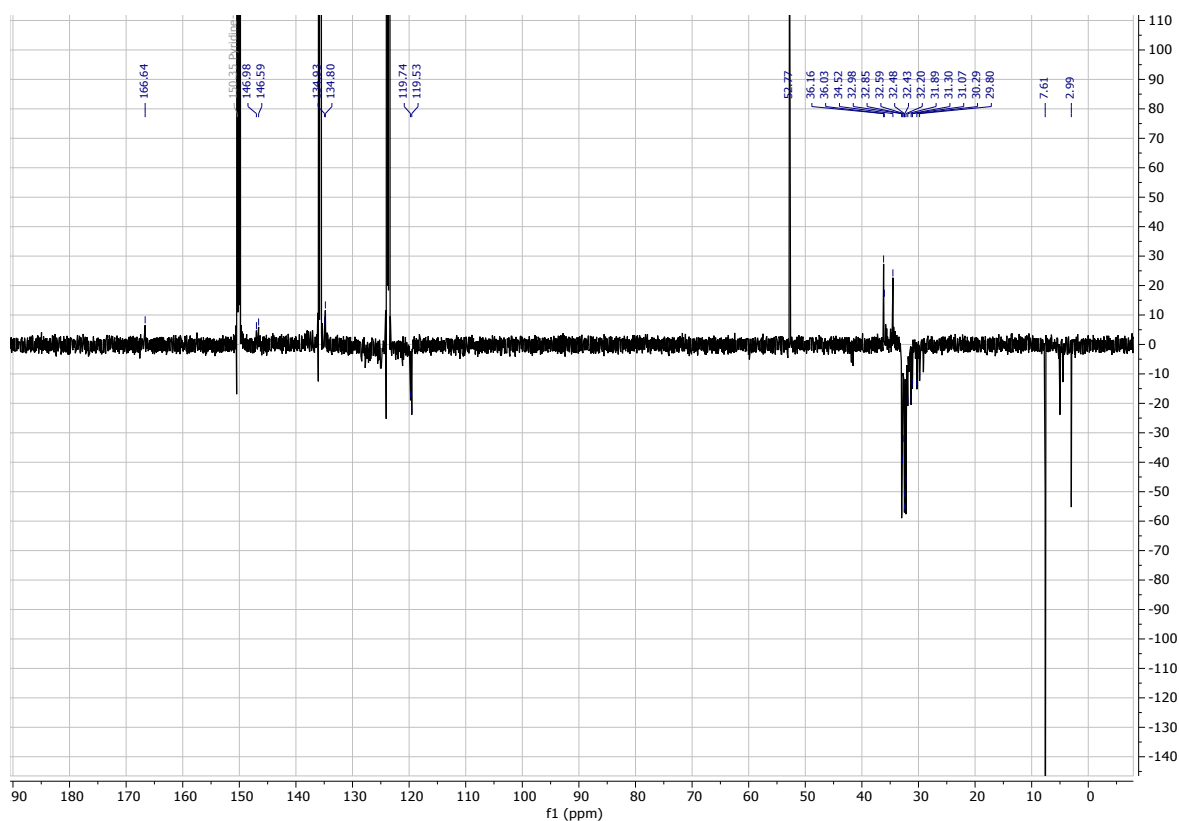
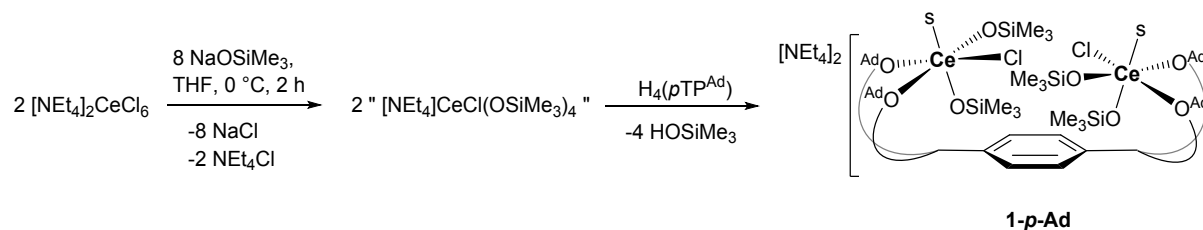


Figure S11: ^{13}C DEPTQ NMR spectrum of $[\text{NEt}_4]_2[\text{Ce}_2\text{Cl}_2(\text{OSiMe}_3)_4(m\text{TP}^t)]$ in $\text{C}_5\text{D}_5\text{N}$.



S2.6 $[\text{NEt}_4]_2[\text{Ce}_2\text{Cl}_2(\text{OSiMe}_3)_4(p\text{TP}^{\text{Ad}})]$



Equation S7: Synthesis of $[\text{NEt}_4]_2[\text{Ce}_2\text{Cl}_2(\text{OSiMe}_3)_4(p\text{TP}^{\text{Ad}})]$.

By analogous procedure to S2.4A.

$[\text{NEt}_4]_2\text{CeCl}_6$ (515 mg, 0.840 mmol, 2 equiv.) and sodium trimethylsiloxide (377 mg, 3.36 mmol, 8 equiv.) were combined in a Schlenk flask, cooled in a salt-ice bath, and suspended in THF (15 mL). The yellow suspension was stirred at 0°C for 2 hours before adding dropwise to a THF solution (15 mL) of $\text{H}_4(p\text{TP}^{\text{Ad}})$ (623 mg, 0.42 mmol, 1 equiv.). An initial green colour was observed which afterwards turned red-brown once the addition was completed. The reaction was stirred for a further 16 hours and worked up in an identical manner to S2.4A. The purple solid $[\text{NEt}_4]_2[\text{Ce}_2\text{Cl}_2(\text{OSiMe}_3)_4(p\text{TP}^{\text{Ad}})]$ **1-p-Ad** was obtained (592 mg, 60%).

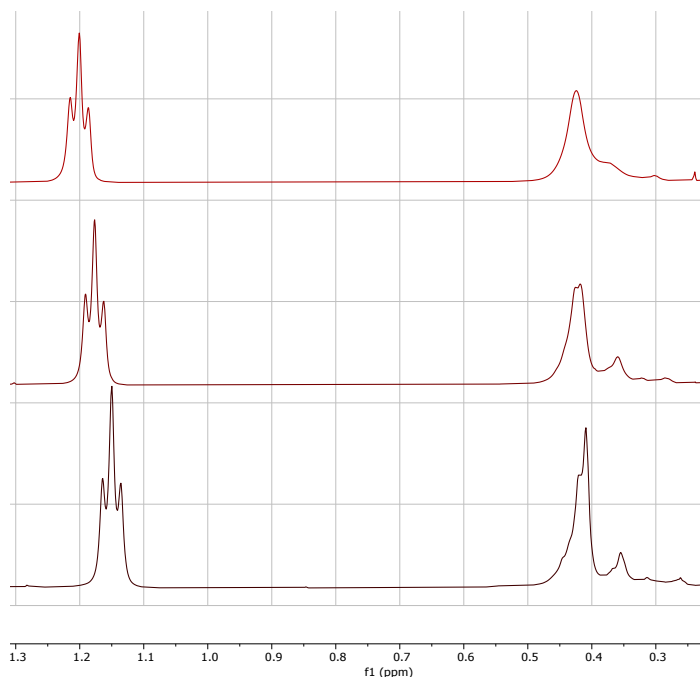
^1H NMR (500 MHz, pyridine- d_5) δ_{H} 7.21 (s, 4H, Ar-H), 7.18-7.13 (m, 4H, Ar-H), 7.02-6.96 (m, 4H, Ar-H), 6.71 (s, 1H, benzylic C-H), 6.40 (s, 1H, benzylic C-H), 3.02 (q, 16H, ($^+\text{N}(\text{CH}_2\text{CH}_3)_4$)), 2.74-2.66 (m, 18H, $-\text{CH}_2$), 2.44 (s, 18H), 2.35 (s, 6H), 2.28-2.20 (m, 6H, $-\text{CH}_2$), 2.10 (s, 6H), 1.96-1.76 (m, 18H), 1.15 (t, 24H, ($^+\text{N}(\text{CH}_2\text{CH}_3)_4$)), 0.40 (s, 36H, OSiMe $_3$).

^{13}C DEPTQ NMR (126 MHz, pyridine- d_5) δ_c 155.9 (q, ArC-O), 138.6 (q, ArC), 137.2 (q, ArC), 129.9 (ArC-H), 129.1 (ArC-H), 128.3 (ArC-H), 127.9 (ArC-H), 126.2 (ArC-H) 53.0 ($^+N(\underline{\text{C}}\text{H}_2\text{C}\text{H}_3)_4$), 42.2, 41.5, 41.3 ($-\text{C}\text{H}_2$), 38.5, 38.3, 37.90 ($-\text{C}\text{H}_2$), 30.5, 30.4, 30.0 ($-\text{C}\text{H}_3$), 7.9 ($^+N(\underline{\text{C}}\text{H}_2\text{C}\text{H}_3)_4$).

^{29}Si NMR (99 MHz, pyridine- d_5) δ_{Si} 10.48

Elemental analysis ($[\text{NEt}_4]_2[\text{Ce}_2\text{Cl}_2(\text{OSiMe}_3)_4(\rho\text{TP}^{\text{Ad}})(\text{THF})_2]$): C 61.82%, H 8.25%, N 1.29% calculated; C 61.37%, H 7.95%, N 1.28% found.

Figure S12: Section of variable temperature ^1H NMR spectra of $[\text{NEt}_4]_2[\text{Ce}_2(\text{OSiMe}_3)_6(\rho\text{TP}^{\text{Ad}})]$ in $\text{C}_5\text{D}_5\text{N}$.



The top spectrum is at 340 K and shows a coalescence of both – OSiMe₃ signals into one, indicating that upon even mild heating, there is sufficient energy for free rotation between the two conformers.

The middle spectrum is at 320 K.

The bottom spectrum is at 300 K and shows two signals for the – OSiMe₃ ligands, at 0.43 and 0.35 ppm – one each for the *anti* and *syn* conformers.

Figure S13: ^1H NMR spectrum of $[\text{NEt}_4]_2[\text{Ce}_2\text{Cl}_2(\text{OSiMe}_3)_4(\rho\text{TP}^{\text{Ad}})]$ in $\text{C}_5\text{D}_5\text{N}$.

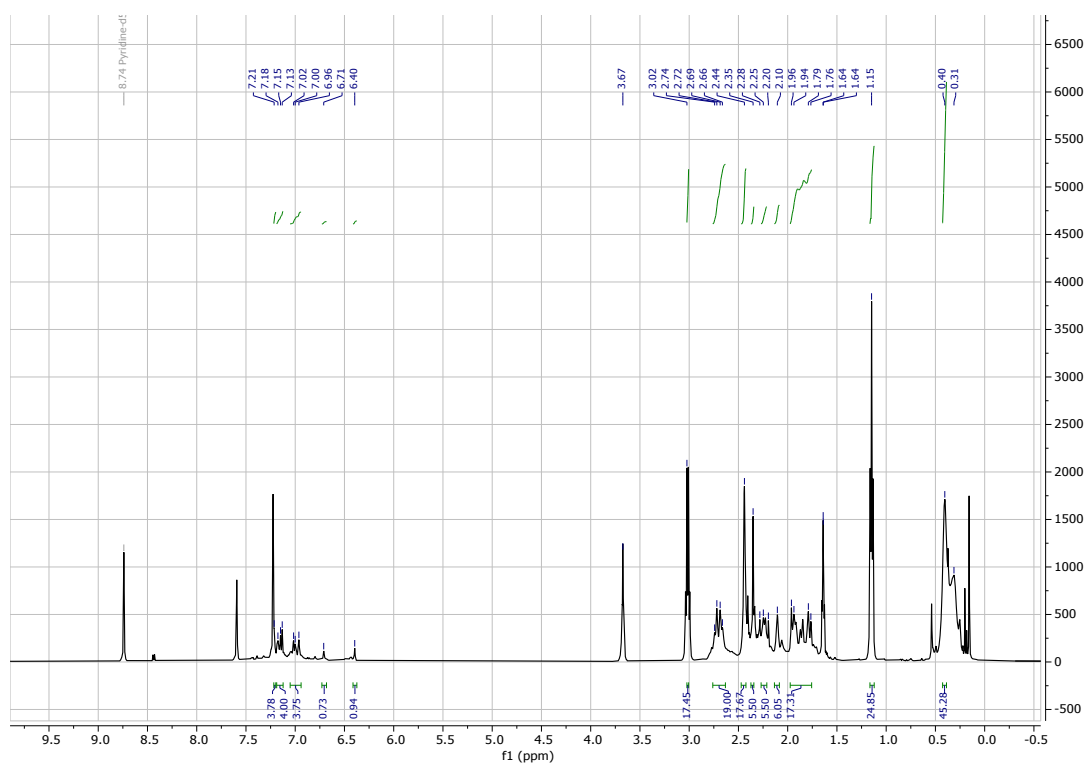
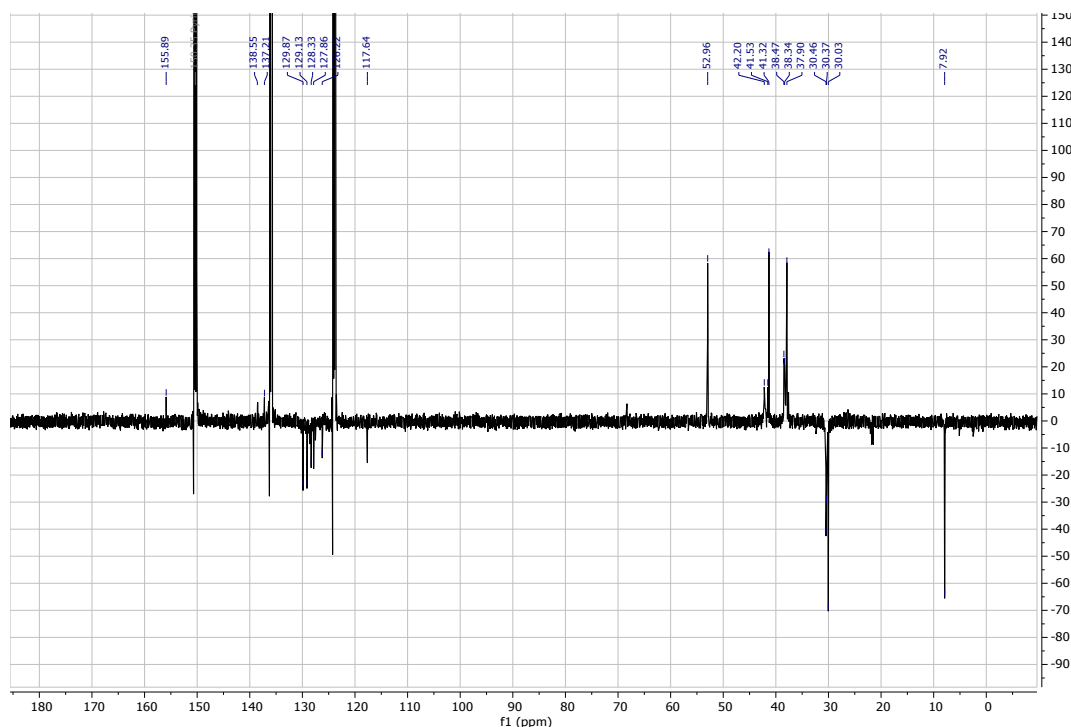
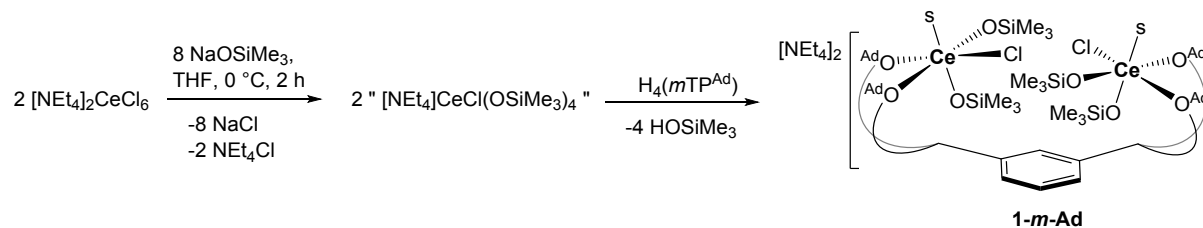


Figure S14: ^{13}C DEPTQ NMR spectrum of $[\text{NEt}_4]_2[\text{Ce}_2\text{Cl}_2(\text{OSiMe}_3)_4(\text{pTP}^{\text{Ad}})]$ in $\text{C}_5\text{D}_5\text{N}$.



S2.7 $[\text{NEt}_4]_2[\text{Ce}_2\text{Cl}_2(\text{OSiMe}_3)_4(\text{mTP}^{\text{Ad}})]$



Equation S8: Synthesis of $[\text{NEt}_4]_2[\text{Ce}_2\text{Cl}_2(\text{OSiMe}_3)_4(\text{mTP}^{\text{Ad}})]$.

By analogous procedure to S2.4A.

$[\text{NEt}_4]_2\text{CeCl}_6$ (515 mg, 0.840 mmol, 2 equiv.) and sodium trimethylsiloxide (377 mg, 3.36 mmol, 8 equiv.) were combined in a Schlenk flask, cooled in a salt-ice bath, and suspended in THF (15 mL). The yellow suspension was stirred at 0°C for 2 hours before adding dropwise to a THF solution (15 mL) of $\text{H}_4(\text{mTP}^{\text{Ad}})$ (623 mg, 0.42 mmol, 1 equiv.). An initial green colour was observed which afterwards turned red-brown once the addition was completed. The reaction was stirred for a further 16 hours and worked up in an identical manner to S2.4A. The purple solid $[\text{NEt}_4]_2[\text{Ce}_2\text{Cl}_2(\text{OSiMe}_3)_4(\text{mTP}^{\text{Ad}})]$ **1-m-Ad** was obtained (648 mg, 65%).

^1H NMR (500 MHz, pyridine- d_5) δ_{H} 7.31-7.28 (m, 2H, Ar-H), 7.20-7.17 (m, 2H, Ar-H), 7.13-7.11 (m, 2H, Ar-H), 7.09-7.06 (m, 2H, Ar-H), 7.02-6.98 (m, 2H, Ar-H), 6.90 (s, 2H, Ar-H), 3.00 (m, 16H, ($^+\text{N}(\text{CH}_2\text{CH}_3)_4$), 2.72-2.67 (m, 12H), 2.44 (m, 12H), 2.37-2.33 (m, 12H), 2.30-2.24 (m, 12H), 1.94-1.70 (m, 24H), 1.14 (m, 24H, ($^+\text{N}(\text{CH}_2\text{CH}_3)_4$), 0.42 (s, 36H, OSiMe₃).

^{13}C DEPTQ NMR (126 MHz, pyridine- d_5) δ_{C} 155.9 (q, ArC-O), 129.9 (ArC-H), 129.1 (ArC-H), 128.3 (ArC-H), 127.9 (ArC-H), 126.2 (ArC-H), 117.7 (ArC-H), 53.0 ($^+\text{N}(\underline{\text{C}}\text{H}_2\text{CH}_3)_4$), 42.2, 41.5, 41.3 (-CH₂), 38.3, 38.1, 37.90 (-CH₂), 30.5, 30.0 (-CH₃), 29.8, 8.0 ($^+\text{N}(\text{CH}_2\underline{\text{C}}\text{H}_3)_4$), 2.49 (CH₃, OSiMe₃).

^{29}Si NMR (99 MHz, pyridine- d_5) δ_{Si} -7.59

Elemental analysis ([NEt₄]₂[Ce₂Cl₂(OSiMe₃)₄(*m*TP^{Ad})(THF)₂]): C 61.82%, H 8.25%, N 1.29% calculated; C 62.21%, H 8.92%, N 1.16% found.

Figure S15: ^1H NMR spectrum of [NEt₄]₂[Ce₂Cl₂(OSiMe₃)₄(*m*TP^{Ad})] in C₅D₅N.

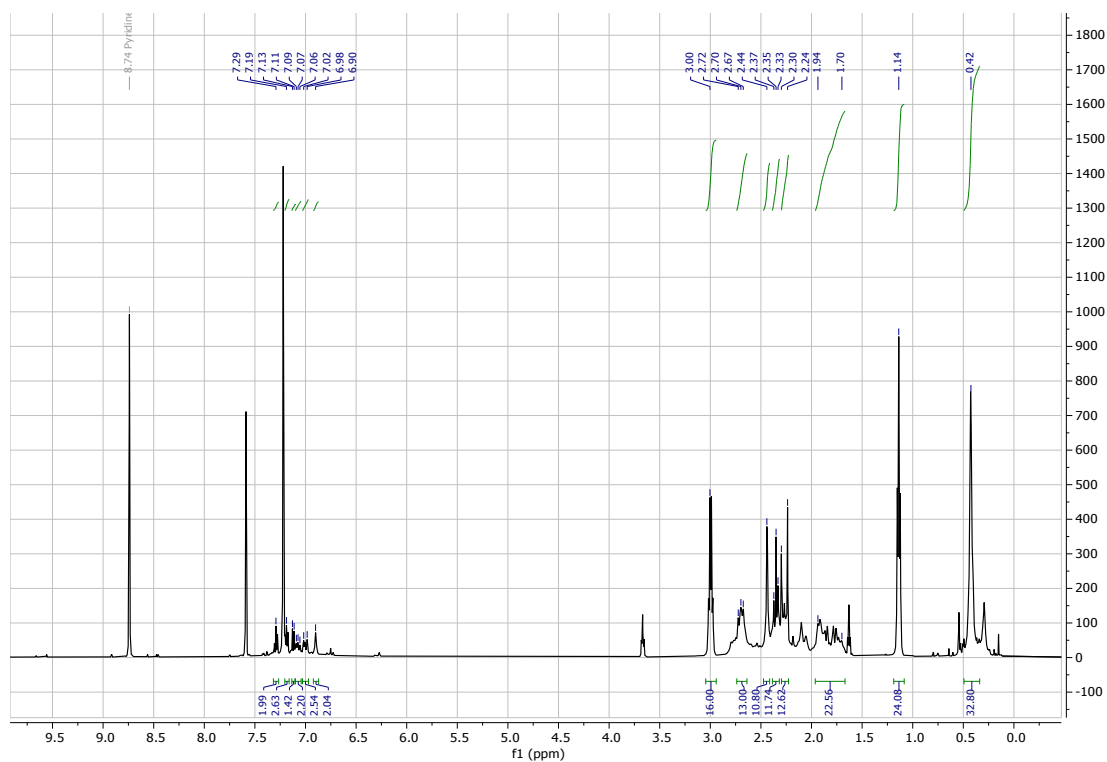
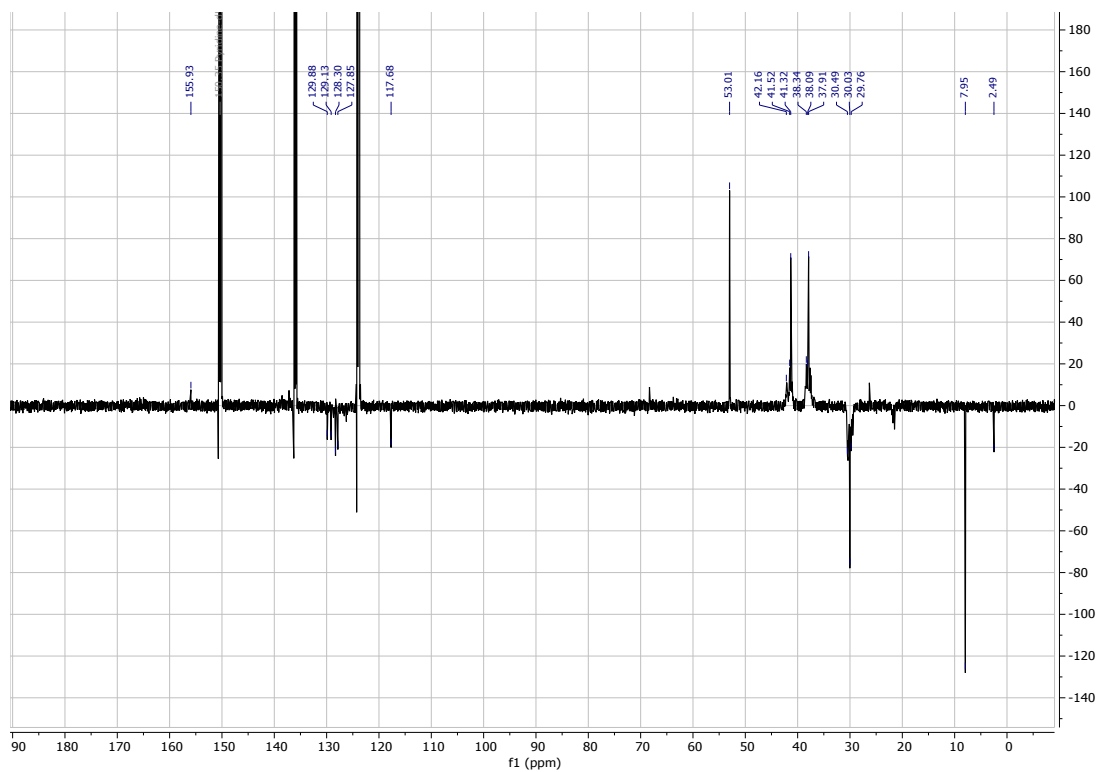
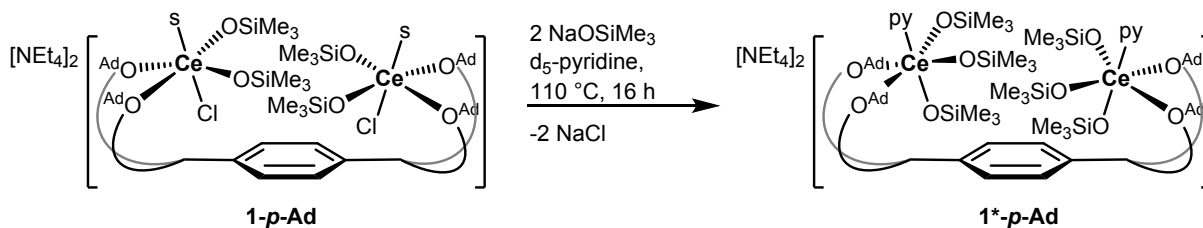


Figure S16: ^{13}C DEPTQ NMR spectrum of $[\text{NEt}_4]_2[\text{Ce}_2\text{Cl}_2(\text{OSiMe}_3)_4(\text{pTP}^{\text{Ad}})]$ in $\text{C}_5\text{D}_5\text{N}$.



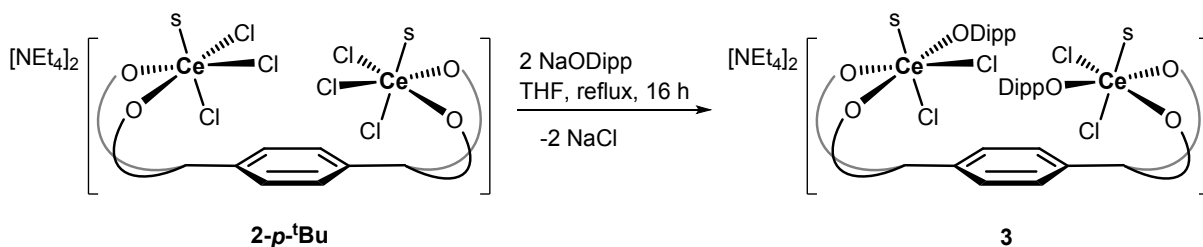
S2.8 $[\text{NEt}_4]_2[\text{Ce}_2(\text{OSiMe}_3)_6(\text{pTP}^{\text{Ad}})]$



Equation S9: Synthesis of $[\text{NEt}_4]_2[\text{Ce}_2(\text{OSiMe}_3)_6(\text{pTP}^t)]$ from **2-p-tBu**.

A. J. Young's tap NMR tube was charged with a d_5 -pyridine solution (0.6 mL) of **1-p-Ad** (25 mg, 0.01 mmol, 1 equiv.) and sodium trimethylsiloxide (2.0 mg, 0.02 mmol, 2 equiv.). Once sealed, the solution was heated at 110 °C for 16 hours. No change was observed in the ^1H NMR spectrum, however a few dark crystals grew from the concentrated solution, identified by X-ray crystallography as **1*-p-Ad**.

S2.9 $[\text{NEt}_4]_2[\text{Ce}_2\text{Cl}_4(\text{ODipp})_2(\text{pTP}^t)]$



Equation S10: Synthesis of $[\text{NEt}_4]_2[\text{Ce}_2\text{Cl}_4(\text{ODipp})_2(\text{pTP}^t)]$.

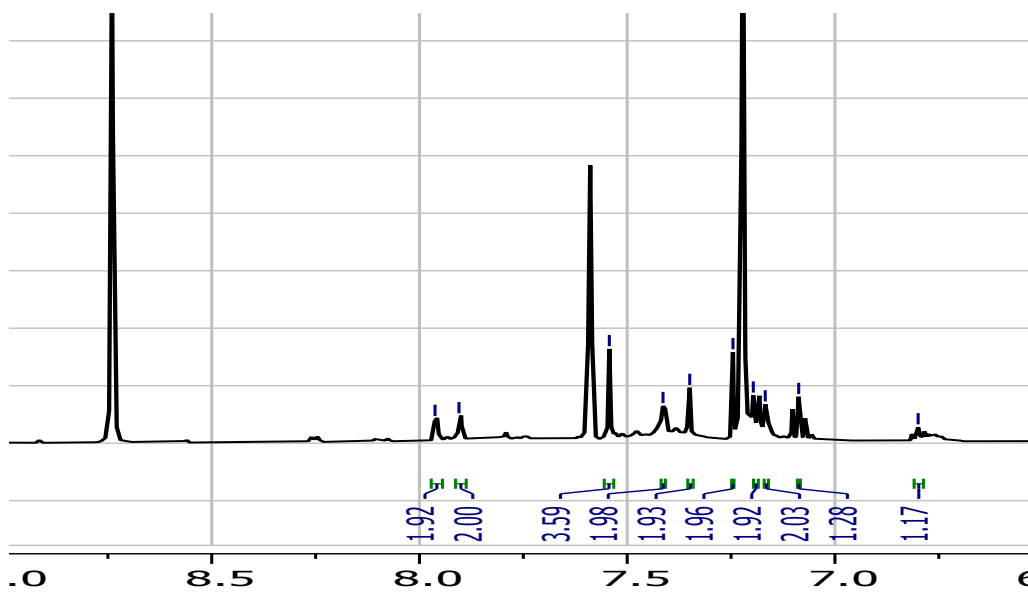
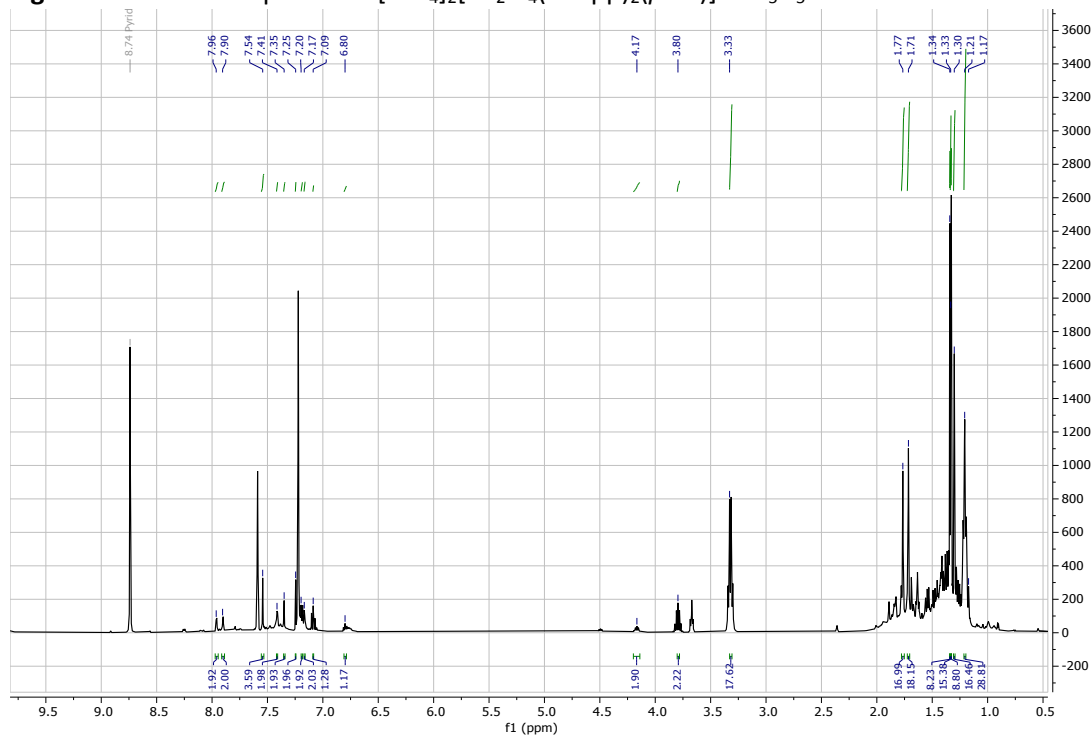
To a purple THF solution (20 mL) of $[\text{NEt}_4]_2[\text{Ce}_2\text{Cl}_6(\text{pTP}^t)]$ (1.00 g, 0.61 mmol, 1 equiv.) was added, with stirring, a clear THF solution (20 mL) of sodium 2,6-diisopropylphenoxide (243 mg, 1.22 mmol, 2 equiv.). The resulting purple solution was heated under reflux for 16 hours before allowing to cool to room temperature, centrifuged, filtered *via* cannula and the solids extracted with THF (2 x 10 mL). The filtrates were combined, solvent was evaporated under reduced pressure and the crude product dried yielding $[\text{NEt}_4]_2[\text{Ce}_2\text{Cl}_4(\text{ODipp})_2(\text{pTP}^t)]$ **3** (910 mg, 76%) as a purple solid.

^1H NMR (500 MHz, pyridine- d_5) δ_{H} 7.96 (d, $J = 2.5$ Hz, 2H), 7.90 (d, $J = 2.5$ Hz, 2H), 7.54 (s, 4H, spacer), 7.41 (d, $J = 2.5$ Hz, 2H), 7.35 (s, 2H, benzylic C-H), 7.27 (d, $J = 7.7$ Hz, 2H, Dipp), 7.19 (d, $J = 7.7$ Hz, 2H, Dipp), 7.17 (d, $J = 2.5$ Hz, 2H), 6.87 (t, $J = 7.7$ Hz, 1H, Dipp), 6.80 (t, $J = 7.7$ Hz, 1H, Dipp), 4.17 (sept, $J = 6.6$ Hz, 2H, Dipp), 3.80 (sept, $J = 6.6$ Hz, 2H, Dipp), 3.33 (q, 16H, $^+\text{N}(\text{CH}_2\text{CH}_3)_4$), 1.76 (s, 18H, ^tBu), 1.71 (s, 18H, ^tBu), 1.34 (d, $J = 6.6$ Hz, 12H, Dipp), 1.33 (s, 18H, ^tBu), 1.30 (s, 18H, ^tBu), 1.23 (t, 24H, $^+\text{N}(\text{CH}_2\text{CH}_3)_4$).

^{13}C DEPTQ NMR (126 MHz, pyridine- d_5) δ_{C} 169.4 (q, ArC-O), 168.9 (q, ArC-O), 167.8 (q, ArC-O), 165.7 (q, ArC-O), 152.8 (q, ArC), 143.7 (q, ArC), 143.1 (q, ArC), 139.9 (q, ArC), 139.2 (q, ArC), 138.4 (q, ArC), 138.1 (q, ArC), 137.8 (q, ArC), 137.1 (q, ArC), 134.4 (q, ArC), 134.2 (q, ArC), 130.1 (ArC-H), 126.5 (ArC-H), 122.9 (ArC-H), 122.8 (ArC-H), 119.3 (ArC-H), 119.1 (ArC-H), 118.1 (ArC-H), 53.2 ($^+\text{N}(\text{CH}_2\text{CH}_3)_4$), 46.1 (benzylic C-H), 36.2 (q, ^tBu), 36.1 (q, ^tBu), 35.1 (q, ^tBu), 34.9 (q, ^tBu), 33.3 (CH_3 , ^tBu), 33.0 (CH_3 , ^tBu), 32.4 (CH_3 , ^tBu), 31.8 (CH_3 , ^tBu), 28.4 ($\text{CH}(\text{CH}_3)_2$), 28.1 ($\text{CH}(\text{CH}_3)_2$), 25.9 ($\text{CH}(\text{CH}_3)_2$), 25.6 ($\text{CH}(\text{CH}_3)_2$), 25.0 ($\text{CH}(\text{CH}_3)_2$), 8.0 ($^+\text{N}(\text{CH}_2\text{CH}_3)_4$).

Elemental analysis ($[\text{NEt}_4]_2[\text{Ce}_2\text{Cl}_4(\text{ODipp})_2(\text{pTP}^t)](\text{THF})_2$): C 64.04%, H 8.45%, N 1.33% calculated; C 64.07%, H 8.35%, N 1.09% found.

Figure S17: ^1H NMR spectra of $[\text{NEt}_4]_2[\text{Ce}_2\text{Cl}_4(\text{ODipp})_2(\rho\text{TP}^t)]$ in $\text{C}_5\text{D}_5\text{N}$.



^1H - ^1H NOESY spectrum of $[\text{NEt}_4]_2[\text{Ce}_2\text{Cl}_4(\text{ODipp})_2(\rho\text{TP}^t)]$ in $\text{C}_5\text{D}_5\text{N}$. The only cross-peaks observable are that related to the NEt_4 counterions – located at 3.3 and 1.2 ppm.

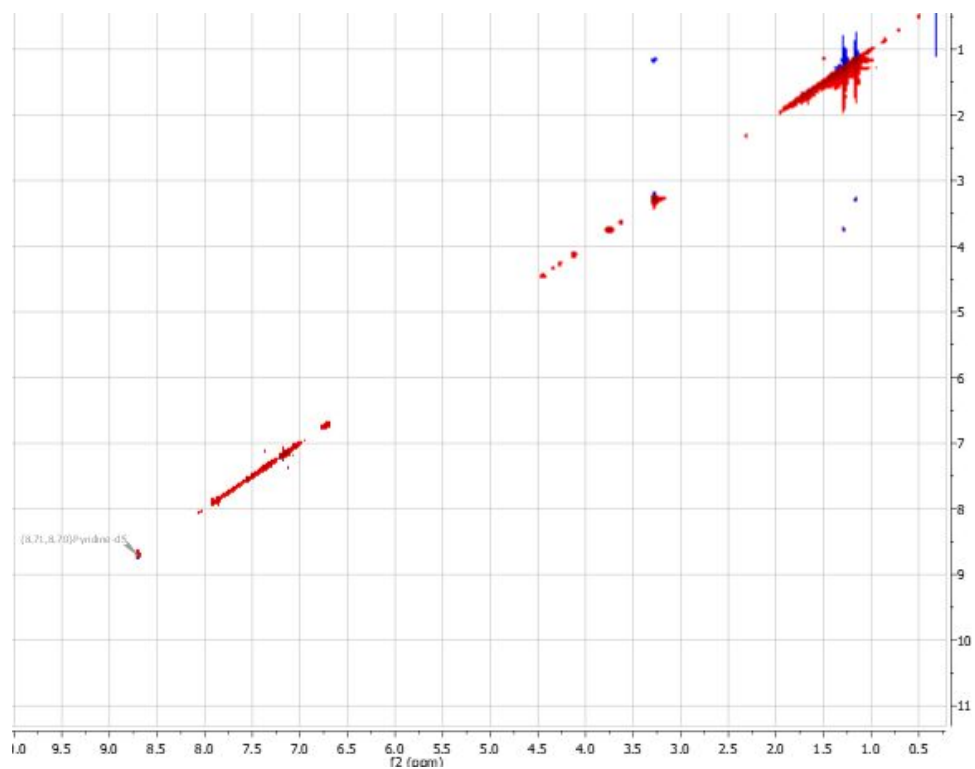
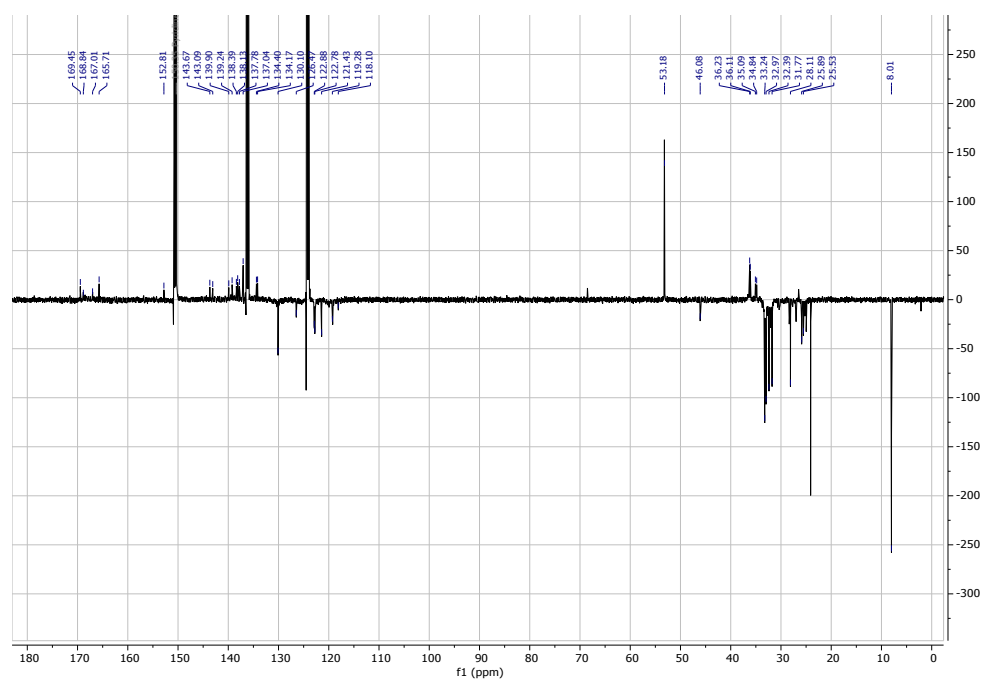
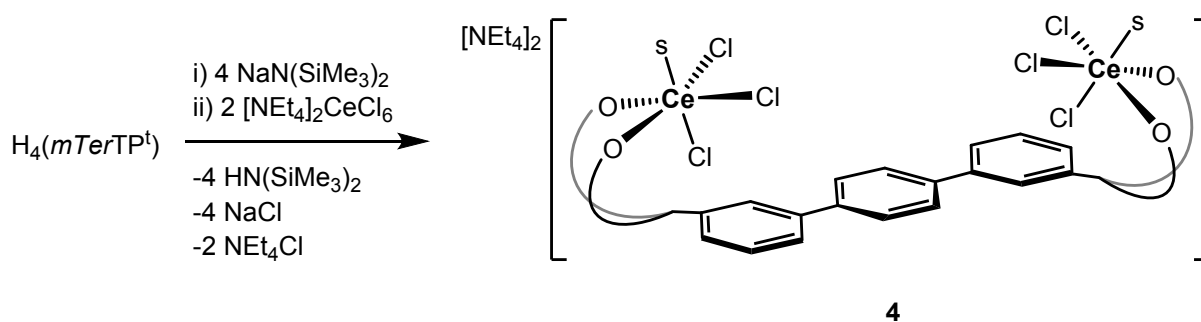


Figure S18: ^{13}C DEPTQ NMR spectrum of $[\text{NEt}_4]_2[\text{Ce}_2\text{Cl}_4(\text{ODipp})_2(\rho\text{TP}^t)]$ in $\text{C}_5\text{D}_5\text{N}$.



S2.10 Synthesis of $[\text{NEt}_4]_2[\text{Ce}_2\text{Cl}_6(m\text{TerTP}^t)]$



Equation S11: Synthesis of $[\text{NEt}_4]_2[\text{Ce}_2\text{Cl}_6(m\text{TerTP}^t)]$.

By analogous procedure to S2.3.

$\text{H}_4(m\text{TerTP}^t)$ (269 mg, 0.25 mmol, 1 equiv.) and $\text{NaN(SiMe}_3)_2$ (183 mg, 1.00 mmol 4 equiv.) were dissolved in THF (10 mL) and the resulting clear solution stirred for 2 hours. $[\text{NEt}_4]_2\text{CeCl}_6$ (307 mg, 0.50 mmol, 2 equiv.) was suspended in THF (10 mL) at 0 °C and to this was slowly added the $\text{Na}_4(m\text{TerTP}^t)$ solution, forming a purple solution which was stirred for 16 hours at room temperature. The mixture was centrifuged and cooled in an ice-bath, filtered *via* cannula whilst cold and the volatiles evaporated under reduced pressure. The crude product was dried, then triturated with hexane (3 x 10 mL) before drying again, yielding $[\text{NEt}_4]_2[\text{Ce}_2\text{Cl}_6(m\text{TerTP}^t)]$ **4** (351 mg, 77%) as a purple solid.

^1H NMR (500 MHz, pyridine- d_5) δ_{H} 8.33 (s, 1H, Ar-H), 8.25 (s, 1H, Ar-H), 8.18 (s, 1H, Ar-H), 7.83 (m, 2H, Ar-H), 7.72 (m, 2H, Ar-H), 7.70 (m, 2H, Ar-H), 7.49 (s, 1H, Ar-H), 7.40 (s, 1H, Ar-H), 7.38 (s, 1H, Ar-H), 7.36 (m, 2H, Ar-H), 7.35 (m, 2H, Ar-H), 7.31 (m, 1H, Ar-H), 7.30 (m, 1H, Ar-H), 7.28 (m, 2H, Ar-H), 6.82 (s, 2H, benzylic C-H), 3.32 (q, 16H, ($^+\text{N}(\text{CH}_2\text{CH}_3)_4$)), 1.86 (br s, 18H, ^tBu), 1.64 (9H, tBu), 1.49 (s, 18H, ^tBu), 1.36 (s, 9H, ^tBu), 1.33 (s, 9H, ^tBu), 1.31 (s, 9H, ^tBu), 1.19 (t, 24H, ($^+\text{N}(\text{CH}_2\text{CH}_3)_4$)).

^{13}C DEPTQ NMR (126 MHz, pyridine- d_5) δ_{C} 168.2 (q, ArC-O), 149.5 (q, ArC), 143.5 (q, ArC), 141.2 (q, ArC), 133.0 (ArC-H), 129.3 (ArC-H), 128.8 (ArC-H), 128.5 (ArC-H), 127.6 (ArC-H), 120.1 (ArC-H), 53.0 ($^+\text{N}(\text{CH}_2\text{CH}_3)_4$), 44.4 (CH_3 , ^tBu), 36.1 (q, ^tBu), 36.0 (q, ^tBu), 34.9 (q, ^tBu), 33.1 (CH_3 , ^tBu), 32.8 (CH_3 , ^tBu), 30.9 (CH_3 , ^tBu), 26.3 (q, ^tBu), 7.8 ($^+\text{N}(\text{CH}_2\text{CH}_3)_4$).

Elemental analysis ($[\text{NEt}_4]_2[\text{Ce}_2\text{Cl}_6(m\text{TerTP}^t)(\text{THF})_2]$): C 60.55%, H 8.65%, N 1.40% calculated; C 60.44%, H 8.76%, N 1.39% found.

Figure S19: ^1H NMR spectrum of $[\text{NEt}_4]_2[\text{Ce}_2\text{Cl}_6(m\text{TerTP}^t)]$ in $\text{C}_5\text{D}_5\text{N}$.

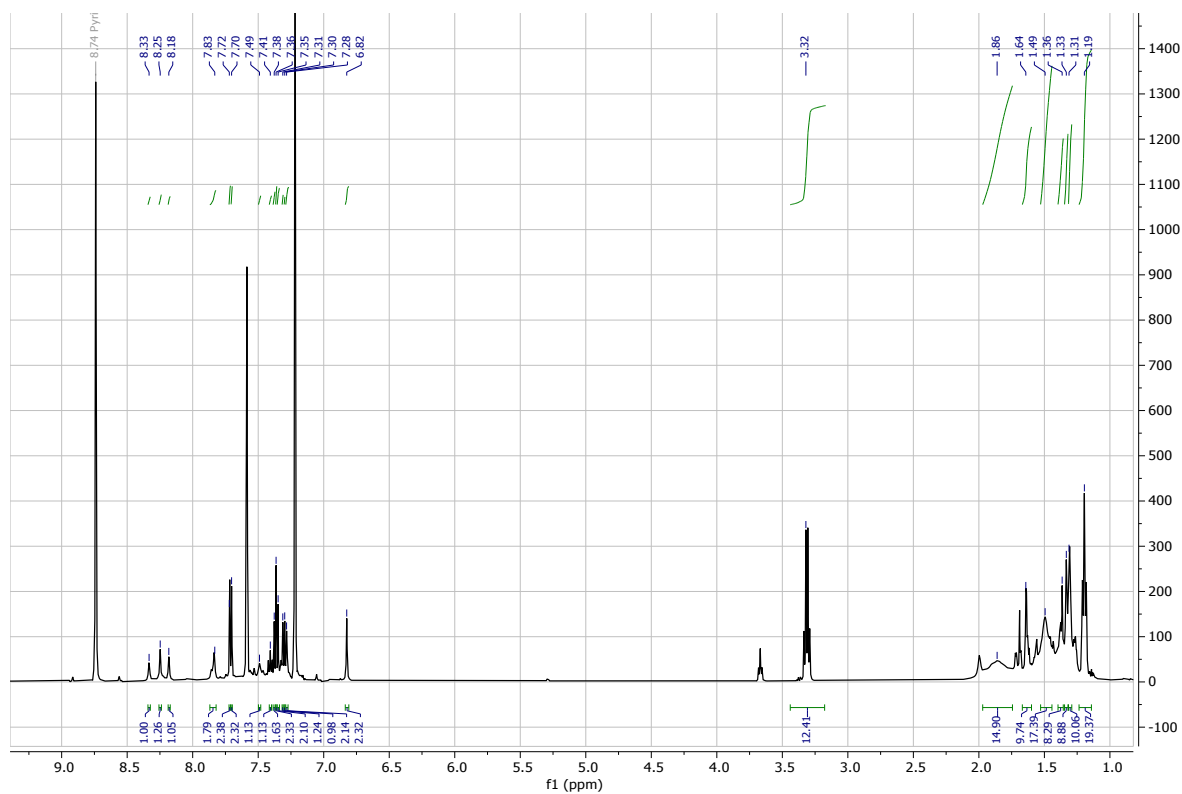
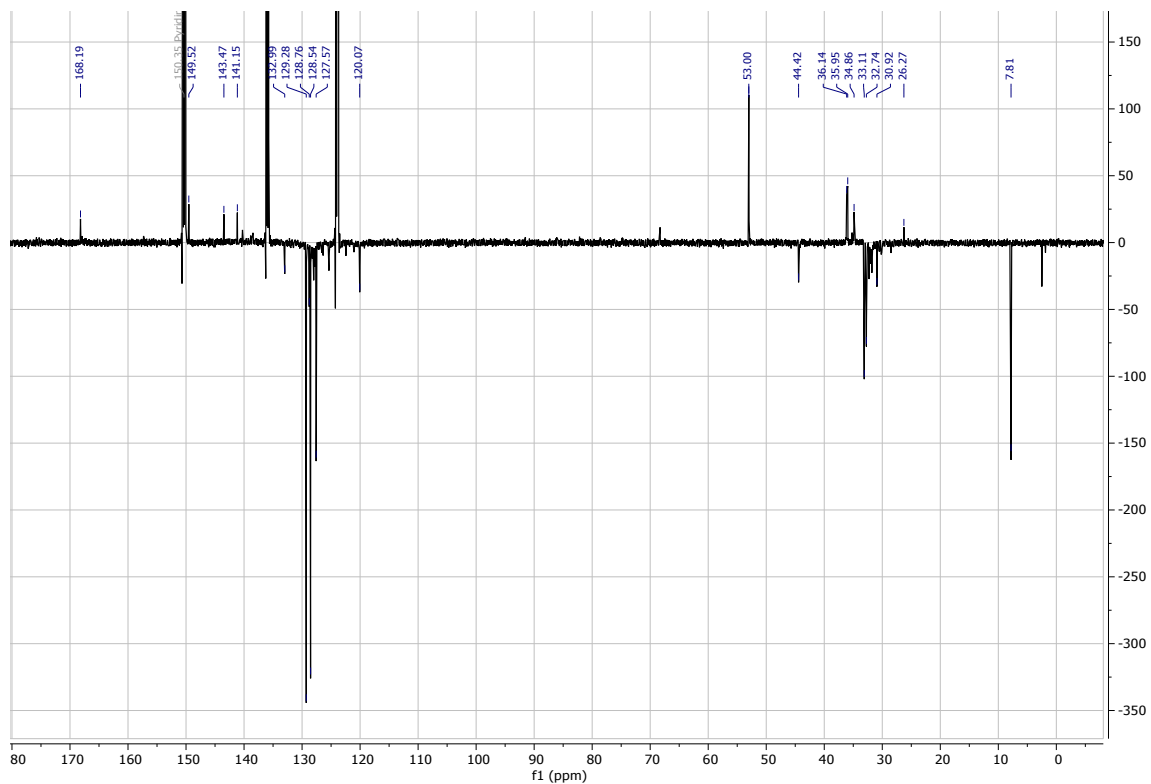
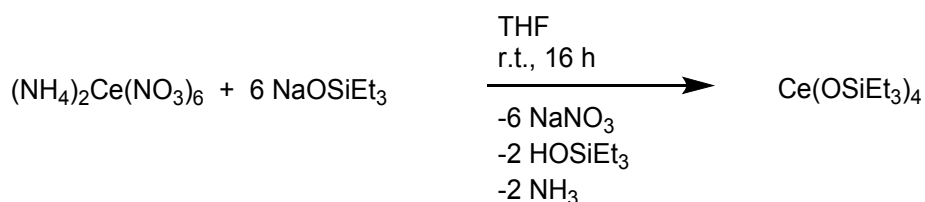


Figure S20: ^{13}C DEPTQ NMR spectrum of $[\text{NEt}_4]_2[\text{Ce}_2\text{Cl}_6(m\text{TerTP}^t)]$ in $\text{C}_5\text{D}_5\text{N}$.



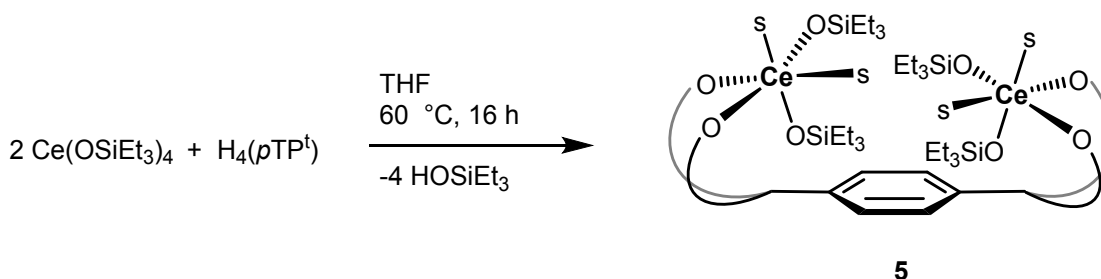
S2.11 Synthesis of neutral di-Ce(IV) complex



Equation S12: Synthesis of $\text{Ce}(\text{OSiEt}_3)_4$.

Prepared using the method described by Anwender et al. and Evans et al.^{8,9} A colourless THF solution (2 mL) of NaOSiEt_3 (212.4 mg, 1.38 mmol, 6 equiv.) was added dropwise to a vigorously stirring orange THF suspension (2 mL) of $(\text{NH}_4)_2\text{Ce}(\text{NO}_3)_6$ (125.8 mg, 0.230 mmol, 1 equiv.). The mixture became a cloudy yellow suspension and gas evolution was observed for about 1 hour. Stirring was continued for 16 hours after which the white suspension was centrifuged, filtered and the filtrate evaporated to dryness by heating under vacuum at 40 °C for 5 hours. A sticky yellow solid was obtained (95 mg, 62%).

^1H NMR (500 MHz, pyridine- d_5) δ_{H} 1.11 (t, $J = 7.5$ Hz, 36H), 0.71 (q, $J = 7.5$ Hz, 24H).



Equation S13: Synthesis of $[\text{Ce}(\text{OSiEt}_3)_4(\rho\text{TP}^{\text{t}})]$; s = solvent

In a Schlenk flask, $\text{H}_4(\rho\text{TP}^{\text{t}})$ (55 mg, 0.060 mmol, 1 equiv.) was dissolved in THF (10 mL). To this clear, stirring solution, a pale yellow THF solution (3 mL) of $\text{Ce}(\text{OSiEt}_3)_4$ (80 mg, 0.120 mmol, 2 equiv.) was added dropwise. The mixture immediately turned a deep purple colour, and the reaction was heated at 60 °C with stirring for 16 hours. Volatiles were evaporated under reduced pressure and the residue washed with hexane (2 x 5 mL) before drying at 50 °C for 6 h. $[\text{Ce}(\text{OSiEt}_3)_4(\rho\text{TP}^{\text{t}})]$ **5** was obtained as a purple solid (70 mg, 68%).

^1H NMR (500 MHz, pyridine- d_5) δ_{H} 7.94 (2H, Ar-H), 7.44 (2H, Ar-H), 7.30 (2H, Ar-H), 7.08 (s, 4H, spacer Ar-H), 7.02 (2H, Ar-H), 1.44 (s, 36H, ^tBu), 1.35 (s, 36H, ^tBu), 1.13 (t, $J = 7.5$ Hz, 36H), 0.73 (q, $J = 7.5$ Hz, 24H).

^{13}C DEPTQ NMR (126 MHz, pyridine- d_5) δ_{C} 166.8 (q, ArC-O), 145.4 (q, ArC), 140.9 (q, ArC), 137.9 (q, ArC), 134.3 (q, ArC), 130.1 (ArC-H), 129.7 (ArC-H), 125.5 (ArC-H), 120.5 (ArC-H), 44.0 (benzylic C-H), 36.0 (q, ^tBu), 35.6 (q, ^tBu), 34.9 (q, ^tBu), 32.7 (CH_3 , ^tBu), 31.2 (CH_3 , ^tBu), 26.3 (q, ^tBu), 8.4 ($\text{OSiCH}_2\text{CH}_3$), 8.2 ($\text{OSiCH}_2\text{CH}_3$), 7.7 ($\text{OSiCH}_2\text{CH}_3$), 7.2 ($\text{OSiCH}_2\text{CH}_3$).

^{29}Si NMR (99 MHz, pyridine- d_5) δ_{Si} 13.09.

Elemental analysis ($[\text{Ce}_2(\text{OSiEt}_3)_4(\rho\text{TP}^{\text{t}})(\text{THF})_4]$): C 62.05%, H 9.54%, N 0.00% calculated; C 62.37%, H 9.81%, N 0.00% found.

Figure S21: ^1H NMR spectrum of $[\text{Ce}(\text{OSiEt}_3)_4(\text{pTP}^t)]$ in $\text{C}_5\text{D}_5\text{N}$. Residual THF is also present.

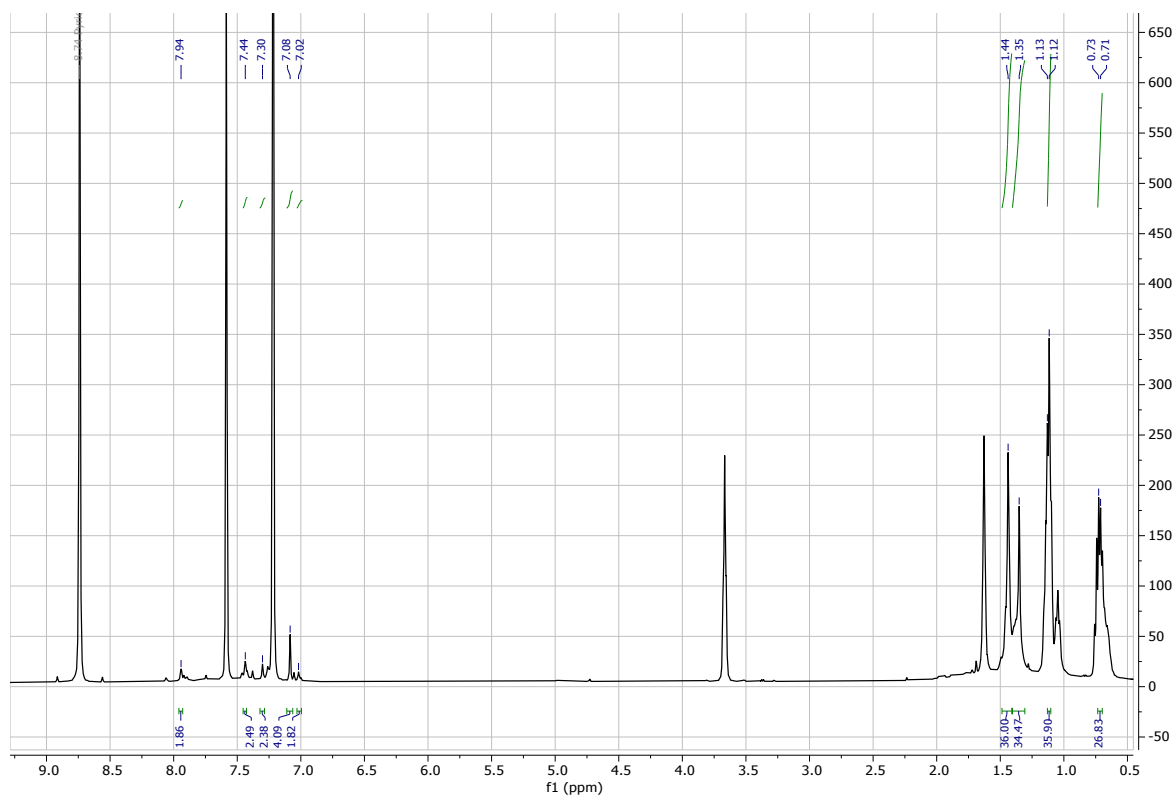
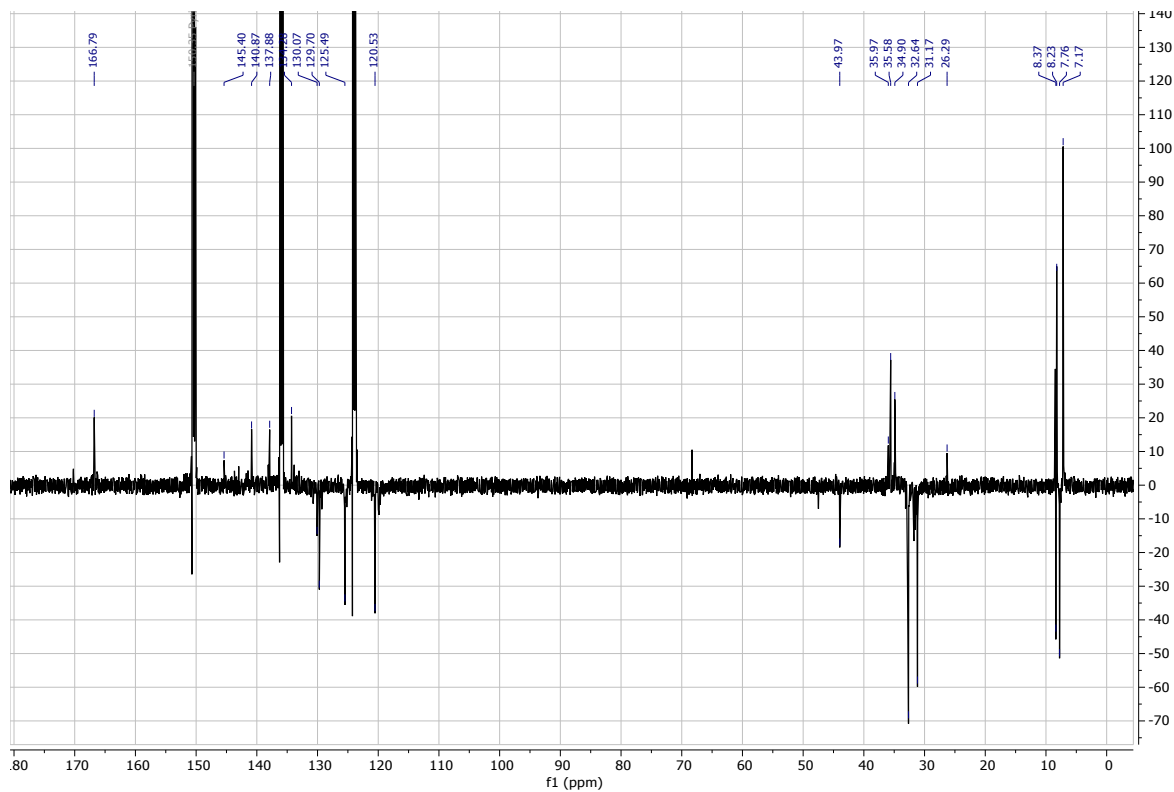


Figure S22: ^{13}C DEPTQ NMR spectrum of $[\text{Ce}(\text{OSiEt}_3)_4(\text{pTP}^t)]$ in $\text{C}_5\text{D}_5\text{N}$.



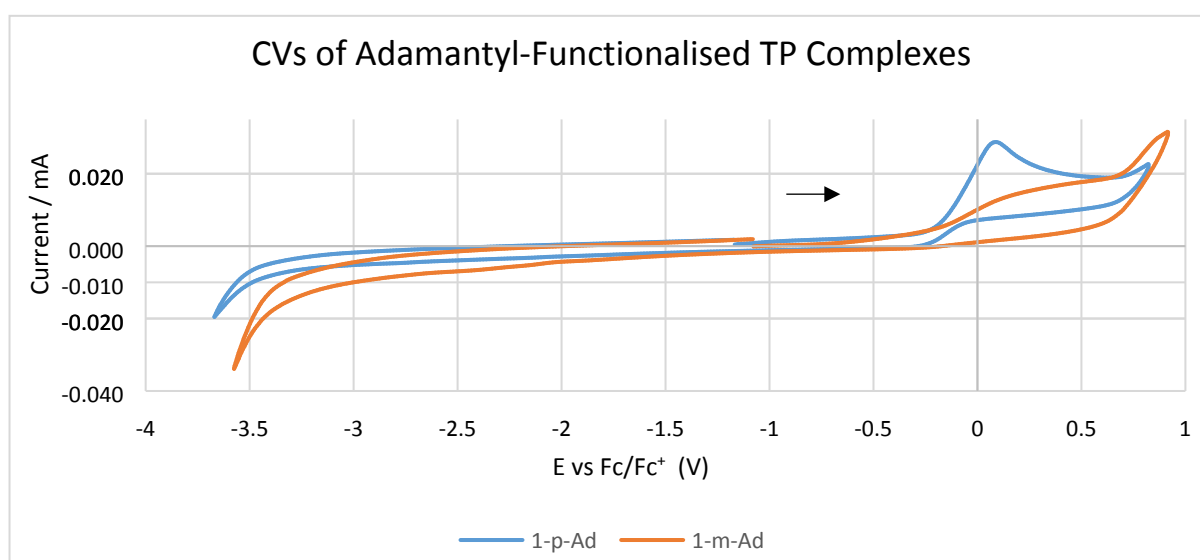
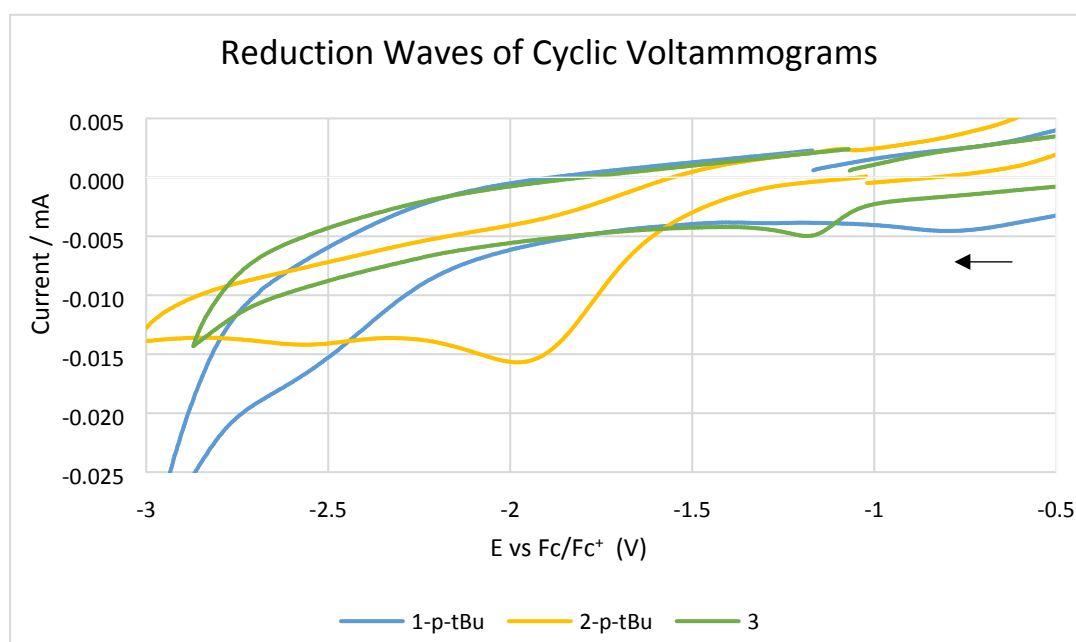
S2.12 Cyclic voltammetry studies

Measurements were conducted in THF using 0.1 M $[n\text{Bu}_4\text{N}][\text{PF}_6]$ as a supporting electrolyte. The mass of complex used was that required to form a 0.01 mM solution.

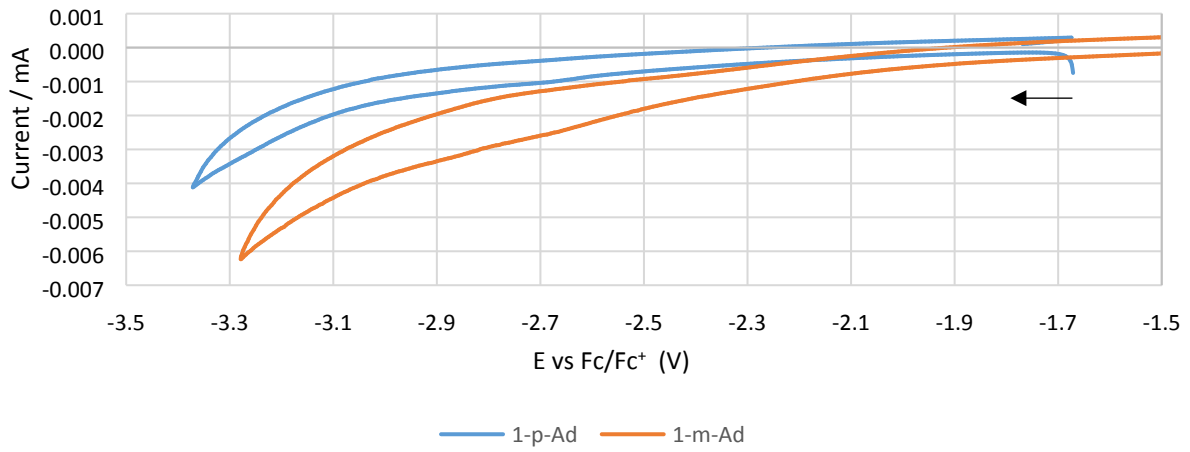
Table S1: Reduction potentials of selected di-Ce(IV) complexes.

Complex	E_{pc} vs Fc/Fc ⁺
	V
1-<i>p</i>-tBu	-2.47
2-<i>p</i>-tBu	-1.98
3	-1.18

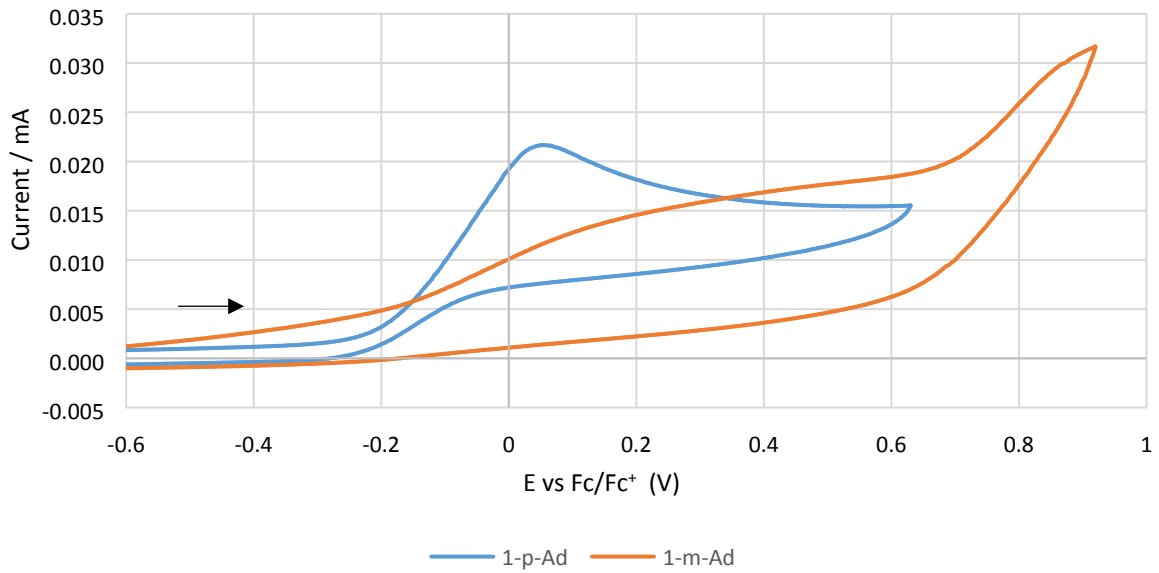
Figure S23: Cyclic voltammograms of selected di-Ce(IV) complexes. → = scan direction



Reduction Waves of Adamantyl-Functionalized TP Complexes



Oxidation Waves of Adamantyl-Functionalized TP Complexes



S2.13 UV-Vis

All UV-Vis spectra were recorded in THF, using concentrations of 3×10^{-5} M for **1-*p*-^tBu**, **1-*m*-^tBu**, **2-*p*-^tBu** and **3**; 1×10^{-5} M for **1-*p*-Ad**; 3×10^{-6} M **1-*m*-Ad**.

Figure S24: UV-Vis spectra of selected di-Ce(IV) complexes.

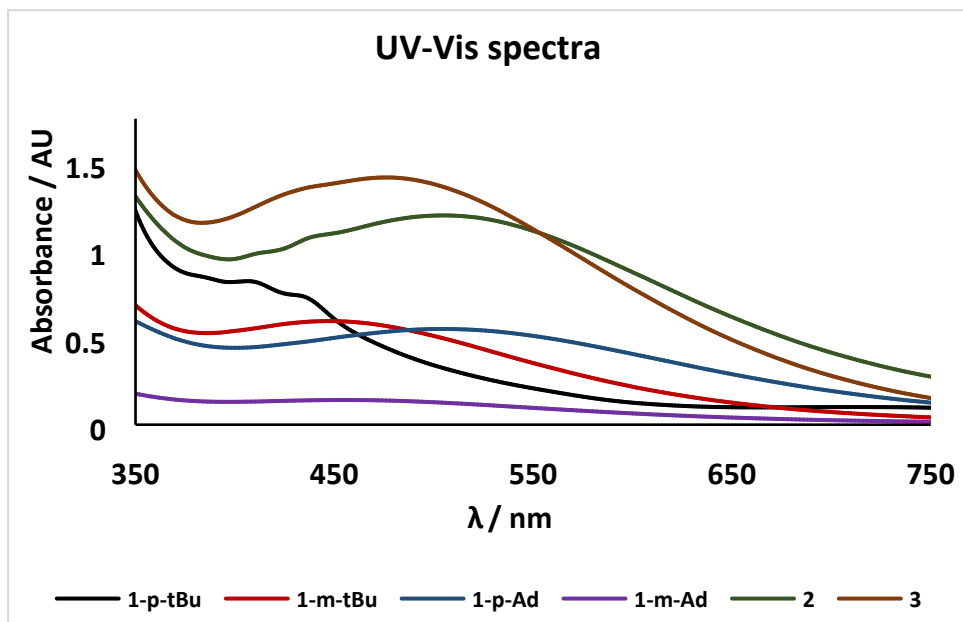
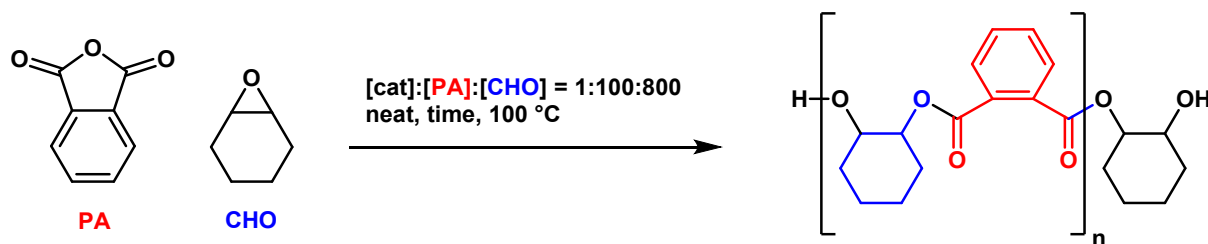


Table S2: λ_{\max} values of selected di-Ce(IV) complexes.

Compound	λ_{\max}
	nm
1-<i>p</i>-^tBu	406.5
1-<i>m</i>-^tBu	447.5
1-<i>p</i>-Ad	504
1-<i>m</i>-Ad	455
2-<i>p</i>-^tBu	505
3	476.5

S3 ROCOP Protocols

S3.1 Example procedure for PA/CHO reactions, using $[\text{NEt}_4]_2[\text{Ce}_2\text{Cl}_2(\text{OSiMe}_3)_4(\rho\text{TP}^t)]$ as catalyst.



Equation S14: General reaction for anhydride/epoxide ROCOP.

In the glovebox a glass vial with Teflon-coated lid was charged with $[\text{NEt}_4]_2[\text{Ce}_2\text{Cl}_2(\text{OSiMe}_3)_4(\rho\text{TP}^t)]$ (14.2 mg, 0.0075 mmol, 1 equiv.) phthalic anhydride (111.1 mg, 0.75 mmol, 100 equiv.) and a stir bar. Cyclohexene oxide (0.60 mL, 6.0 mmol, 800 equiv.) was added, the vial closed and then taken out of the glovebox. The reaction mixture was heated to 100 °C with constant stirring and after the appropriate reaction time the vial was opened to air and quenched by addition of CDCl_3 (0.5 mL). A sample of the crude polymer was analysed by ^1H NMR spectroscopy. The polymer was purified by evaporating volatiles under vacuum, dissolving the residue in a minimum volume of dichloromethane and precipitating the polymer by addition to stirring pentane.

SEC samples were prepared by filtering a solution ($4 \text{ mg}\cdot\text{mL}^{-1}$ in SEC grade THF) of the purified polymer.

For MALDI-ToF samples, the purified polymer, dithranol matrix and KI (cationizing agent) were dissolved in THF at $10 \text{ mg}\cdot\text{mL}^{-1}$, and the solutions were mixed in a 2:2:1 volume ratio, respectively. A droplet ($2 \mu\text{L}$) of the resultant mixture was spotted on to the sample plate and submitted for MALDI-ToF MS analysis.

Diagnostic resonances of poly(cyclohexene phthalate): 10 ^1H NMR (500 MHz, CDCl_3) δ_{H} 7.59 (br m, 2 x Ar-H), 7.41 (br m, 2 x Ar-H), 5.15 (br, 2 x OC-H), 2.23 (br m, $-\text{CH}_2$), 1.76 (br m, $-\text{CH}_2$), 1.53 (br m, $-\text{CH}_2$), 1.37 (br m, $-\text{CH}_2$). $^{13}\text{C}\{^1\text{H}\}$ NMR (500 MHz, CDCl_3) δ_{C} 166.8 (O-CH-CH-OC=O), 132.2 (ArC), 131.2 (ArC), 129.0 (ArC), 74.8 (O-CH-CH-OC=O), 30.0 ($\text{CH}_2\text{-CH}_2\text{-CH-O}$), 23.5 ($\text{CH}_2\text{-CH}_2\text{-CH-O}$).

Figure S25: ^1H NMR spectrum of poly(cyclohexene phthalate) in CDCl_3 , produced by a 2.5 h reaction with catalyst **3**.

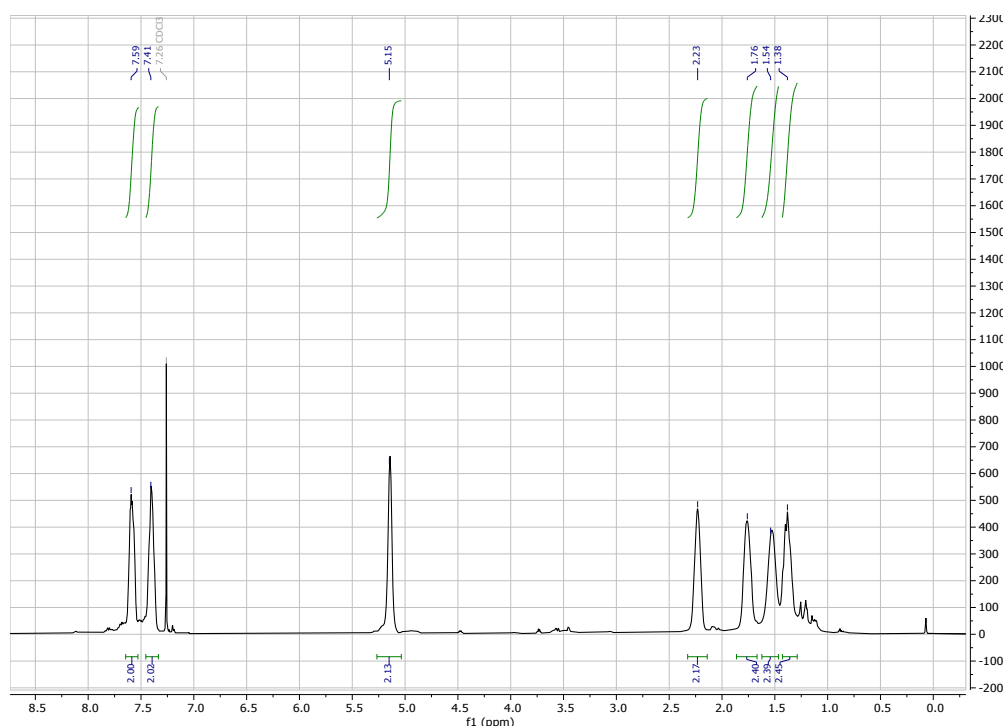


Figure S26: $^{13}\text{C}\{^1\text{H}\}$ NMR spectrum of poly(cyclohexene phthalate) in CDCl_3 , produced by a 2.5 h reaction with catalyst **3**, 100 equiv. PA and 800 equiv. CHO.

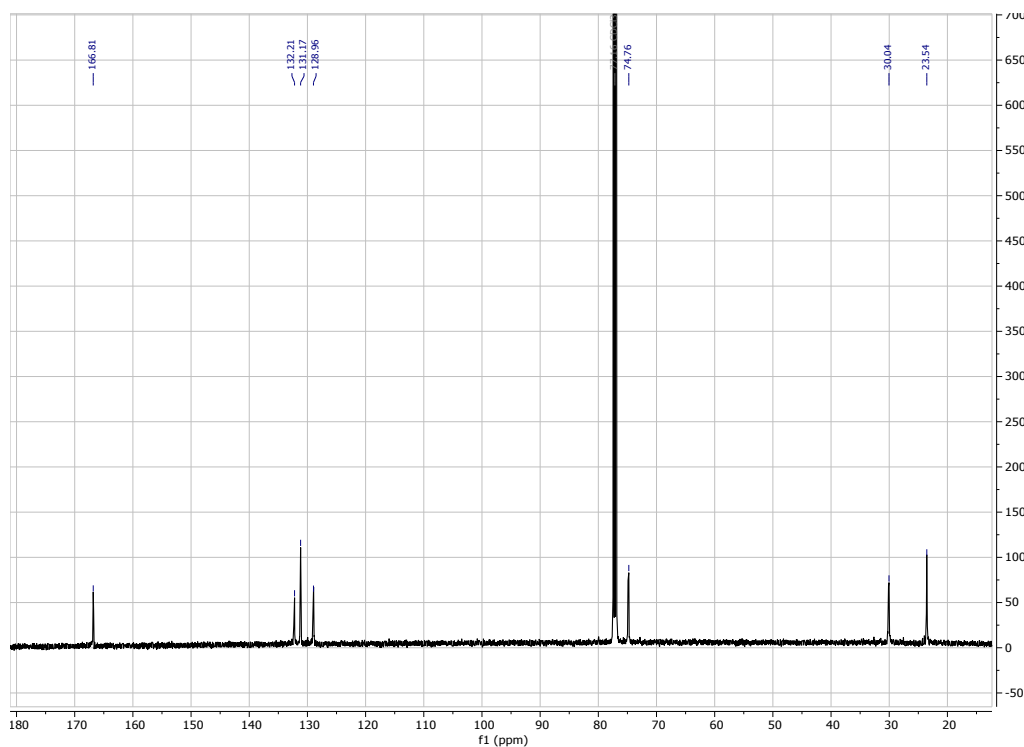


Figure S27: ^1H NMR spectrum of poly(cyclohexene phthalate) in CDCl_3 , produced by a 2 h reaction with catalyst **1-p-tBu**, 10 equiv. PA and 80 equiv. CHO. The small peak at 0.07 ppm can be attributed to silicone grease present in the CDCl_3 (confirmed in a spectrum of blank solvent). It is also observed in the spectrum in Figure S7 above, therefore is not due to a $-\text{OSiMe}_3$ initiated polymer. Trace polyether, THF and hexane are also visible.

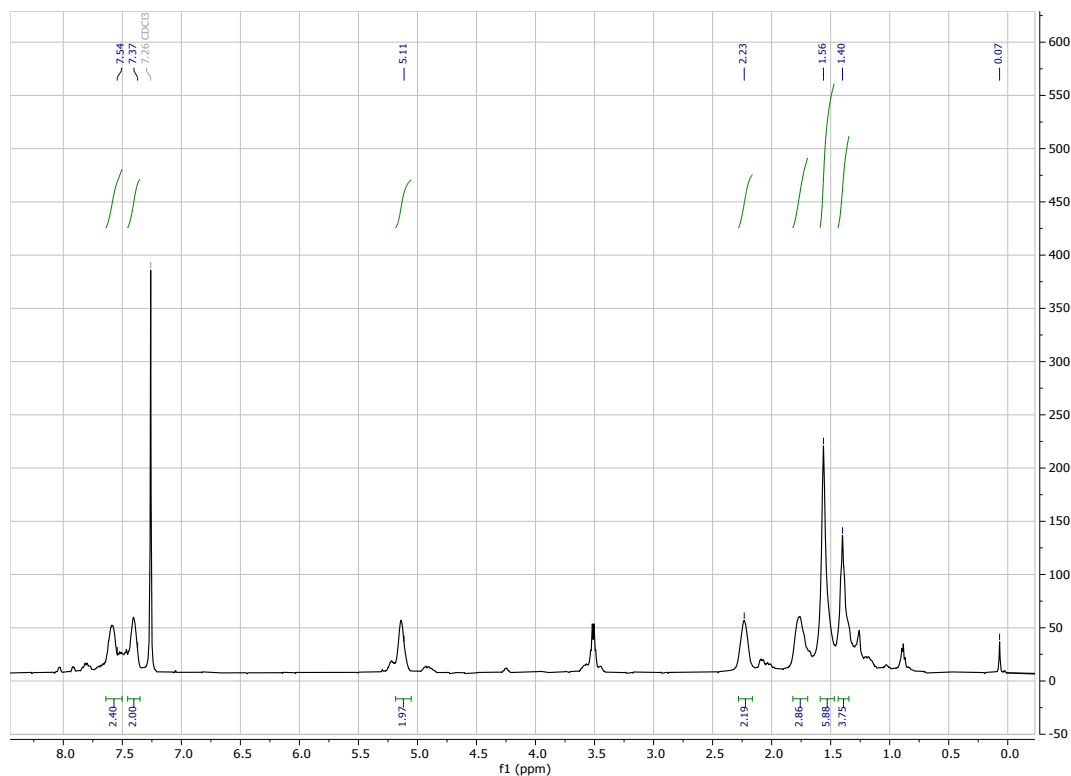


Table S3: Data for PA/CHO ROCOP at multiple time-points^a

Entry	Catalyst	Loading	Time	% PA Conversion ^b	% Ester Linkages ^c	TOF ^e	M_n (exp) ^d	\bar{D} ^d
		mol%	h			mol.h ⁻¹	g.mol ⁻¹	
1	1- <i>m</i> - ^t Bu	1.0	0.50	49	94	98	4690	1.29
2	1- <i>m</i> - ^t Bu	1.0	0.75	86	97	115	5240	1.31
3	1- <i>m</i> - ^t Bu	1.0	1.25	99	97	79	7120	1.32
4	1- <i>p</i> - ^t Bu	1.0	0.50	29	94	58	7730 (5180)	1.07 (1.24)
							3420	1.05
5	1- <i>p</i> - ^t Bu	1.0	1.25	83	96	66	6070	1.23
6	1- <i>p</i> - ^t Bu	1.0	2.00	100	96	50	7360	1.22
7	1- <i>m</i> -Ad	1.0	0.17	38	91	229	2700	1.09
8	1- <i>m</i> -Ad	1.0	0.33	82	97	246	2800	1.08
9	1- <i>m</i> -Ad	1.0	0.50	99	97	198	4400	1.10
10	1- <i>p</i> -Ad	1.0	0.50	51	97	102	3940	1.12
11	1- <i>p</i> -Ad	1.0	0.75	84	97	112	10100 (6200)	1.06 (1.27)
							4130	1.07
12	1- <i>p</i> -Ad	1.0	1.25	99	99	79	10620 (6730)	1.07 (1.28)
							4460	1.07
13	2- <i>p</i> - ^t Bu	1.0	0.50	30	93	60	4420	1.05
14	2- <i>p</i> - ^t Bu	1.0	1.25	67	92	54	6620 (4230)	1.07 (1.26)
							2580	1.09
15	2- <i>p</i> - ^t Bu	1.0	2.00	99	89	50	9140 (5700)	1.05 (1.24)
							4090	1.07
16	3	1.0	0.50	23	88	46	15920 (7720)	1.07 (1.32)
							4530	1.22
17	3	1.0	2.00	85	95	43	16230 (7840)	1.08 (1.35)
							5860	1.14
18	3	1.0	2.50	99	99	40	17890 (8360)	1.07 (1.38)
							6490	1.14
19	4	1.0	1.00	42	93	42	-	-
20	4	1.0	2.00	97	94	49	10180 (6530)	1.05 (1.23)
							4590	1.06
21	5	1.0	1.00	27	61	27	-	-
22	5	1.0	2.00	87	71	49	9400	1.38
23	[NEt ₄] ₂ CeCl ₆ ^f	2.0	2.00	87	83	22	2700	1.23

^aStandard conditions: Reactions were run at 100 °C with a molar ratio of catalyst:PA:CHO of 1:100:800.

^bDetermined by ¹H NMR spectroscopy (CDCl₃) by integrating the normalized resonances for PA (7.95 ppm) and the phenylene signals in polyester (7.30–7.70 ppm). ^cDetermined by ¹H NMR spectroscopy (CDCl₃) by integrating the normalized resonances for ester linkages (5.10 ppm). ^dDetermined by SEC in THF using narrow- M_n polystyrene standards to calibrate the instrument; M_n multiplied by a correction factor of 1.85.¹¹ Double entries represent bimodal distributions; the numbers in parentheses represent the total M_n and \bar{D} values. ^eTurnover frequency (TOF) = (number of moles of anhydride consumed/number of moles of catalyst)/time. ^f2.0 mol% catalyst loading.

Table S4: Raw M_n and M_w data corresponding to runs in Table S3.

Entry	Catalyst	M_w (raw, exp) ^a	M_n (raw, exp) ^a	M_n (corr, exp) ^b	\bar{D} ^c
		g.mol ⁻¹	g.mol ⁻¹	g.mol ⁻¹	
1	1- <i>m</i> - ^t Bu	3270	2540	4690	1.29
2	1- <i>m</i> - ^t Bu	3710	2830	5240	1.31
3	1- <i>m</i> - ^t Bu	5090	3850	7120	1.32
4	1- <i>p</i> - ^t Bu	4465 (3480)	4180 (2800)	7730 (5180)	1.07 (1.24)
		1950	1850	3420	1.05
5	1- <i>p</i> - ^t Bu	4050	3280	6070	1.23
6	1- <i>p</i> - ^t Bu	4870	3980	7360	1.22
7	1- <i>m</i> -Ad	1600	1460	2700	1.09
8	1- <i>m</i> -Ad	1630	1510	2800	1.08
9	1- <i>m</i> -Ad	2620	2380	4400	1.10
10	1- <i>p</i> -Ad	2380	2130	3940	1.12
11	1- <i>p</i> -Ad	5770 (4260)	5460 (3350)	10100 (6200)	1.06 (1.27)
		2440	2230	4130	1.07
12	1- <i>p</i> -Ad	6120 (4650)	5740 (3640)	10620 (6730)	1.07 (1.28)
		2590	2410	4460	1.07
13	2- <i>p</i> - ^t Bu	2500	2390	4420	1.05
14	2- <i>p</i> - ^t Bu	3820 (2890)	3580 (2290)	6620 (4230)	1.07 (1.26)
		1520	1400	2580	1.09
15	2- <i>p</i> - ^t Bu	5190 (3800)	4940 (3080)	9140 (5700)	1.05 (1.24)
		2362	2210	4090	1.7
16	3	9210 (5500)	8610 (4170)	15920 (7720)	1.07 (1.32)
		3000	2450	4530	1.22
17	3	9500 (5720)	8770 (4240)	16230 (7840)	1.08 (1.35)
		3600	3170	5860	1.14
18	3	10310 (6230)	9670 (4520)	17890 (8360)	1.07 (1.38)
		4000	3510	6490	1.14
19	4	-	-	-	-
20	4	5780 (4330)	5500 (3530)	10180 (6530)	1.05 (1.23)
		2640	2480	4590	1.06
21	5	-	-	-	-
22	5	7020	5080	9400	1.38
23	[NEt ₄] ₂ CeCl ₆ ^f	1790	1460	2700	1.23

^aDouble entries represent bimodal distributions; the numbers in parentheses represent the total M_w , M_n and \bar{D} values. ^b M_n multiplied by a correction factor of 1.85. ^c $\bar{D} = M_w/M_n$. For total molar masses, the entire peak and shoulders were integrated; for bimodal samples the minimum between the two peaks was chosen as the boundary between the two integrated areas.

S3.2 Example procedure for ROCOP substrate scope

In the glovebox a glass vial with Teflon-coated lid was charged with **1-*m*-Ad** (18.1 mg, 0.0075 mmol, 1 equiv.) and the relevant anhydride (0.75 mmol, 100 equiv.), and a stir bar.

For CHO and LO reactions, the relevant epoxide (6.0 mmol, 800 equiv.) was added, the vial closed and then taken out of the glovebox.

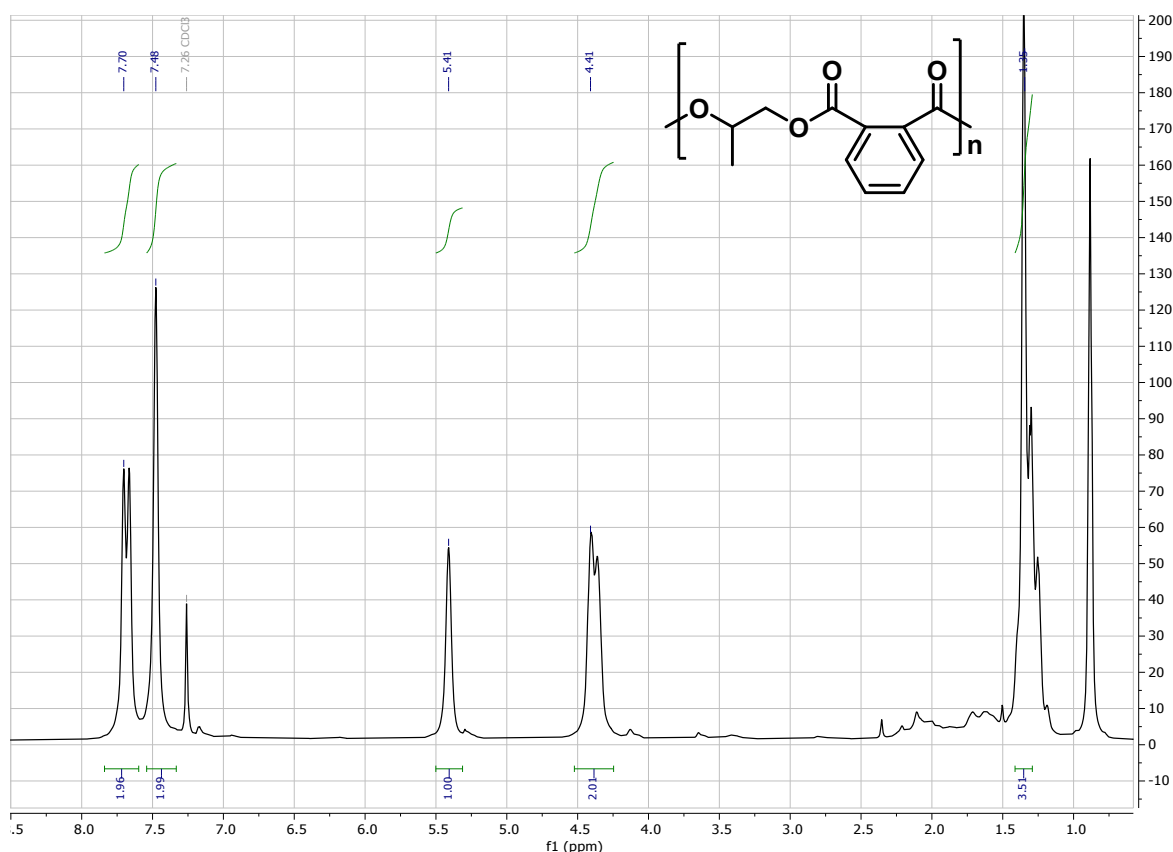
For PO reactions, propylene oxide (0.42 mL, 6.0 mmol, 800 equiv.) and toluene (1.5 mL) were added the vial closed and then taken out of the glovebox.

The reaction mixture was heated to 100 °C with constant stirring. After the appropriate reaction time the vial was opened to air and the contents rinsed into a round-bottom flask with dichloromethane, volatiles were removed under vacuum and the crude polymer analysed by ¹H NMR spectroscopy (CDCl₃). The polymer was purified by dissolving in a minimum volume of dichloromethane and precipitating by addition to stirring pentane.

SEC/MALDI-TOF sample preparations are identical as for the PA/CHO reactions.

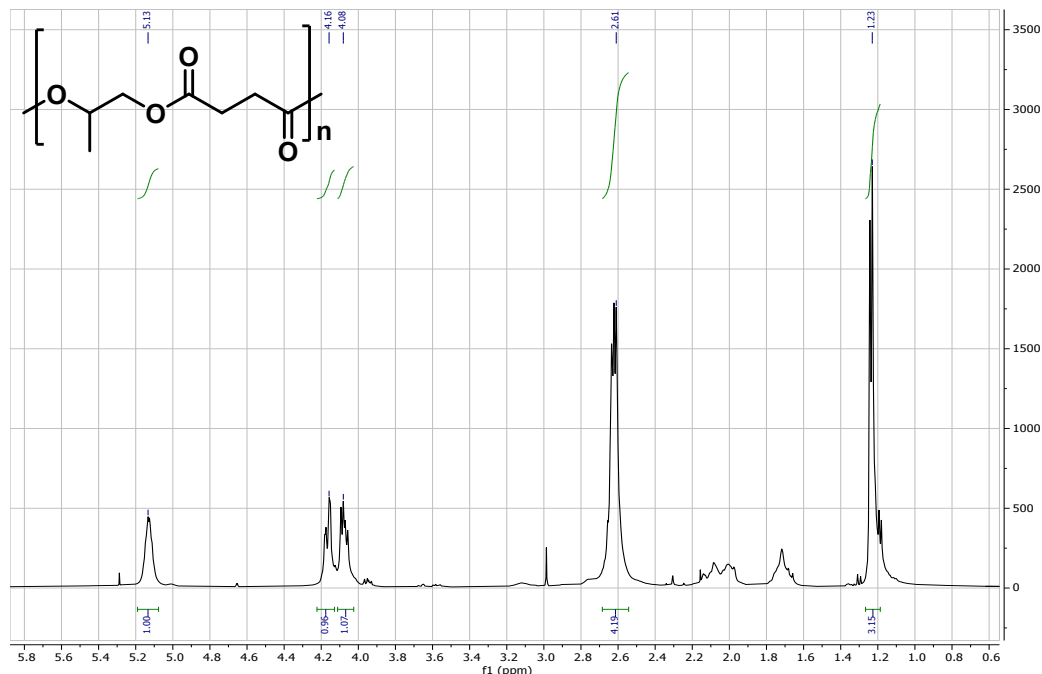
Diagnostic resonances of poly(propylene phthalate):¹² ¹H NMR (600 MHz, CDCl₃) δ_H 7.70 (br m, 2H, Ar-H), 7.48 (br m, 2H, Ar-H), 5.41 (br, 1H, (CO)O-CH(CH₃)-CH₂), 4.40 (br m, 2H, (CO)O-CH(CH₃)-CH₂), 1.35 (br, 3H, (CO)O-CH(CH₃)-CH₂). (Residual pentane visible in spectrum below.)

Figure S28: ¹H NMR spectrum of poly(propylene phthalate) in CDCl₃, produced by a 2.5 h reaction with catalyst **1-*m*-Ad**, 100 equiv. PA and 800 equiv. PO.



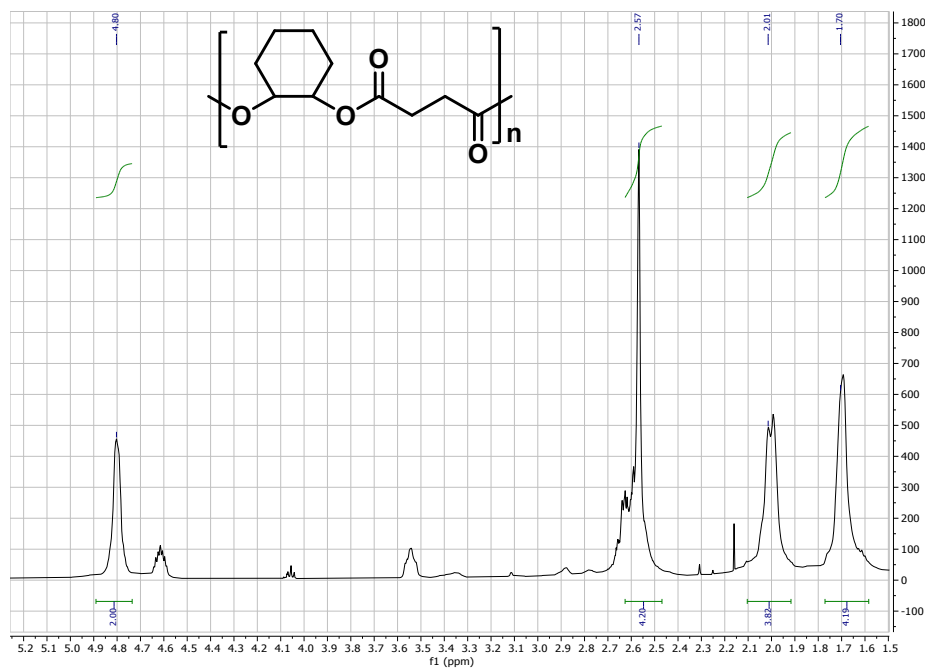
Diagnostic resonances of poly(propylene succinate):¹³ ¹H NMR (500 MHz, CDCl₃) δ_H 5.12 (br, 1H, (CO)O-CH(CH₃)-CH₂), 4.17 (m, 1H, (CO)O-CH(CH₃)-CH₂), 4.07 (m, 1H, (CO)O-CH(CH₃)-CH₂), 2.61 (m, 4H, (CO)-CH₂-CH₂-(CO)), 1.22 (d, 4H, (CO)O-CH(CH₃)-CH₂).

Figure S29: ¹H NMR spectrum of poly(propylene succinate) in CDCl₃, produced by a 2.5 h reaction with catalyst **1-*m*-Ad**, 100 equiv. SA and 800 equiv. PO.



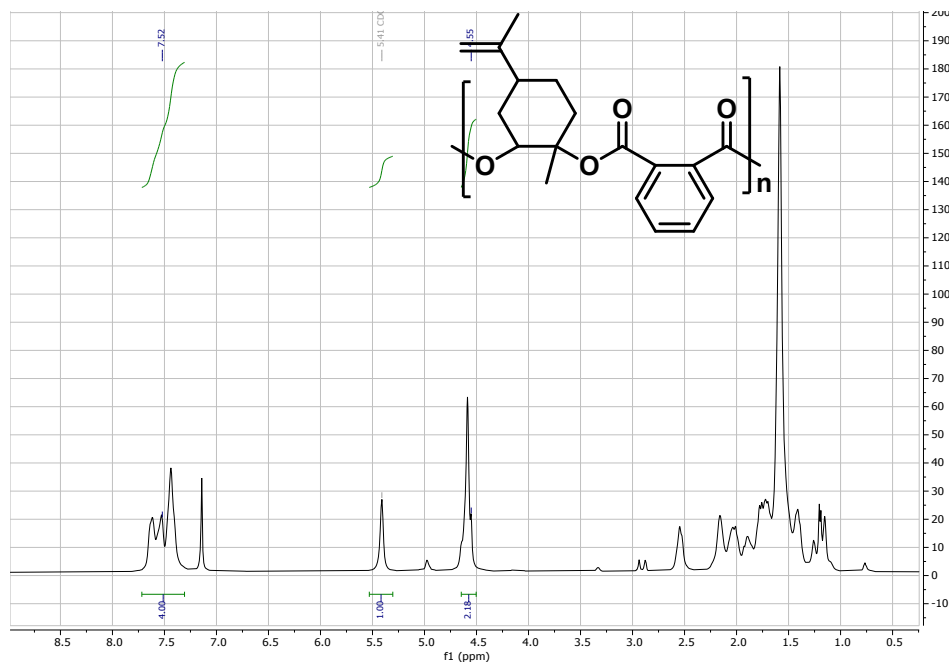
Diagnostic resonances of poly(cyclohexene succinate):¹⁴ ¹H NMR (500 MHz, CDCl₃) δ_H 4.80 (br, 2 x OC-H), 2.54 (br, 4H, (CO)-CH₂-CH₂-(CO)), 2.01 (br, 4H, cyclohexyl CH₂), 1.70 (br, 4H, cyclohexyl CH₂).

Figure S30: ¹H NMR spectrum of poly(cyclohexene succinate) in CDCl₃, produced by a 0.5 h reaction with catalyst **1-*m*-Ad**, 100 equiv. SA and 800 equiv. CHO.



Diagnostic resonances of poly(limonene phthalate):¹⁵ ^1H NMR (500 MHz, CDCl_3)
 δ_{H} 7.64-7.30 (br m, 4H, ArH), 5.41 (br, 1H, OCCH), 4.55 (m, 2H, $\text{C}=\text{CH}_2$).

Figure S31: ^1H NMR spectrum of poly(limonene phthalate) in CDCl_3 , produced by a 18 h reaction with catalyst **1-*m*-Ad**, 100 equiv. PA and 800 equiv. LO.



Diagnostic resonances of poly(limonene succinate):¹⁶ ^1H NMR (500 MHz, CDCl_3) δ_{H} 5.20 (br, 1H, OCCH), 4.82 (m, 2H, $\text{C}=\text{CH}_2$), 2.65 (br, 4H, $(\text{CO})\text{-CH}_2\text{-CH}_2\text{-(CO)}$).

Figure S32: ^1H NMR spectrum of poly(limonene succinate) in CDCl_3 , produced by a 18 h reaction with catalyst **1-*m*-Ad**, 100 equiv. SA and 800 equiv. LO.

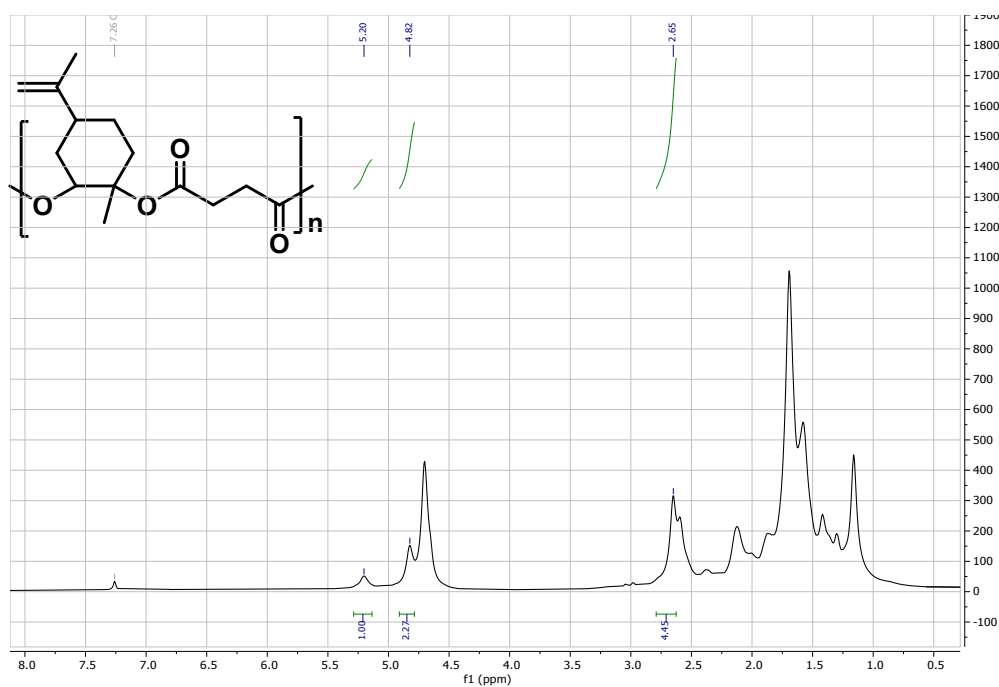


Table S5: Substrate scope using 1-*m*-Ad as catalyst.^a

Entry / catalyst loading	Monomer Combination	Solvent	TON ^b	TOF	% Ester ^b	M _w (exp) ^e	M _n (exp) ^e	Đ ^e
				mol.h ⁻¹		g.mol ⁻¹	g.mol ⁻¹	
1 / 1 mol%	PO/PA	toluene	100	40	96	5330 (5520)	4990 (3890)	1.07 (1.42)
						1790	1640	1.09
2^c / 0.5 mol%	PO/PA	toluene	99	11	97	23853 (20660)	19370 (13510)	1.23 (1.53)
						6290	5750	1.09
3^c / 1 mol%	LO/PA	neat	82	5	94	8490 (6370)	7740 (4740)	1.10 (1.34)
						3280	3020	1.09
4^d / 1 mol%	CHO/SA	neat	92	184	90	4070	2790	1.46
5^c / 0.5 mol%	CHO/SA	neat	98	11	88	5200	3860	1.35
6 / 1 mol%	PO/SA	toluene	98	39	92	5320 (1560)	3890 (1220)	1.37 (1.28)
						1090	1070	1.02
7^c / 1 mol%	LO/SA	neat	89	5	86	1720 (1890)	1540 (1250)	1.11 (1.51)
						768	760	1.01

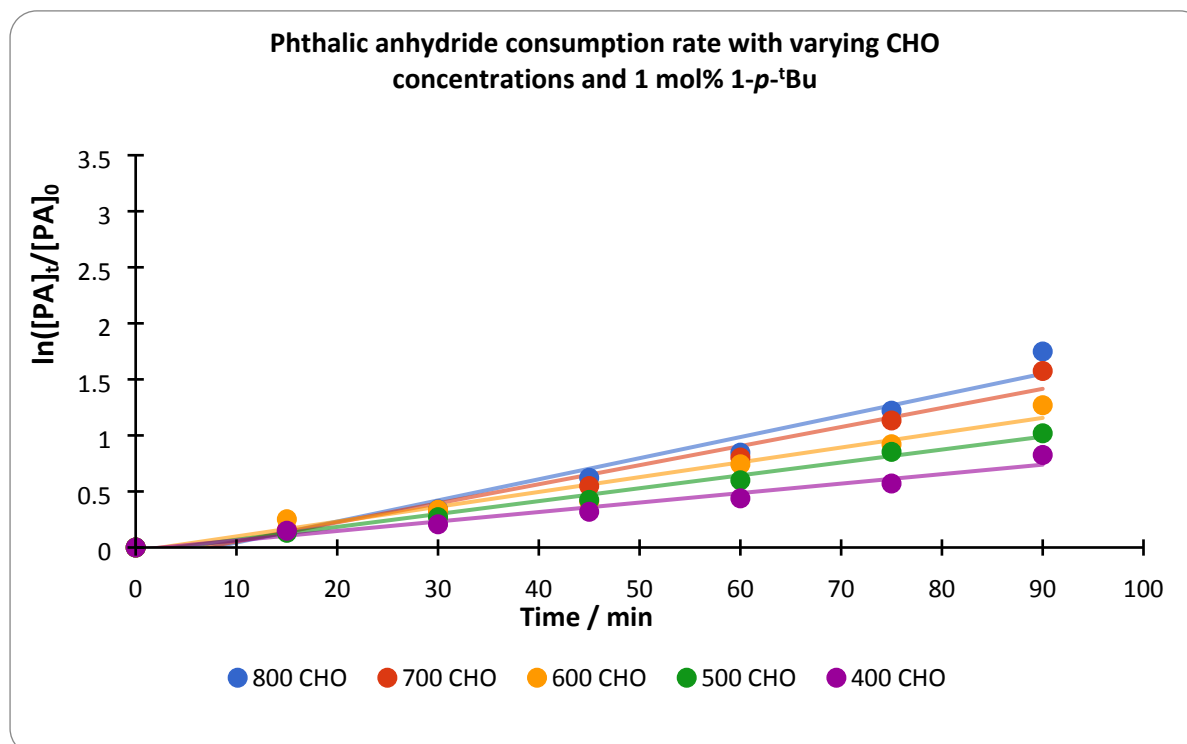
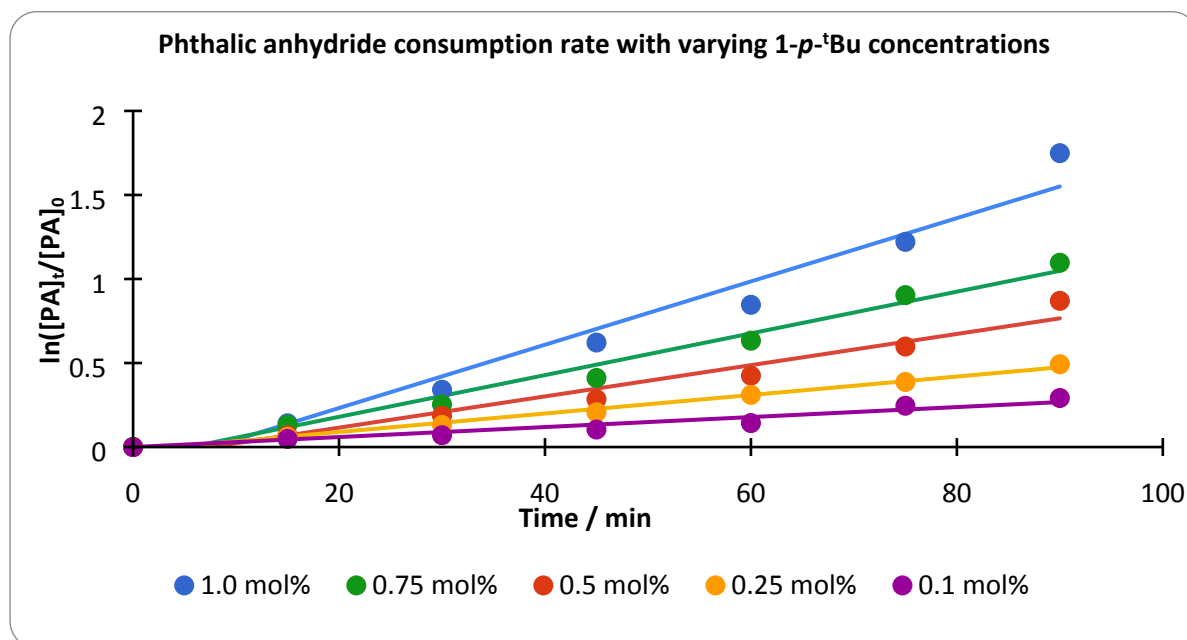
^aStandard conditions: Reactions were run at 100 °C for 2.5 h with a molar ratio of **1-*m*-Ad**:anhydride:epoxide of 1:100:800. Due to the low boiling point of PO toluene was used as solvent in the indicated reactions.

^bDetermined by ¹H NMR spectroscopy (CDCl₃) by integrating the normalized resonances for anhydride and polyester (conversion); and for ester and ether linkages (selectivity). ^c18 h reaction time. ^d0.5 h reaction time.

^eNo correction factor has been applied for M_n. Double entries represent bimodal distributions, the numbers in parentheses represent the total M_n and Đ values. Đ = M_w/M_n. ^fBased on two polymer chains formed per catalyst molecule, where M_n (calc) = (molar mass of repeat unit x %anhydride conversion)/(catalyst loading x 2). To the best of our knowledge, no correction factors have been reported for these monomer combinations which limits the comparison of the observed and calculated M_n values for these monomer combinations.

S3.3 Rate equation determination experiments

In the glovebox a 10 cm³ ampoule was charged with **1-*p*-^tBu** (56.6 mg, 0.03 mmol, 1 equiv.) and phthalic anhydride (444.3 mg, 3.0 mmol, 100 equiv.), and a stir bar. Cyclohexene oxide (2.4 mL, 24 mmol, 800 equiv.) was added and the reaction mixture was then heated to 100 °C with constant stirring. At the start of the reaction and every 15 minutes thereafter, a few drops of the reaction mixture were transferred *via* cannula, and any reaction halted, by addition to a NMR tube containing 0.5 mL CDCl₃ at 0 °C. The ¹H NMR spectrum of each sample was recorded, allowing monitoring of PA conversion and % ester linkages over time. [**1-*p*-^tBu**] was varied by changing the mass of **1-*p*-^tBu** and keeping all other variables constant. [CHO] was altered by decreasing the volume used from the standard 800 equiv. CHO and replacing the lost volume with the same volume of toluene. [PA] was calculated from the ¹H NMR spectra.



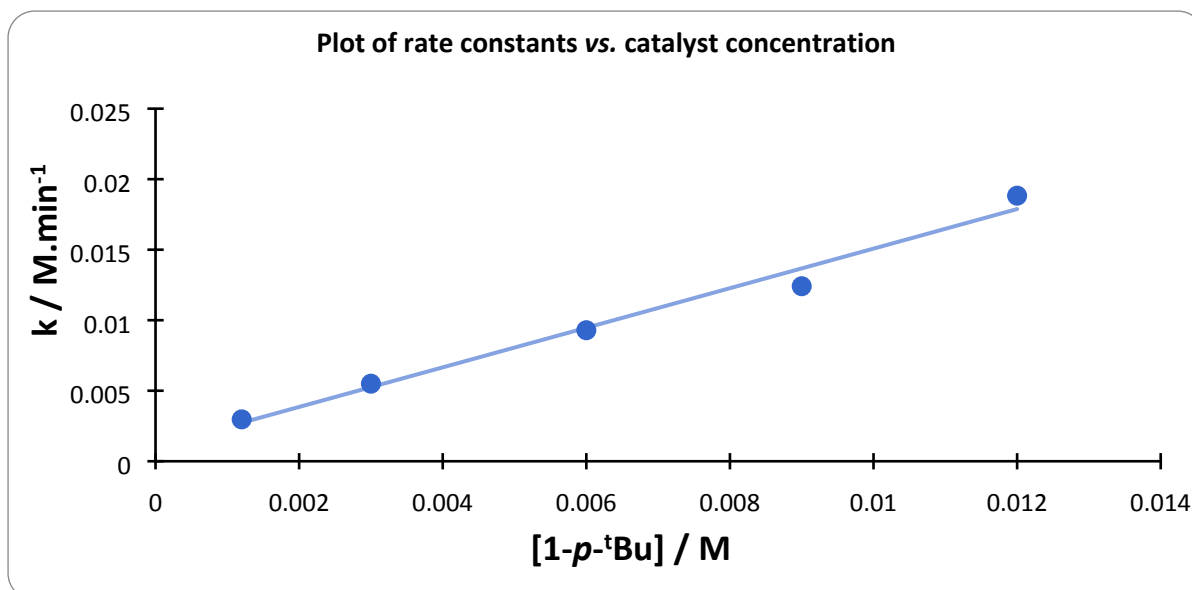


Figure S33: Kinetic plots. Top: Plot showing how the rate of PA consumption changes with different loadings of **1-p-tBu**. Each line represents a different % catalyst loading (i.e., concentration), and it is clear that the steeper lines for higher catalyst concentrations represent faster PA consumption. Middle: Plot showing how the rate of PA consumption changes with different concentrations of CHO, but a constant concentration of **1-p-tBu**. Each line represents a different CHO concentration, written in terms of CHO equivalents here for simplicity. We observe higher rates for higher CHO concentrations. Bottom: Plot of the rate constants (k) determined at each value of **[1-p-tBu]** against the values of **[1-p-tBu]**. The data fit a straight line of best fit, suggesting that the overall polymerisation reaction has a first order dependence on catalyst concentration.

S3.4 ROCOP Mechanistic discussion

By considering all of the kinetic data we have obtained, together with that published elsewhere, some details around the general ROCOP mechanism can be summarised.^{17, 18} Initial reaction rates are not affected by the amount of anhydride consumption, suggesting a zero order dependence on anhydride concentration. The initiation is deduced to be first order with respect to both catalyst concentration and epoxide concentration. Therefore the rate expression for this process can be expressed as: $rate = k[\text{catalyst}][\text{epoxide}]$. For the initiation step, MALDI-ToF mass spectrometry is useful for identifying possible end-groups for polymer chains, which are effectively also the initiating groups for starting polymerisations, i.e. the anion which first attacks and ring-opens an epoxide coordinated to a metal.

The propagation step, however, is more complicated to investigate compared to the initiation, and with respect to studying plausible mechanisms. The simplest, or most ideal, possibility is for the opened epoxide to attack a coordinated anhydride molecule, with the epoxide tether now disassociating from the metal. This is followed by a new epoxide molecule coordinating, which is in turn attacked by the now ring-opened anhydride, leaving space for a new anhydride molecule and the process repeats. All of this could occur around a single metal center, or a “chain-shuttling” mechanism could exist based upon two proximal metal centers – the latter is depicted in Figure S28. The propagation step can be further complicated by the presence of competing processes such as transesterification and ether insertions.

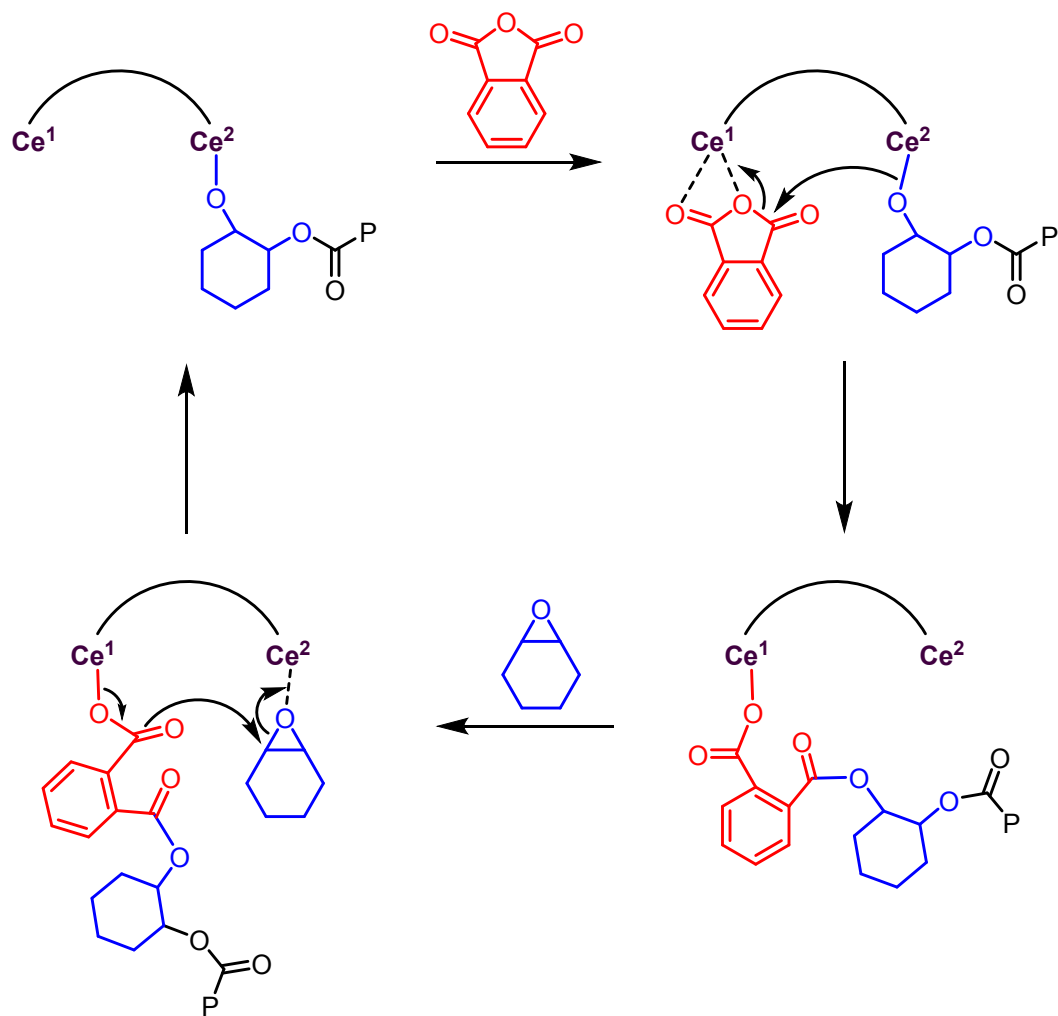


Figure S34: Plausible mechanism for propagation step that involves metal-metal cooperativity.

S3.5 SEC Traces

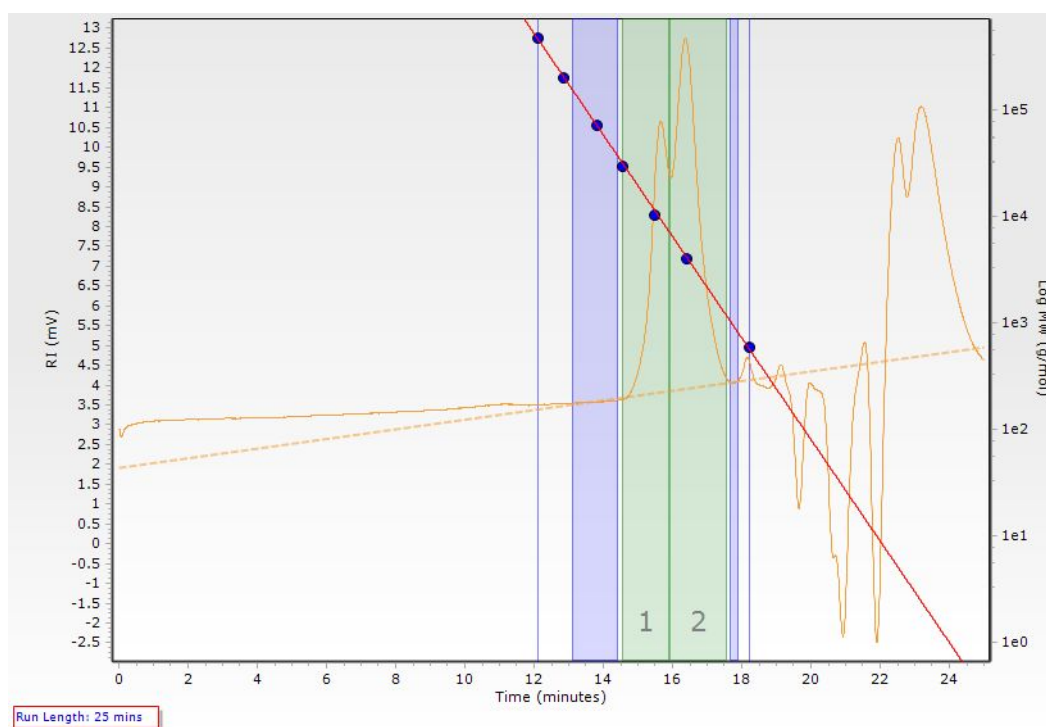


Figure S35: SEC trace for PA/CHO co-polyester formed by **1-*m*-^tBu** (Table S3 Entry 3).

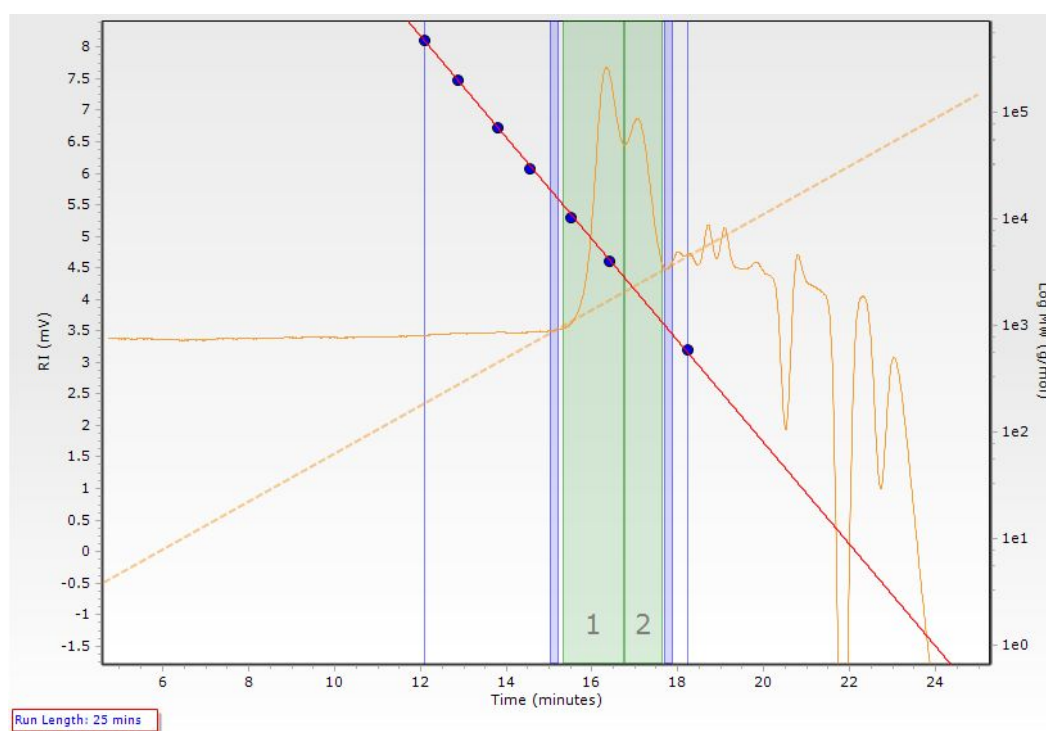


Figure S36: SEC trace for PA/CHO co-polyester formed by **1-*p*-^tBu** (Table S3 Entry 4).

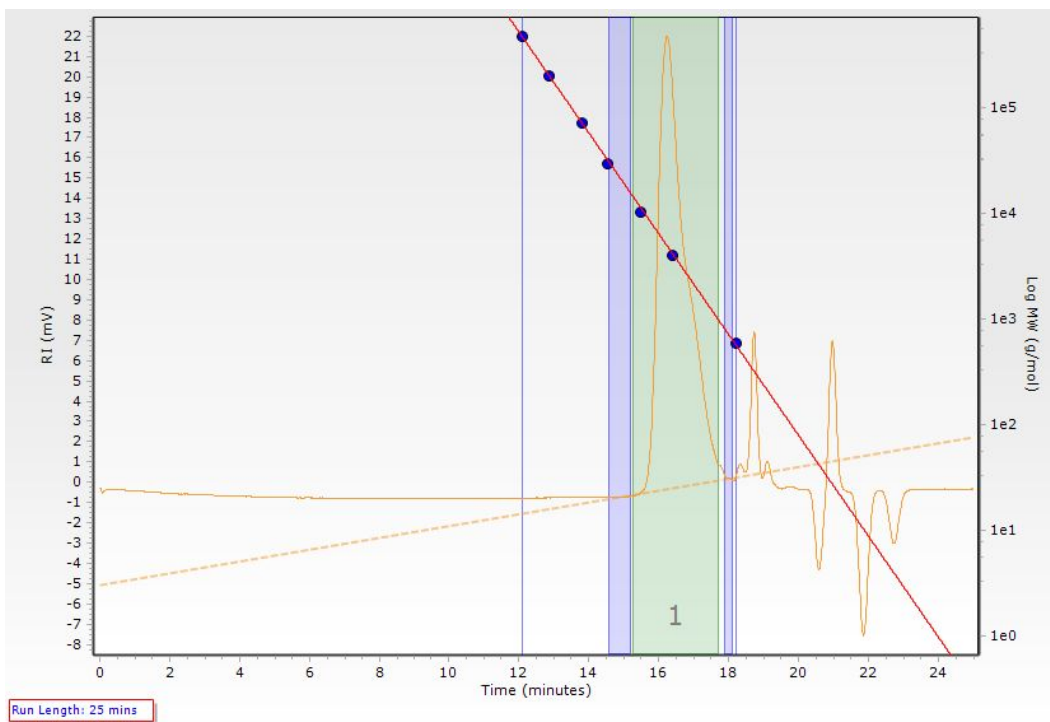


Figure S37: SEC trace for PA/CHO co-polyester formed by **1-*p*-tBu** (Table S3 Entry 5).

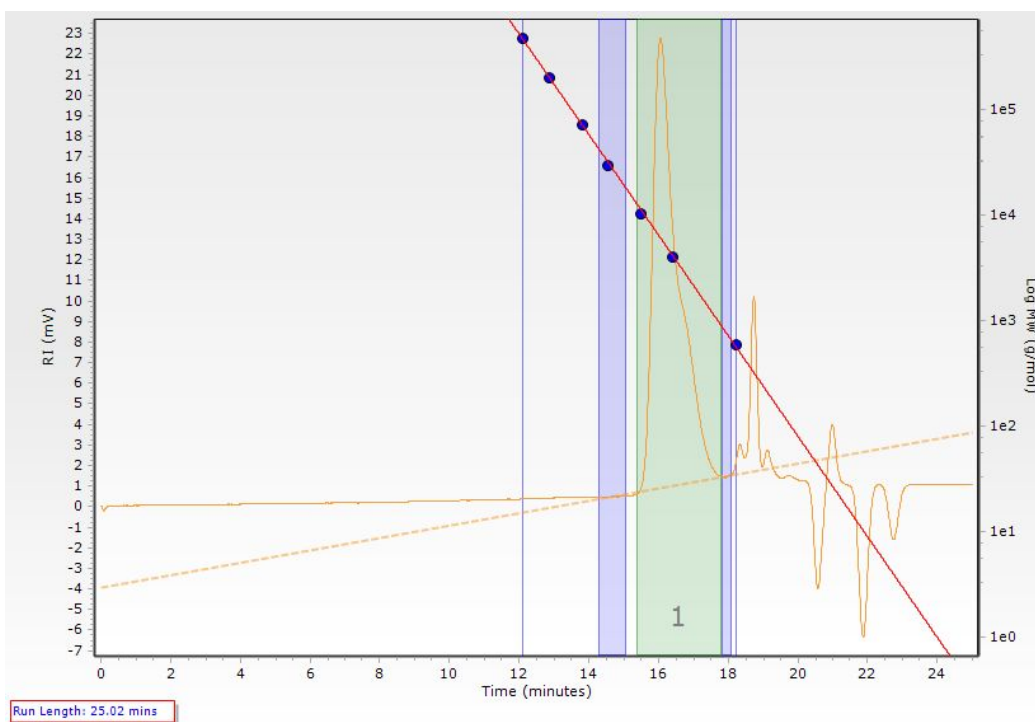


Figure S38: SEC trace for PA/CHO co-polyester formed by **1-*p*-tBu** (Table S3 Entry 6).

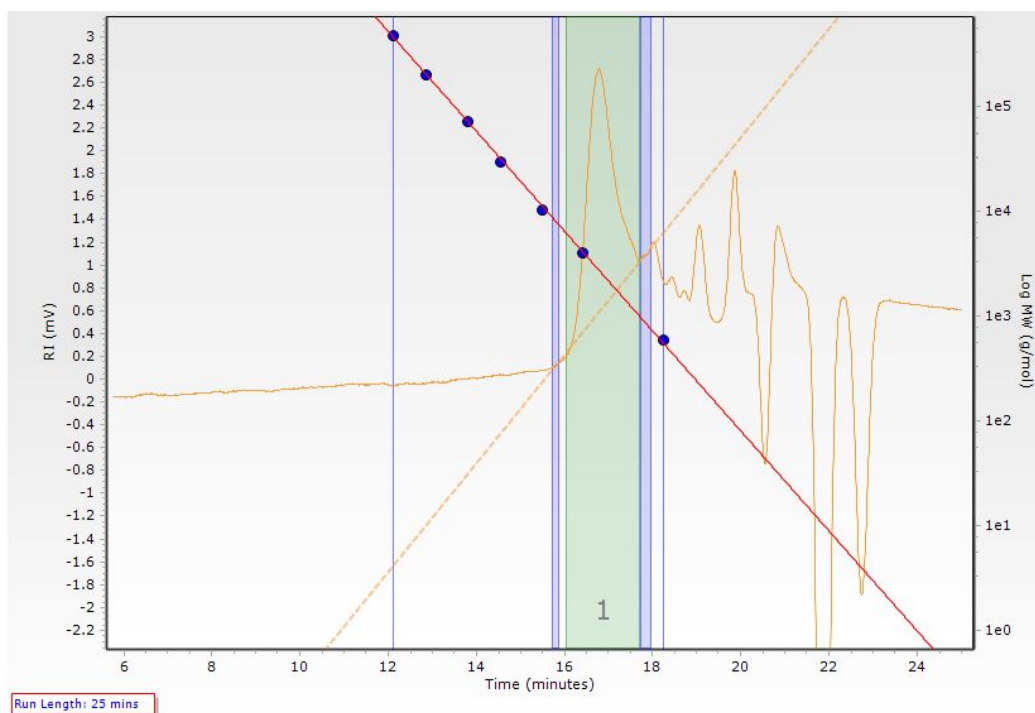


Figure S39: SEC trace for PA/CHO co-polyester formed by **1-*m*-Ad** (Table S3 Entry 9).

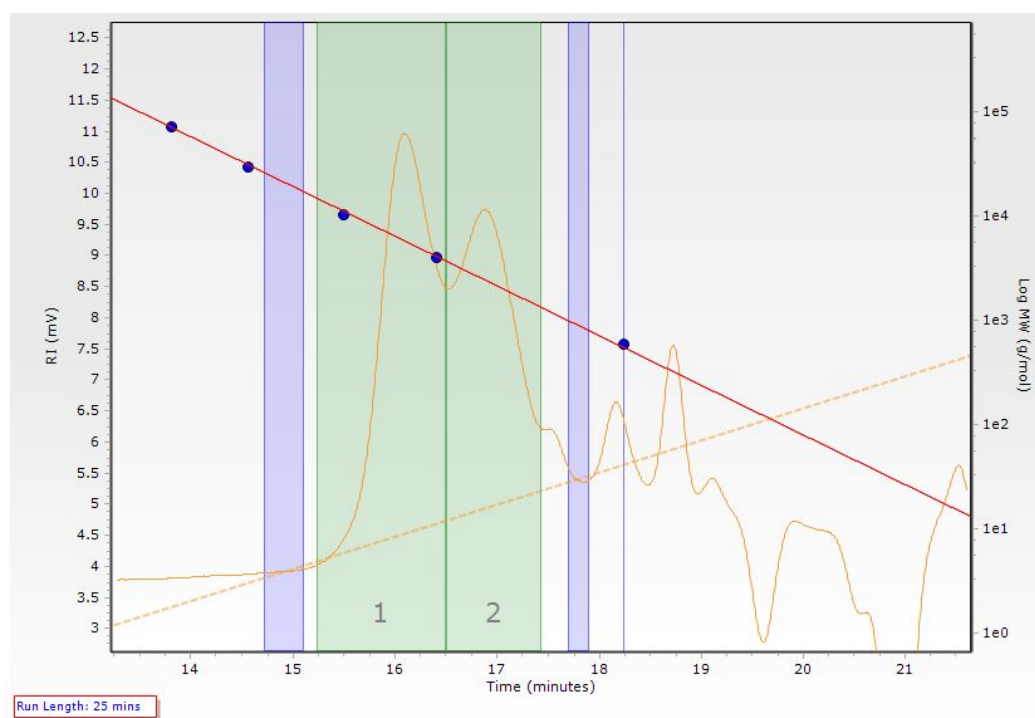


Figure S40: SEC trace for PA/CHO co-polyester formed by **1-*p*-Ad** (Table S3 Entry 11).

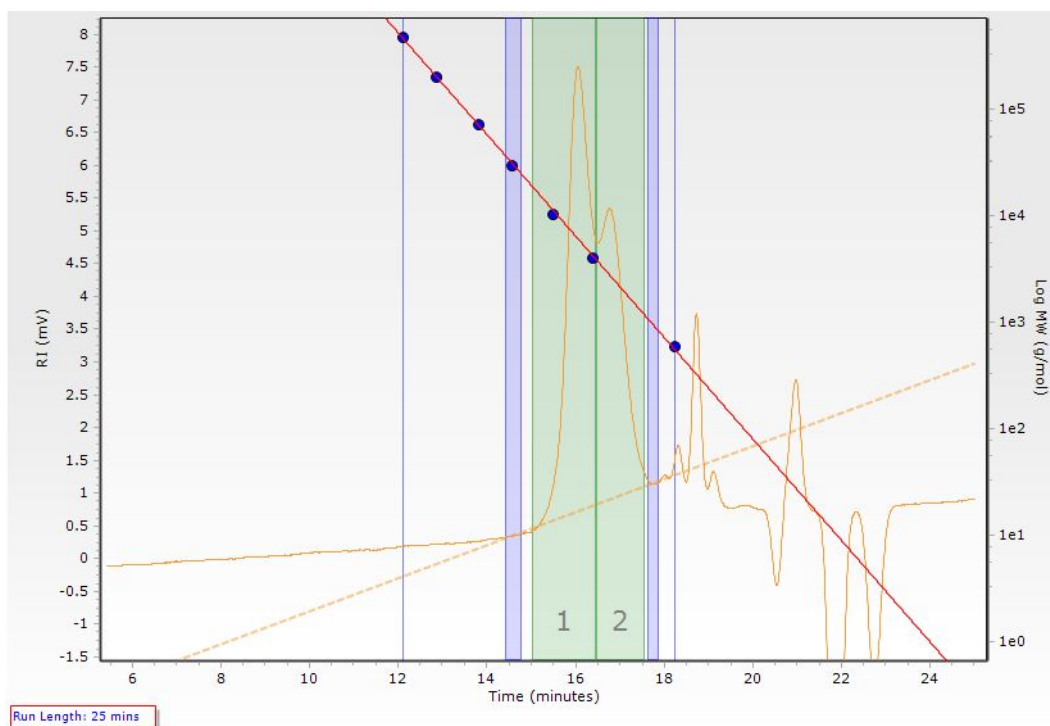


Figure S41: SEC trace for PA/CHO co-polyester formed by **1-*p*-Ad** (Table S3 Entry 12).

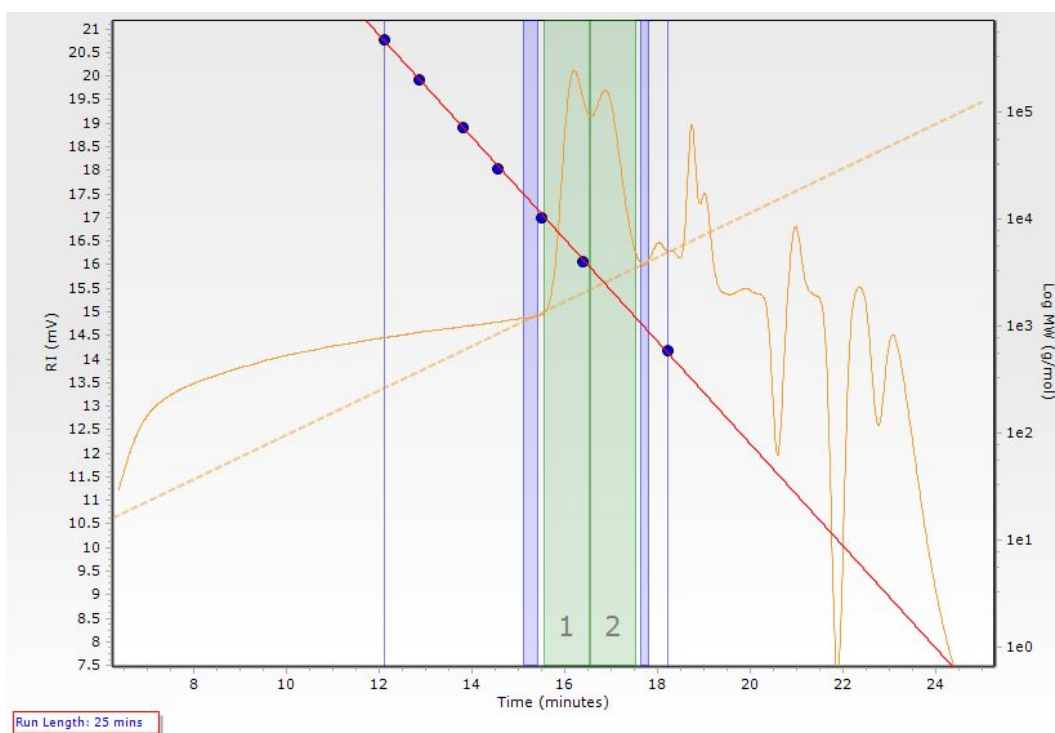


Figure S42: SEC trace for PA/CHO co-polyester formed by **2-*p*-^tBu** (Table S3 Entry 15).

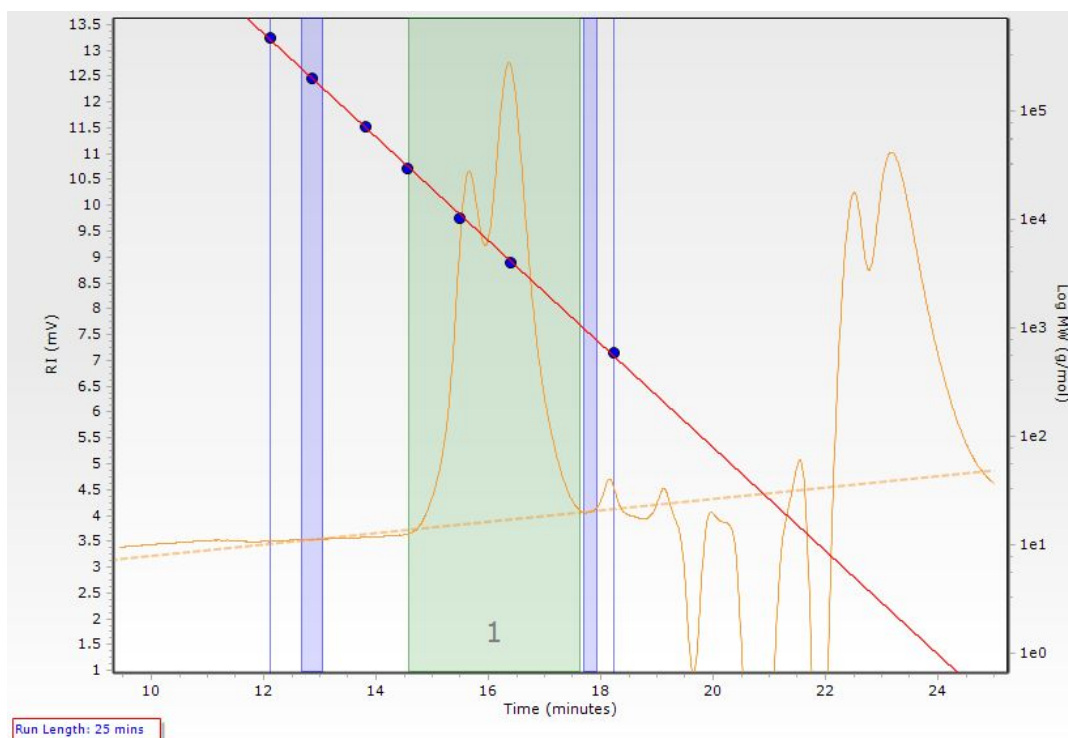


Figure S43: SEC trace for PA/CHO co-polyester formed by **3** (Table S3 Entry 18).

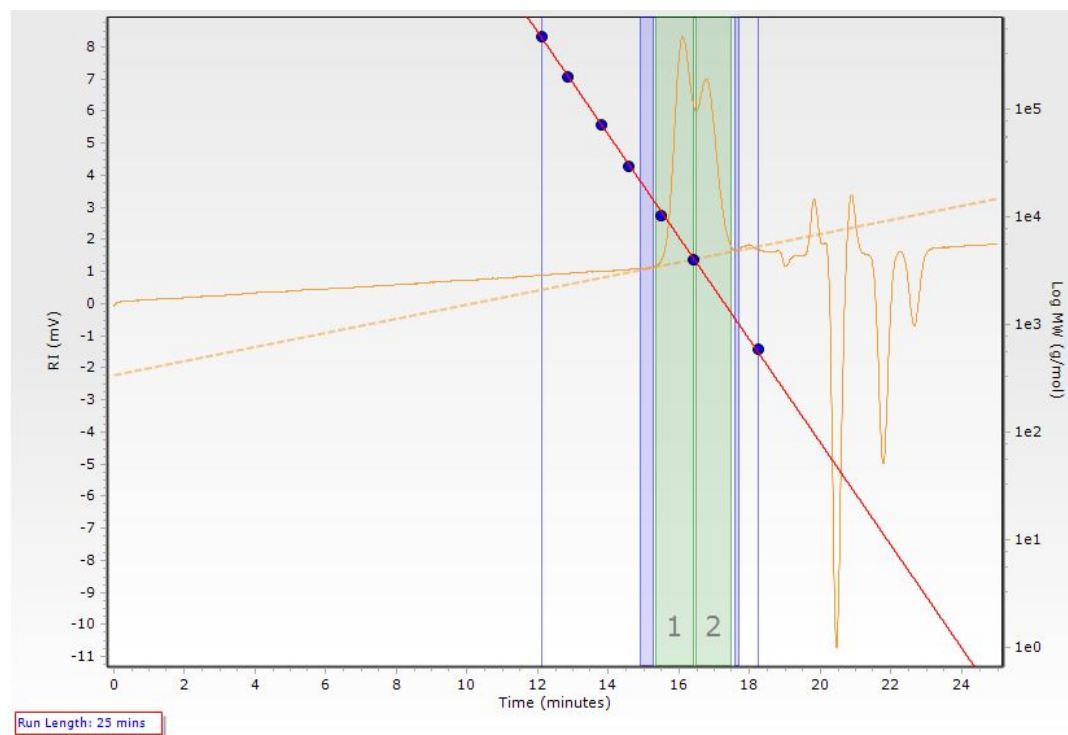


Figure S44: SEC trace for PA/CHO co-polyester formed by **4** (Table S3 Entry 20).

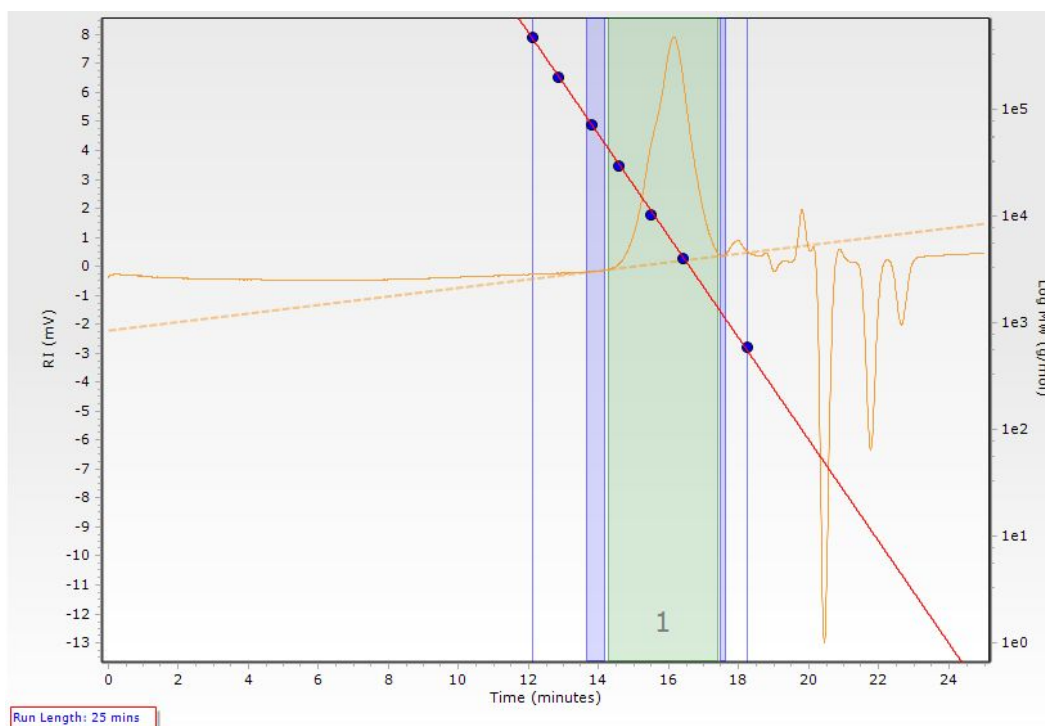


Figure S45: SEC trace for PA/CHO co-polyester formed by **5** (Table S3 Entry 22).

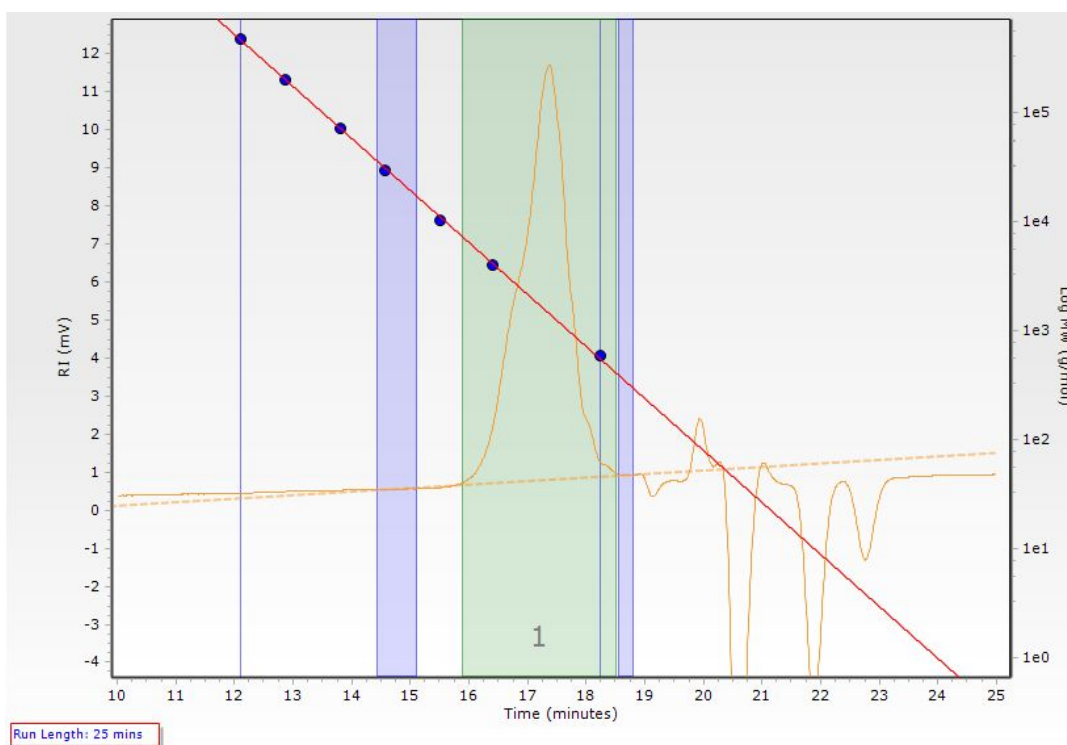


Figure S46: SEC trace for PA/CHO co-polyester formed by $[\text{NEt}_4]_2\text{CeCl}_6$ (Table S3 Entry 23).

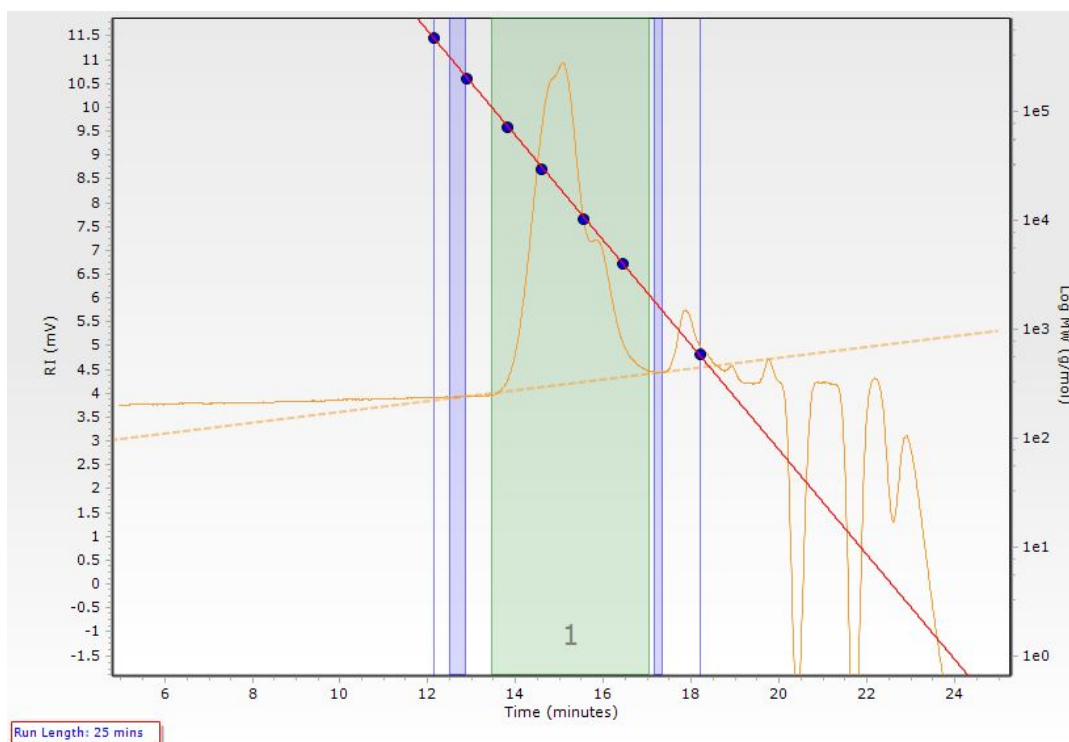


Figure S47: SEC trace for PA/PO co-polyester formed by **1-*m*-Ad** (Table S5 Entry 2).

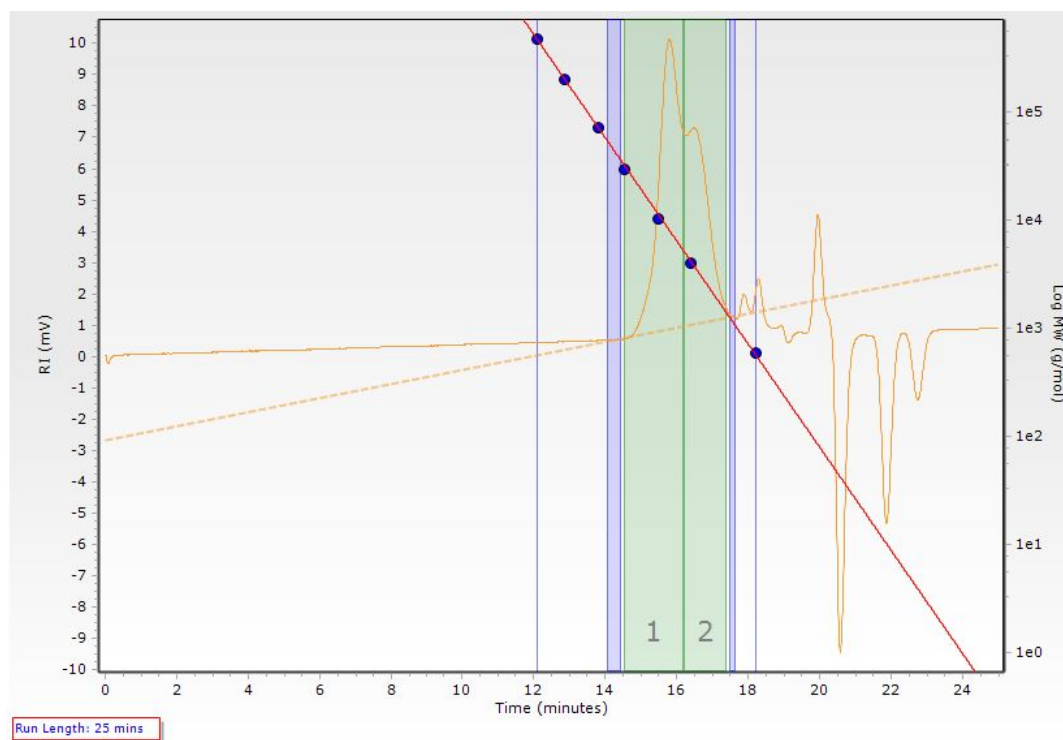


Figure S48: SEC trace for PA/LO co-polyester formed by **1-*m*-Ad** (Table S5 Entry 3).

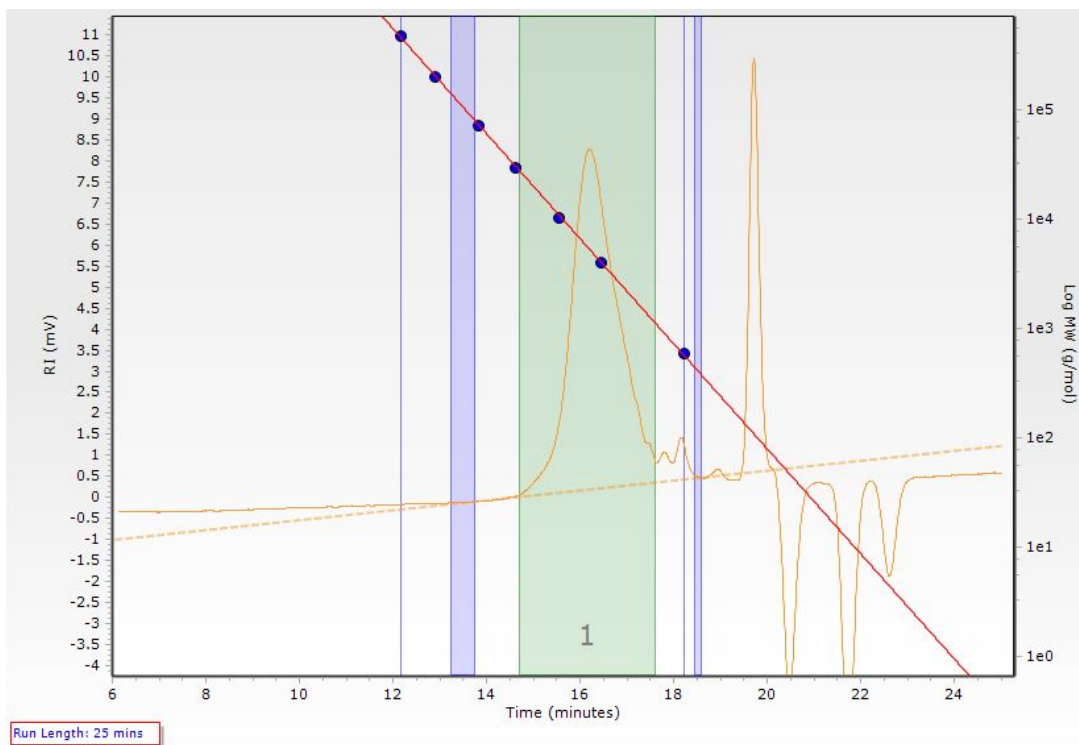


Figure S49: SEC trace for SA/CHO co-polyester formed by **1-*m*-Ad** (Table S5 Entry 5).

S3.6 MALDI Data

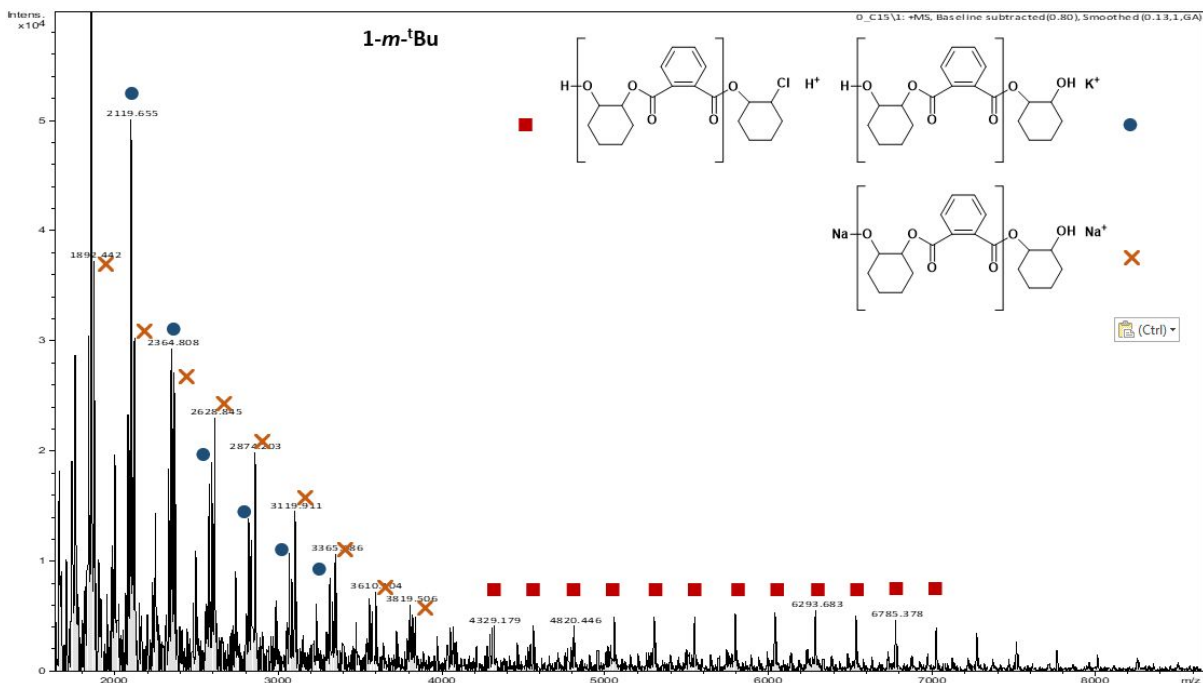


Figure S50: MALDI-ToF spectrum for PA/CHO co-polyester formed by **1-*m*-tBu** (Table S3 Entry 3).

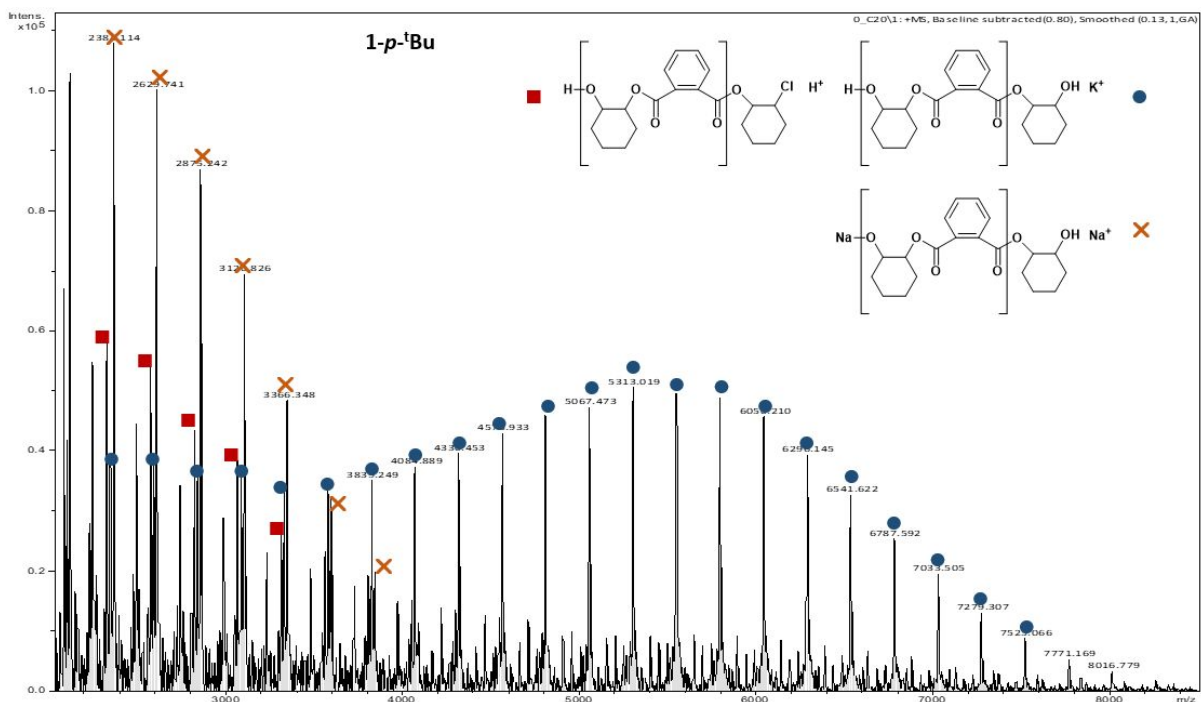


Figure S51: MALDI-ToF spectrum for PA/CHO co-polyester formed by **1-*p*-tBu** (Table S3 Entry 5).

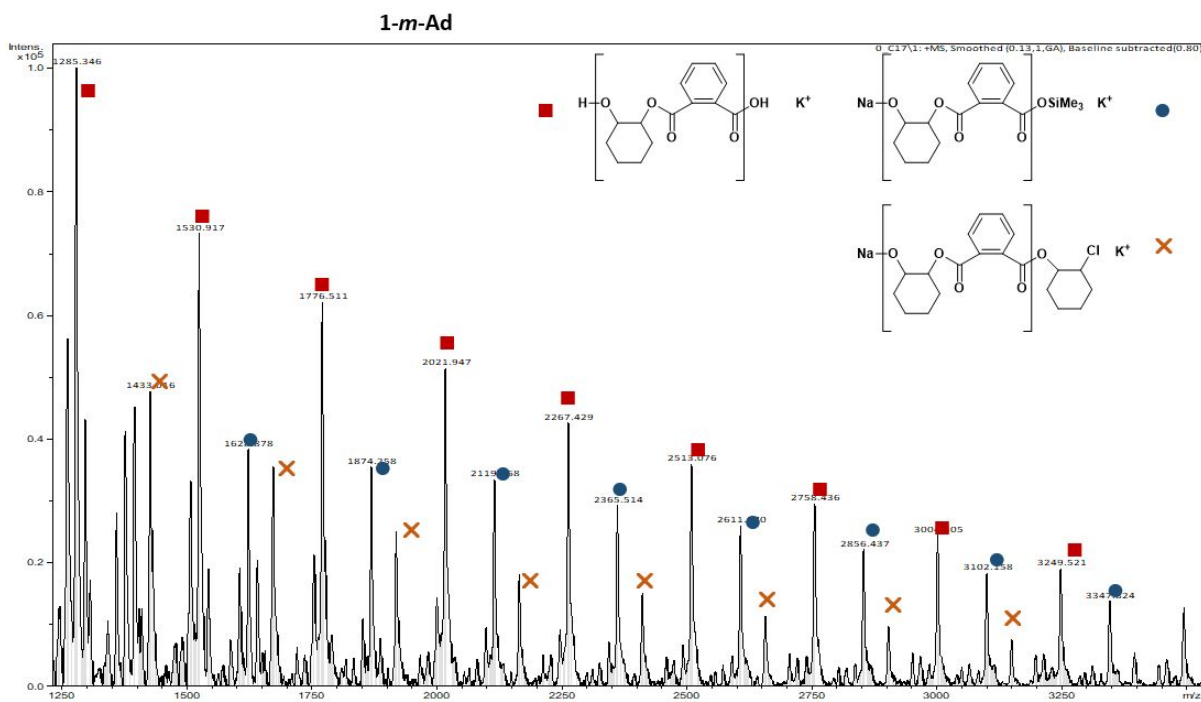


Figure S52: MALDI-ToF spectrum for the PA/CHO co-polyester formed by **1-*m*-Ad** (Table S3 Entry 9).

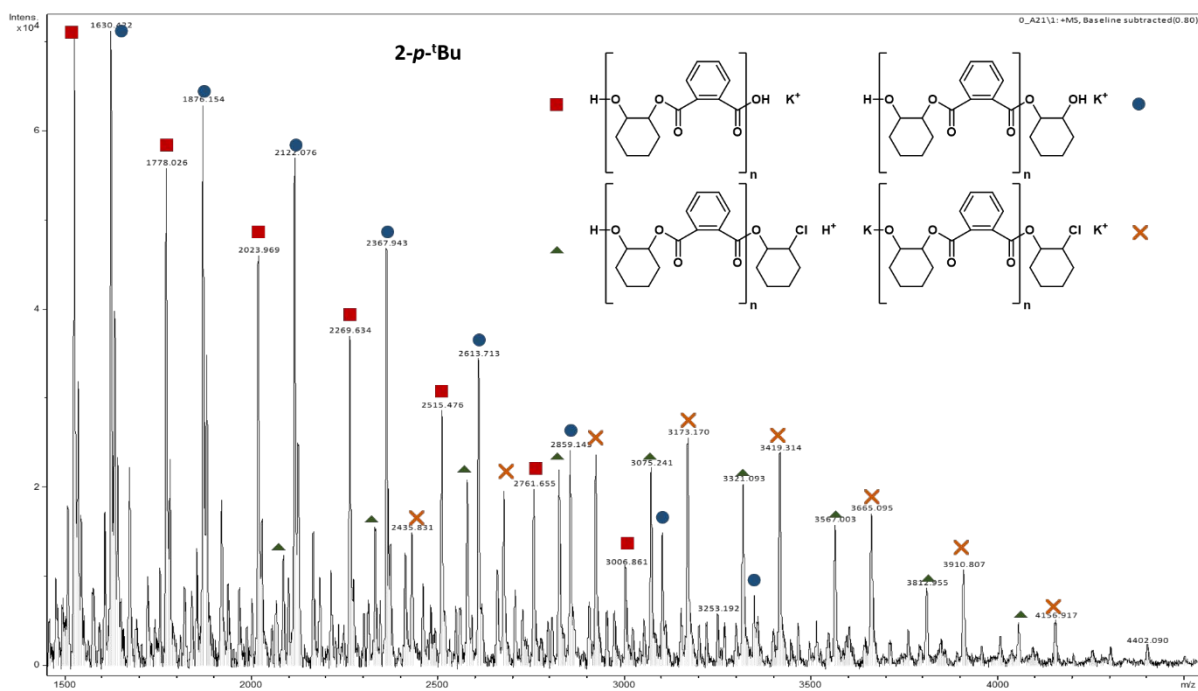


Figure S53: MALDI-ToF spectrum for the PA/CHO co-polyester formed by **2-p-tBu** (Table S3 Entry 13).

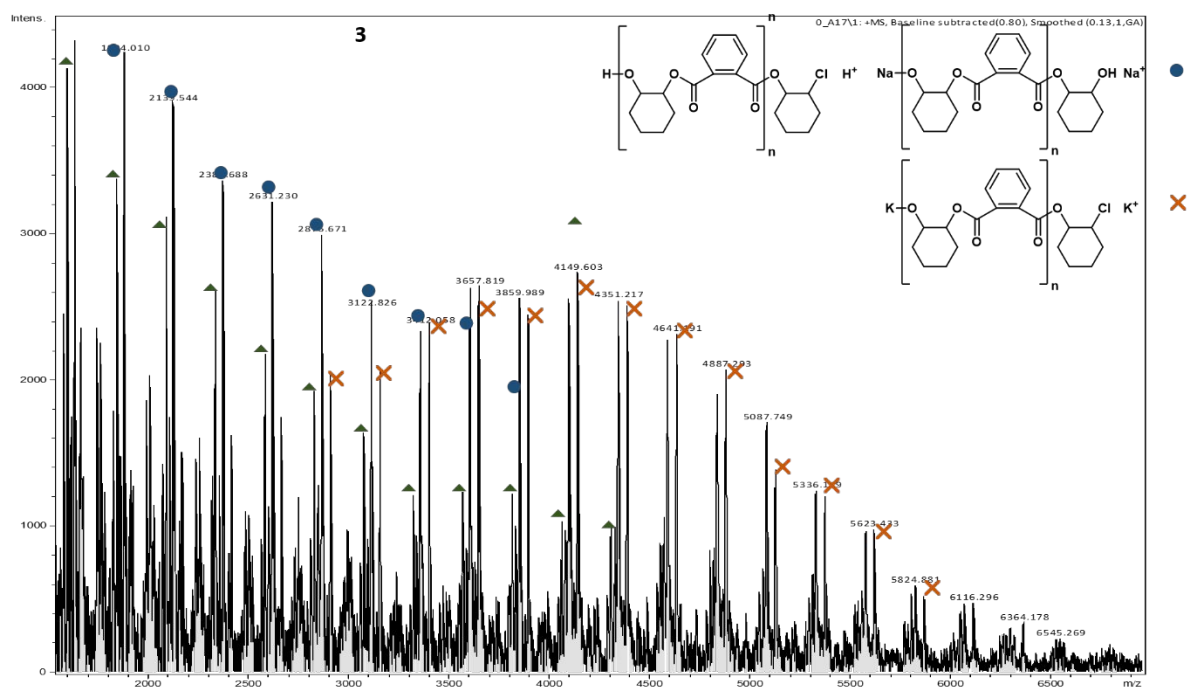


Figure S54: MALDI-ToF spectrum for PA/CHO co-polyester formed by **3** (Table S3 Entry 17).

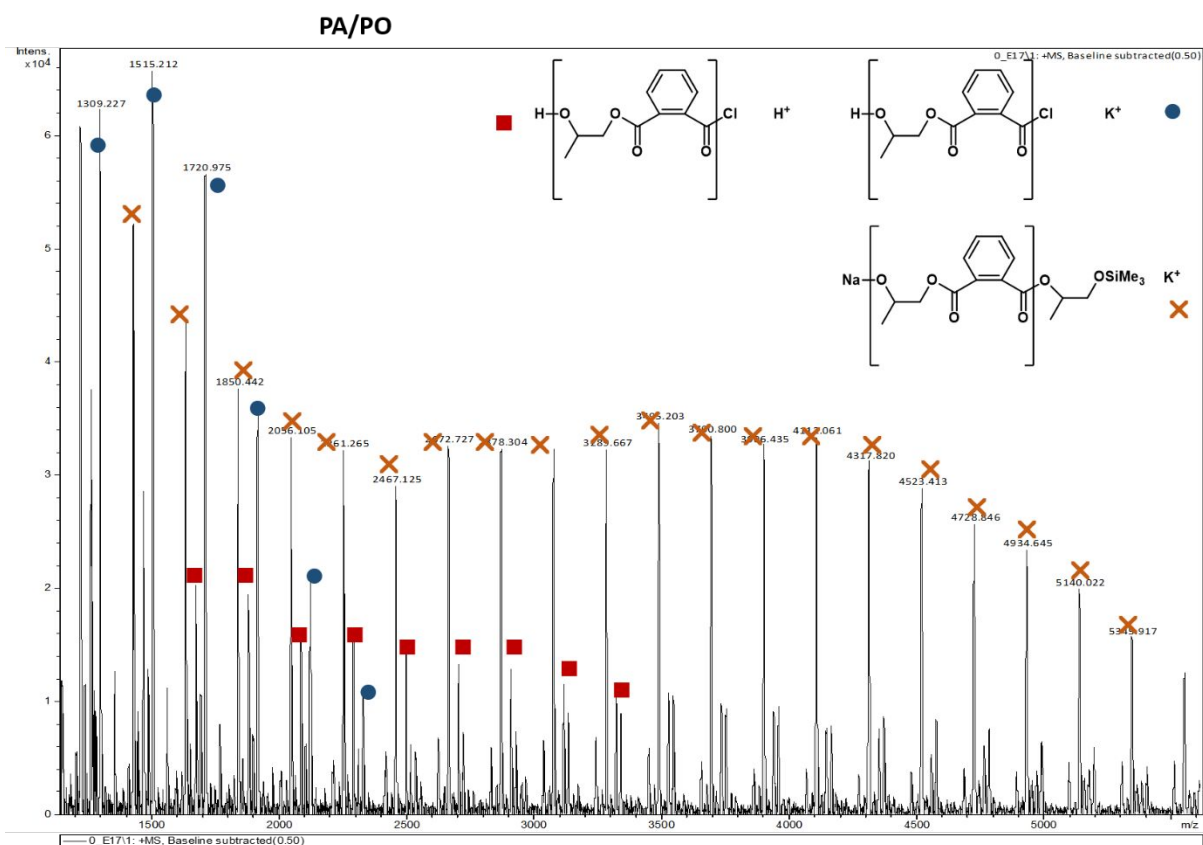


Figure S55: MALDI-ToF spectrum for PA/PO co-polyester formed by **1-*m*-Ad** (Table S4 Entry 1).

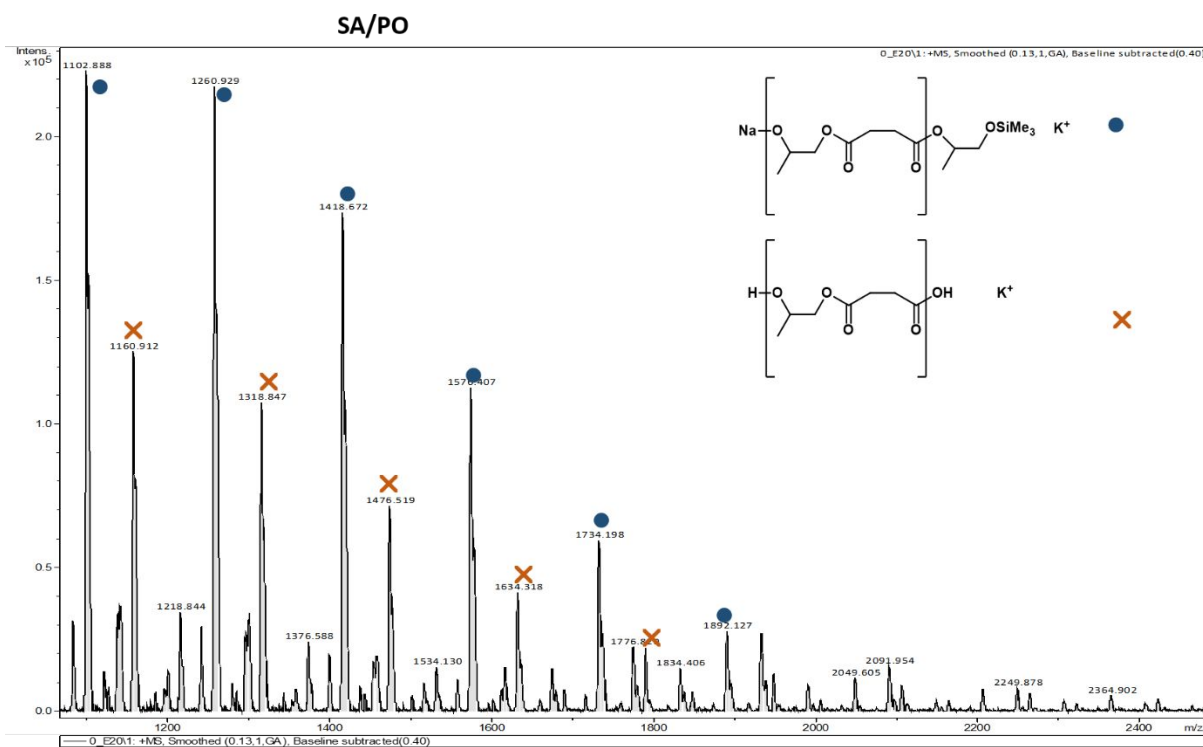


Figure S56: MALDI-ToF spectrum for SA/PO co-polyester formed by **1-*m*-Ad** (Table S4 Entry 4).

S4. Crystallography

Single crystal X-ray diffraction data were collected using an Excalibur Eos diffractometer, fitted with a CCD area detector and using MoK α radiation ($\lambda = 0.71073 \text{ \AA}$) at 190 K. The molecular structure of **1^{*}-p-Ad** was solved using SHELXT¹⁹ and least-square refined using SHELXL²⁰ in Olex2.²¹ Hydrogen atoms were treated by constrained refinement.

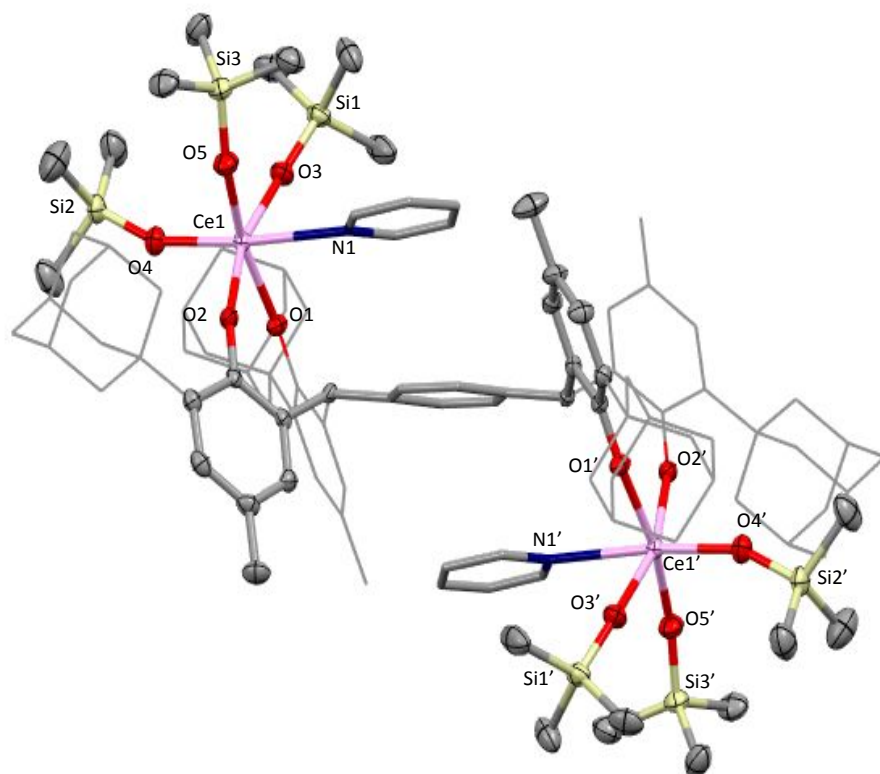


Figure S57: Solid-state structure of the dianion $[1^*-\text{p-Ad}]^{2-}$ with selected C and non-C/H atoms shown at 50% ellipsoid probability, coordinated solvent and selected C atoms drawn capped stick, peripheral C & O atoms drawn wireframe. Tetraethylammonium cations, all H atoms and two pyridine lattice solvent molecules omitted for clarity. Selected bond distances (\AA) and angles ($^\circ$) for **1^{*}-p-Ad**: Ce1-O1 2.231(2), Ce1-O2 2.209(2), Ce1-O3 2.151(3), Ce1-O4 2.154(3), Ce1-O5 2.168(3), Ce1-N1 2.659(3), O1-Ce1-O2 85.35(9), O1-Ce1-O3 87.96(10), O2-Ce1-O4 98.58(10), O2-Ce1-O5 90.47(10), O3-Ce1-O4 98.45(11), O3-Ce1-N1 79.46(11).

Table S6: Crystallographic data for **1^{*}-p-Ad**.

Crystal data	
CCDC deposition no.	2032589
Chemical formula	$C_{104}H_{150}Ce_2N_2O_{10}Si_6 \cdot 2(C_8H_{20}N) \cdot 4(C_5H_5N)$
<i>M</i> _r	2613.93
Crystal system, space group	Triclinic, <i>P</i> 1
Temperature (K)	190
<i>a</i> , <i>b</i> , <i>c</i> (Å)	14.1625 (7), 14.4859 (7), 19.8390 (8)
α , β , γ (°)	97.975 (4), 105.839 (4), 112.170 (4)
<i>V</i> (Å ³)	3490.0 (3)
<i>Z</i>	1
Radiation type	Mo <i>K</i> α
μ (mm ⁻¹)	0.75
Crystal size (mm)	0.19 × 0.14 × 0.08
Data collection	
Diffractometer	Xcalibur, Eos
Absorption correction	Analytical <i>CrysAlis PRO</i> 1.171.40.54a (Rigaku Oxford Diffraction, 2019) Analytical numeric absorption correction using a multifaceted crystal model based on expressions derived by R.C. Clark & J.S. Reid. (Clark, R. C. & Reid, J. S. (1995). <i>Acta Cryst.</i> A51, 887-897) Empirical absorption correction using spherical harmonics, implemented in SCALE3 ABSPACK scaling algorithm.
<i>T</i> _{min} , <i>T</i> _{max}	0.805, 0.896
No. of measured, independent and observed [<i>I</i> > 2σ(<i>I</i>)] reflections	66835, 14152, 11546
<i>R</i> _{int}	0.084
(<i>sin</i> θ/λ) _{max} (Å ⁻¹)	0.625
Refinement	
<i>R</i> [<i>F</i> ² > 2σ(<i>F</i> ²)], <i>wR</i> (<i>F</i> ²), <i>S</i>	0.054, 0.123, 1.08
No. of reflections	14152
No. of parameters	763
H-atom treatment	H-atom parameters constrained
Δρ _{max} Δρ _{min} (e Å ⁻³)	1.69, -0.80

S5. References

1. Wells, J. A. L.; Seymour, M. L.; Suvova, M.; Arnold, P. L., Dinuclear Uranium Complexation and Manipulation Using Robust Tetraaryloxides. *Dalton Trans.* **2016**, 45 (40), 16026-16032.
2. Arnold, P. L.; Cowie, B. E.; Halliday, C. J. V., Isolation of f-Block Cation Pairs by Stretched Dinucleating Aryloxide Platforms. *manuscript in preparation*.
3. Gademann, K. C.; David E.; Jacobsen, Eric N., Highly Enantioselective Inverse-Electron-Demand Hetero-Diels-Alder Reactions of α,β -Unsaturated Aldehydes. *Angew. Chem. Int. Ed.* **2002**, 41 (No. 16), 3059-3061.
4. Mansell, S. M.; Perandones, B. F.; Arnold, P. L., New U^{III} and U^{IV} Silylamides and an Improved Synthesis of NaN(SiMe₂R)₂ (R = Me, Ph). *J. Organomet. Chem.* **2010**, 695 (25-26), 2814-2821.
5. Loble, M. W.; Keith, J. M.; Altman, A. B.; Stieber, S. C.; Batista, E. R.; Boland, K. S.; Conradson, S. D.; Clark, D. L.; Lezama Pacheco, J.; Kozimor, S. A.; Martin, R. L.; Minasian, S. G.; Olson, A. C.; Scott, B. L.; Shuh, D. K.; Tyliszczak, T.; Wilkerson, M. P.; Zehnder, R. A., Covalency in Lanthanides. An X-ray Absorption Spectroscopy and Density Functional Theory Study of LnCl₆(x-) (x = 3, 2). *J. Am. Chem. Soc.* **2015**, 137 (7), 2506-23.
6. Cetinkaya, B.; Gumrukcu, I.; Lappert, M. F., Lithium and Sodium 2,6-Di-tert-butylphenoxides and the Crystal and Molecular Structure of [Li(OC₆H₂Me-4-Bu,2-2,6)(OEt₂)₂]. *J. Am. Chem. Soc.* **1980**, 102 (6), 2086-2088.
7. Chen, H.-Y.; Mialon, L.; Abboud, K. A.; Miller, S. A., Comparative Study of Lactide Polymerization with Lithium, Sodium, Magnesium, and Calcium Complexes of BHT. *Organometallics* **2012**, 31 (15), 5252-5261.
8. Friedrich, J.; Maichle-Mössmer, C.; Schrenk, C.; Schnepf, A.; Anwander, R., Ceric Ammonium Nitrate and Ceric Ammonium Chloride as Precursors for Ceric Siloxides: Ammonia and Ammonium Inclusion. *Eur. J. Inorg. Chem.* **2019**, 19 (1), 79-90.
9. Gradeff, P. S.; Yunlu, K.; Deming, T. J.; Olofson, J. M.; Doedens, R. J.; Evans, W. J., Synthesis of Yttrium and Lanthanide Silyloxy Complexes from Anhydrous Nitrate and Oxo Alkoxide Precursors and the X-ray Crystal Structure of [Ce(OSiPh₃)₃(THF)₃](THF). *Inorg Chem* **1990**, 29, 420-424.
10. Garden, J. A.; Saini, P. K.; Williams, C. K., Greater than the Sum of Its Parts: A Heterodinuclear Polymerization Catalyst. *J. Am. Chem. Soc.* **2015**, 137 (48), 15078-81.
11. Romain, C.; Garden, J. A.; Trott, G.; Buchard, A.; White, A. J. P.; Williams, C. K., Di-Zinc-Aryl Complexes: CO₂ Insertions and Applications in Polymerisation Catalysis. *Chemistry* **2017**, 23 (30), 7367-7376.
12. Jeon, J. Y.; Eo, S. C.; Varghese, J. K.; Lee, B. Y., Copolymerization and Terpolymerization of Carbon Dioxide/Propylene Oxide/Phthalic Anhydride Using a (salen)Co(III) Complex Tethering Four Quaternary Ammonium Salts. *Beilstein J. Org. Chem.* **2014**, 10, 1787-95.
13. Longo, J. M.; DiCiccio, A. M.; Coates, G. W., Poly(propylene succinate): A New Polymer Stereocomplex. *J. Am. Chem. Soc.* **2014**, 136 (45), 15897-900.
14. Isnard, F.; Santulli, F.; Cozzolino, M.; Lamberti, M.; Pellicchia, C.; Mazzeo, M., Tetracoordinate Aluminum Complexes Bearing Phenoxy-Based Ligands as Catalysts for Epoxide/Anhydride Copolymerization: some Mechanistic Insights. *Catal. Sci. Technol.* **2019**, 9 (12), 3090-3098.
15. Peña Carrodegas, L.; Martín, C.; Kleij, A. W., Semiaromatic Polyesters Derived from Renewable Terpene Oxides with High Glass Transitions. *Macromolecules* **2017**, 50 (14), 5337-5345.
16. Martinez de Sarasa Buchaca, M.; de la Cruz-Martinez, F.; Martinez, J.; Alonso-Moreno, C.; Fernandez-Baeza, J.; Tejada, J.; Niza, E.; Castro-Osma, J. A.; Otero, A.; Lara-Sanchez, A., Alternating Copolymerization of Epoxides and Anhydrides Catalyzed by Aluminum Complexes. *ACS Omega* **2018**, 3 (12), 17581-17589.
17. Trott, G.; Garden, J. A.; Williams, C. K., Heterodinuclear Zinc and Magnesium Catalysts for Epoxide/CO₂ Ring Opening Copolymerizations. *Chem. Sci.* **2019**, 10 (17), 4618-4627.
18. Saini, P. K.; Romain, C.; Zhu, Y.; Williams, C. K., Di-Magnesium and Zinc Catalysts for the Copolymerization of Phthalic Anhydride and Cyclohexene Oxide. *Polym. Chem.* **2014**, 5 (20), 6068-6075.

19. Sheldrick, G. M., SHELXT – Integrated Space-Group and Crystal-Structure Determination. *Acta Cryst.* **2015**, *A71*, 3-8.
20. Sheldrick, G. M., Crystal Structure Refinement with SHELXL. *Acta Cryst.* **2015**, *C71*, 3-8.
21. Dolomanov, O. V.; Bourhis, L. J.; Gildea, R. J.; Howard, J. A. K.; Puschmann, H., OLEX2: A Complete Structure Solution, Refinement and Analysis Program. *J. Appl. Crystallogr.* **2009**, *42* (2), 339-341.